PERFORMANCE OF UHPC MIXTURES SUBJECTED TO ELEVATED TEMPERATURES AND CYCLIC EXPOSURES

BY

MEHBOOB RASUL

A Thesis Presented to the

DEANSHIP OF GRADUATE STUDIES

KING FAHD UNIVERSITY OF PETROLEUM & MINERALS

DHAHRAN, SAUDI ARABIA

In Partial Fulfillment of the
Requirements for the Degree of

MASTER OF SCIENCE

In

CIVIL ENGINEERING

MAY 2016

KING FAHD UNIVERSITY OF PETROLEUM & MINERALS

DHAHRAN- 31261, SAUDI ARABIA

DEANSHIP OF GRADUATE STUDIES

This thesis, written by **MEHBOOB RASUL** under the direction of his thesis advisor and approved by his thesis committee, has been presented and accepted by the Dean of Graduate Studies, in partial fulfillment of the requirements for the degree of **MASTER OF SCIENCE IN CIVIL ENGINEERING.**

Dr. Shamsad Ahmad
(Advisor)

Dr. Salah U. Al-Dulaijan
Department Chairman

Dr. Mohammed Maslehuddin
(Member)

Dr. Salam A. Zummo
Dean of Graduate Studies

Dr. Salah U. Al-Dulaijan
(Member)

21/6/16

Date

Dedicated To

My beloved parents and brothers

ACKNOWLEDGMENTS

All praises and thanks are due to ALLAH Subhanaho wa taala for blessing me with the countless blessings, health, knowledge and patience to complete this thesis. May the peace and blessings of ALLAH be upon the Prophet Muhammad (Peace be upon him), his family, and his companions.

I would like to acknowledge King Fahd University of Petroleum and Minerals and Department of Civil and Environmental Engineering KFUPM for granting me opportunity to pursue my master studies with scholarship in state of the art academic and research facilities. I want to thank Deanship of Scientific Research for providing financial support during my research work.

I want to express my heartiest gratitude to my respected advisor Dr. Shamsad Ahmad, Committee members Dr. Mohammed Maslehuddin and Dr. Salah U. Al-Dulaijan for their sincere continuous guidance and kind support. It is a vital life time experience for me to work under the umbrella of such great experts of my field. They not only technically supported me during my research but also helped me to boost up my morale and confidence. I also want to thank all other faculty, staff members and secretaries for their support throughout my studies and research.

I also acknowledge the sincere support of Engr. Imran Syed, Engr. Omer Hussein, Engr. Syed Khaja Najamuddin and Engr. M. Rizwan Ali during my research, especially in experimental works.

I am really grateful to my senior colleagues and all friends especially, Mr. Saheed Kolawole Adekunle and Mr. Muhmmad Umar for their technical and moral support throughout my research work.

Last but not the least, I want to acknowledge my parents and brothers for their unconditional love, support, prayers and encouragement throughout my life.

TABLE OF CONTENTS

LIST OF TABLES

LIST OF FIGURES

ABSTRACT

FULL NAME: MEHBOOB RASUL

THESIS TITLE: PERFORMANCE OF UHPC MIXTURES SUBJECTED TO ELEVATED TEMPERATURES AND CYCLIC EXPOSURES

MAJOR FIELD: CIVIL ENGINEERING

DATE OF DEGREE: MAY, 2016

Ultra-high performance concrete (UHPC) is a specific type of modern era concrete possessing excellent mechanical properties (compressive strength more than 150 MPa, high fracture toughness, etc.) with excellent durability. The constituents of UHPC include high cement content, fine quartz sand, high dosage of silica fume and superplasticizer at a very low water to binder ratio. Fibers are also added to improve the mechanical properties, specifically for post-cracking behavior.

Recently, some research studies were carried out in KFUPM for the production of UHPC mixtures using local materials and for study of their mechanical properties and durability characteristics. However, the performance of the locally developed UHPC mixtures against elevated temperature and long cyclic exposures, such as heat-cool and wet-dry cycles, has not been studied. Such investigations are needed considering the risk of fire and frequent changes in weather conditions. Wet-dry cycles are representation of concrete structures in tidal zone which are exposed to alternate wetting and drying, whereas heat-cool cycles are representative of the daily ambient temperature variation in hot-arid regions. Hence, there was an immense need of research on performance evaluation of already developed UHPC mixtures exposed to elevated temperatures and cyclic exposures (wet-dry, heat-cool cycles).

In this work, three mixtures of UHPC, already developed at KFUPM under previous research projects, were considered for evaluation of their performance against elevated temperature exposure with varying durations and against exposure to the heat-cool and wet-dry cycles. For wet-dry cyclic exposure, specimens were submerged into the water containing 5% Cl^- for six hours and left to dry for remaining 18 hours in one cycle. For heat-cool cyclic exposure, specimens were heated at 70^oC for five hours and cooled down for 19 hours in one cycle. The UHPC specimens, containing the metallic and non-metallic fibers in varying quantity, were exposed to an elevated temperature of 300^oC for different exposure durations. After completion of exposures, specimens were tested to evaluate the performance in terms of residual compressive, flexural and splitting tensile strength, and modulus of elasticity. The performance of UHPC specimens subjected to cyclic exposures were evaluated in terms of residual compressive strength, flexural and splitting tensile strength, modulus of elasticity, fracture toughness, water permeability, rapid chloride ion permeability, and corrosion current density.

UHPC mixtures with steel fibers have shown excellent performance even after five hours of exposure to 300^oC. Although UHPC mixtures with polypropylene fibers have shown satisfactory results even after five hours of exposure to 300^oC, their failure was sudden without warning. Up to 180 cycles of heating and cooling and wetting and drying, there was no significant adverse effect of the cyclic exposures on mechanical properties and durability characteristics. Rather almost all mechanical properties were slightly improved due the curing effect of cyclic exposure. The data developed in this study indicate that UHPC mixtures are suitable for use under elevated temperature and thermal and moisture variations.

ملخص الرسالة

الاسم الكامل: محبوب رسول

عنوان الرسالة : أداء الخلطات الخرسانية فائقة الاداء (UHPC) المعرضة لدرجات حرارة مرتفعة و تغيرات دورية

التخصص: هندسة مدنية (انشاءات)

تاريخ الحصول على الدرجة: مايو 2016 م

الخرسانة فائقة الأداء (UHPC) هي نوع خاص من خرسانات العصر الحديث والتي تتمتع بخواص ميكانيكية ممتازة (قوة ضغط الخرسانة أكثر من 150 ميقا باسكال، متانة عالية، إلخ.) و دوامية ممتازة. تشتمل الخرسانة فائقة الأداء (UHPC) على محتوى اسمنت عالي، رمل، كمية كبيرة من غبار السيليكا، و ملدن (Superplasticizer) بحيث تكون نسبة الماء الى المواد الاسمنتية منخفضة. تم إضافة الالياف المعدنية لتحسين الخواص الميكانيكية خاصة لمرحلة ما بعد التشقق.

حديثا، تم عمل بعض الأبحاث في جامعة الملك فهد للبترول والمعادن (KFUPM) لانتاج خلطات الـ (UHPC) باستخدام المواد المحلية و ذلك لدراسة خواصها الميكانيكية و دوامية الخرسانة. و مع ذلك، أداء هذه الخلطات لم يفحص عند تعرضها لدرجات حرارة مرتفعة و تغيرات دورية مثل التسخين ثم التبريد و التبليل ثم التجفيف. مثل هذه الاختبارات مهمة لدراسة مقاومة الحريق و التغيرات المناخية. دورات التبليل و التجفيف عبارة عن محاكاة للمنشآت الخرسانية الواقعة في المناطق المعرضة للمد والجزر بينما دورات التسخين والتبريد عبارة عن محاكاة لتغير درجة الحرارة اليومية في المناطق الساخنة القاحلة. بالتالي هناك حاجة ملحة للبحث في تقييم أداء الخلطات المختارة بعد تعريضها لدرجات حرارة عالية و تغيرات دورية (التسخين ثم التبريد و التبليل ثم التجفيف).

في هذا البحث، تم اعتبار ثلاث خلطات من (UHPC)، تم تطويرها في أبحاث سابقة في KFUPM، لتقييم أدائها في تحمل درجات حرارة مرتفعة لفترات زمنية مختلفة و مقاومة التغيرات الدورية للحرارة و الرطوبة. بالنسبة لدورة التبليل ثم التجفيف، تم غمر العينات في الماء المحتوي على 5% من الكلوريد لمدة 6 ساعات ثم تركت تجف لمدة الـ 18 ساعة اللاحقة في دورة واحدة. اما بالنسبة لدورة التسخين و التبريد، فقد تم تسخين العينات الى 70 درجة مئوية لمدة 5 ساعات ثم تبريدها لمدة الـ 19 ساعة اللاحقة في دورة واحدة. عينات الخرسانة فائقة الأداء (UHPC)، المحتوية

على الالياف المعدنية و اللامعدنية بنسب مختلفة، تم تعريضها لدرجة حرارة 300 درجة مئوية لفترات زمنية مختلفة. بعد الانتهاء من تعريض الخرسانة، تم اختبار العينات لقياس قوة الضغط المتبقية، مقاومة الانحناء، مقاومة الشد، و معامل المرونة. أداء عينات الخرسانة فائقة الأداء (UHPC) المعرضة للتغيرات الدورية تم تقييمه عن طريق قياس قوة الضغط المتبقية، مقاومة الانحناء، مقاومة الشد، معامل المرونة، المتانة، نفاذية الماء، نفاذية الكلوريد، و كثافة تيار التآكل.

نتائج خلطات الـ (UHPC) المحتوية على الالياف المعدنية كانت ممتازة حتى بعد تعريضها الى 300 درجة مئوية لمدة 5 ساعات، انهيار العينات كان مفاجئ و بدون أي إشارات. حتى 180 دورة من التسخين و التبريد و التبليل و التجفيف لم يكن هناك تأثير كبير على الخواص الميكانيكية و دوامية الخرسانة. بدلا من ذلك كل الخواص الميكانيكية تحسنت بشكل طفيف نتيجة تأثير المعالجة الذي احدثه التعرض الدوري. المعلومات التي تم التحصل عليها في هذا البحث تدل على ان خلطات الخرسانة فائقة الأداء (UHPC) تعتبر مناسبة للاستخدام تحت درجات حرارة مرتفعة و كذلك تحت التغيرات في الحرارة و الرطوبة.

درجة الماجستير في العلوم الهندسية

جامعة الملك فهد للبترول والمعادن

الظهران – ٣١٢٦١

المملكة العربية السعودية

CHAPTER 1

INTRODUCTION

1.1 Introduction

The environmental conditions of Arabian Gulf are characterized as severe due to hot weather, wide fluctuations in temperature, humidity, and salts laden air, water and soil. Splash zone is also of much importance due to long costal line. These conditions are highly detrimental to the normal concrete and therefore require high performance concrete to ensure the targeted service life for the concrete structures.

In the present era, Ultra-High Performance Concrete (UHPC) also named as Reactive Powder Concrete (RPC) has become popular, owing to its very high compressive strength exceeding 200 MPa [1] and other superior mechanical properties and durability characteristics. Its homogeneity and dense microstructure, which offer excellent mechanical properties, are enhanced by eliminating the coarse aggregate and using ultra-fine materials (cement, silica fume, fine quartz sand, etc.) minimizing internal defects like voids and micro cracks. Its ductility is improved by adding small size fine steel fibers. UHPC besides having excellent mechanical behavior also possess excellent resistance against permeation of aggressive substances minimizing the risk of reinforcement corrosion. Although the cement content of UHPC is kept on a higher side, it has high resistance against shrinkage due to use of a very low amount of water. UHPC has resistance against shrinkage cracking due to its high tensile strength offered by the fibers used in it.

Moreover, it has high abrasion resistance especially in case of bridge decks and industrial floors as well [2].

UHPC or RPC is the generic name of a cementitious composite material developed in the 90's by Lafarge, Bouygues, and Rhodia jointly with the commercial name Ductal® [3, 4]. UHPC can be produced using relatively higher cement content, silica fume, fine quartz, with very low water-to-binder ratio (0.145 to 0.24) and relatively higher dosage of superplasticizer. Coarse aggregate is replaced by fine quartz sand of size 150 to 600 μm, crushed quartz of size <10 μm as fine aggregate, 25 to 30% silica fume is used to make very dense and impermeable mass. Small-size steel fibers for improving ductility and toughness are also added [1, 3, 5-7]. Presence of high amount of cement which leaves sufficient amount of un-hydrated cement as well, provides potential of self-healing against the cracks [2].

First practical application of UHPC was in construction of a pedestrian bridge, Sherbrooke Bridge Canada, built in 1997 [8]. Afterwards, the Footbridge of Peace in Seoul, South Korea and canopies of The Shawnessy light rail transit station in Calgary, Canada, were built in 2003 using UHPC. As UHPC is a smart and relatively costly material, it should be used only for special purposes. Its utility has more potential where steel is dominant. Especially, utility of UHPC for containing nuclear waste and radioactive materials has a lot of scope. Other possibly viable applications of UHPC can be security bunkers, sewerage pipes and pipes and containers for different liquids [2].

In the last five years, several research works were conducted at KFUPM in the area of UHPC. The first research project was an exploratory one, exploring the possibility of

preparing and testing of UHPC mixture made with a proprietary material, named as Ductal® [3]. Second project was on developing and evaluating the mechanical properties and durability characteristics of UHPC mixtures considering different levels of key parameters that included water/binder ratio, cement content and silica fume content [7, 9]. Third research project was on developing and evaluating the mechanical properties and durability characteristics of UHPC mixtures made using locally available industrial by-products (natural pozzolana, limestone powder, cement kiln dust, pulverized steel slag, bag house dust, metakaolin, etc.) as partial replacement of silica fume, keeping water/binder ratio and cement content constant [5]. The above-mentioned research studies focused mainly on production of UHPC mixtures using locally available materials targeting the excellent mechanical properties and durability characteristics under aggressive exposure conditions. However, performance of developed mixtures of UHPC made using the local materials against elevated temperatures and long cyclic exposures (alternate wet-dry and heat-cool for long durations) was still unknown. Therefore, a detailed study was needed for evaluating the performance of the already developed mixtures of UHPC exposed to elevated temperatures and heat-cool and wet-dry cycles. The findings of the proposed study integrated with the previous outcomes regarding UHPC mixtures would result into generation of sufficient data which can be used for producing and utilizing UHPC for locally prevailed environmental conditions.

1.2 Need for Research

From the literature review, it is found that some research works have been carried out for the performance evaluation of UHPC exposed to elevated temperature and cyclic exposures

for limited durations. However, ample information referring to the performance of UHPC mixtures against elevated temperatures and long cyclic exposures was not available, specifically for Arabian Gulf conditions. This study was aimed to evaluate the performance of three-selected superior UHPC mixtures (already developed using locally available materials during recently conducted research projects in KFUPM) exposed to elevated temperatures and cyclic exposures. The results obtained from this study can be employed in addition to the previous data pertaining to the performance of UHPC against other exposure conditions. This would facilitate to make suitable selection of UHPC mixture for any requires exposure condition during service life of structures.

1.3 Objectives

The main objective of the proposed study was to evaluate the performance of already developed UHPC mixtures under elevated temperature, heat-cool cycles and wet-dry cycles.

The specific objectives of this study were the following:

1. Expose the specimens of selected UHPC mixture to elevated temperatures, heat-cool and wet-dry cycles.
2. Evaluate the performance of the UHPC mixtures in terms of residual mechanical properties and durability characteristics before and after exposures.
3. Analyze the experimental data generated through the proposed work.
4. Provide recommendations for applications of these mixtures for meeting the requirements of different exposure conditions besides the structural requirements.

CHAPTER 2

LITERATURE REVIEW

The literature review presented here summarizes the information pertaining to the production of UHPC mixtures (highlighting its constituents, mixture optimization and basic mechanical properties) and performance of UHPC mixtures subjected to elevated temperatures and long-term cyclic exposures.

2.1 Constituents, Mixture Optimization and Principal Properties of UHPC

2.1.1 Constituents

An Ordinary Portland Cement (Type I) with low C_3A content is used as binder and silica fume (0.1 to 10 μm) is normally used as mineral admixture which also possess cementing properties. Fine quartz sand (150 to 600 μm) is used as aggregate and coarse aggregate is eliminated. Quartz powder (10 μm) is used as micro-filler. Water to binder ratio is kept very low and a high amount of superplasticizer is used to achieve the desirable flow properties [1, 6]. Introduction of fly ash (FA), Ground granulated blast furnace slag (GGBFS) , natural pozzolana (NP), limestone powder (LSP), cement kiln dust (CKD), pulverized steel slag (PSS), etc. as an alternative to silica fume in UHPC are also reported in the literature [5, 10, 11]. Addition of high volume binary (SF–FA or SF–GGBFS) and ternary (SF–FA–GGBFS) mineral admixtures in production of UHPC exhibited their effectiveness towards satisfactory mechanical performance. Cement and silica fume

content can be reduced by the addition of mentioned admixtures (FA, GGBFS, NP, FA, LSP, CKD, and PSS). Furthermore, the reduction in silica fume content reduced the dosage of superplasticizer significantly. Therefore, these substitutes are not only bifocal in reducing the heat of hydration and shrinkage but proved to be environment friendly as well [10]. The narrated optimum level of replacing SF by NP and FA is generally 60%, whereas 20% in case of LSP, CKD, and PSS. Dune sand also can be replaced by CKD, LSP and PSS by 5%, 10% and 20%, respectively [5].

2.1.2 Mixture Optimization

In literature, different techniques are reported to optimize the UHPC mixtures. An approach based on solid suspension model is available for optimizing the UHPC mixtures [12]. In this packing model approach, the fine sand is used as aggregate and a moderate viscosity is selected first, then to confine the paste by keeping the reasonable volume of aggregate, a very low final matrix porosity is taken. Later step determines the silica/cement ratio. In second step if aggregate volume is increased, it results into the increased matrix porosity to maintain the viscosity. In this scenario, maximum paste thickness becomes infinite which is then minimized by using the optimal size of the aggregate to get maximum density matrix with reasonable flow properties. To minimize the wall effect, the size of the sand particles should be larger than the maximum size of the cement particles.

Another method, which is reported in literature to optimize the high-performance concrete mixtures, uses the rheological and strength models. First, according to the strength model of modified mortars, the optimal silica fume (SF) content and superplasticizer (SP) dosage are selected. SF content is kept within 10–15% and SP dosage is set to 10% of SF for optimal performance. Second, the optimum amount of aggregates is specified to fit a

particular grading curve. Then using the strength model water to binder ratio is selected [13].

Basic approach is to minimize the amount of mixing water, using adequate amount of superplasticizers, well-graded particles and packing the particles to improve fluidity and packing density with minimized water additions and to maximize the load-carrying capacity of the mixture [14, 15].

The parameters considered in the mix design of UHPC are mainly, water to binder ratio, cement content, micro silica to cement ratio, total cementitious material content, total fine aggregate content, fiber content and water to binder ratio. The ranges for these parameters as reported in literature are as follows [5, 7, 16].

Water to total binder ratio: 0.145-0.24

Cement content: 710-1100 kg/m^3

Silica fume content: 150-300 kg/m^3

Silica fume to cement ratio: 0.15-0.35

Cement and silica fume content: 940-1400 kg/m^3

Quartz sand: 1000-1400 kg/m^3

Fiber Content: 156-250 kg/m^3

Fiber to total binder ratio: 0.14-0.30

2.1.3 Properties of UHPC

From the literature survey, the ranges of various properties of UHPC are summarized below [5, 7, 17, 18]:

Compressive Strength at 28 days: 130-800 MPa

Modulus of Elasticity: 40-74 GPa

Static Poisson's ratio: 0.19-0.28

Dynamic Poisson's ratio: 0.22-0.24

Linear elastic limit in % of ultimate strength: 60

Flexural Tensile Strength: 15-150 MPa

Direct Tensile Strength: 6-8 MPa

Fracture Energy: 1-47.3 kJ/m^2

Drying Shrinkage at 90 days: 700×10^{-6} - 900×10^{-6} mm/mm

Ultimate tensile strain (10^{-6}): 2000-8000

Abrasion Coefficient: 1.3

Resistivity: 1.13×10^3 KΩ.cm

D_{eff}: 0.02×10^{-12} m^2/s

Air Permeability: 2.5×10^{-18} m^2

I_{corr}: 0.01 $\mu A/cm^2$

2.2 Performance of UHPC Subjected to Elevated Temperatures

2.2.1 Effect of Elevated Temperature on the Microstructure and Mechanical Properties of UHPC

Cheyrezy et al. [19] conducted research on microstructural analysis of RPC considering the effect of high temperature on microstructure of RPC. They reported that at 300^{o}C only around 10% free water remained inside concrete and when temperature was increased to 400^{o}C, no free water remained inside concrete. A large amount of water was found to be lost at temperature ranging between 230^{o}C and 250^{o}C, which attributed to the possible production of another crystal hydrate, called xonotlite (C_6S_6H). The formation of the crystal hydrate in the temperature range of 230^{o}C and 250^{o}C resulted in the dense microstructure of the RPC reducing the porosity. The pozzolanic activity was also mobilized by increase in the temperature. While around 72% of the pozzolanic reaction was completed at room temperature, the exposure to a temperature of 250^{o}C resulted into completion of the pozzolanic reaction by more than 95%. The finding of this study indicate that the pozzolanic reaction as well as evolvement of dense microstructure are supported at higher temperature.

Zanni et al. [20] investigated the hydration and pozzolanic reactions in RPC at elevated temperatures. They reported that the hydrates formation ratio was 10% and pozzolanic activity of silica fume was 5% after 3 days of heat curing at 20^{o}C. A very small increase in the hydrates formation and pozzolanic activity was noted even after 28 days of heat curing at 20^{o}C (hydrates formation ratio raised from 10% to 15% and pozzolanic activity of silica fume raised from 5% to 10%). However, when the RPC was subjected to an elevated temperature of 250^{o}C, the value of hydrates formation ratio reached to 55% and pozzolanic activity of silica fume reached to 75% in an exposure period of only 8 hours. The increased

formation of hydrates and pozzolanic activity resulted into formation of long hexamer or heptamer crystals and xonotlite, which reduce the porosity of the RPC.

Zheng et al. [21] observed an increase in the compressive strength of RPC exposed up to temperature less than 400 °C as compared to the RPC at room temperature. They attributed this finding to the fact that the hydration of cement and pozzolanic reaction promote each at the temperatures below 400 °C. However, at temperature in the range of 400 to 800 °C, they found the compressive strength decreasing gradually. The decrease in compressive strength at temperature more than 400 °C is due to expansion in RPC because of shift of C-S-H gel from continuous block form to the dispersed form causing cracks at the fiber-mortar interface.

The stress-strain behavior of RPC subjected to elevated temperature in the range of 200 to 800 °C, investigated by Tai et al. [22], indicated that there was an increase in compressive strength with an increase in temperature within the range of 200 to 300 °C. For temperature beyond 300 °C the compressive strength was found decreasing. The peak strain increased up to temperature of 500 °C and thereafter it decreased. However, the modulus of elasticity continuously decreased with an increase in temperature.

Liu et al. [23] observed significant loss of the strength of RPC subjected to a high temperature only when temperature exceeded beyond 300°C. Further, they noted a 45% loss of compressive strength of RPC samples subjected to a constant furnace temperature of 500 ± 50°C for 120 min.

2.2.2 Effect of Elevated Temperature on Explosive Spalling of UHPC

Explosive spalling of concrete is a major problem encountered when a high strength concrete is exposed to high temperatures. It is characterized by the violent damage of concrete from the surface when exposed to high temperature raised at a faster rate [24]. Although the mechanism of explosive spalling of high strength concrete is not well-established, there are various hypotheses used to describe the reason of the explosive spalling. Kodur [24] and Bazant et al. [25] explained the mechanism of explosive spalling under elevated temperature using a hypothesis according to which the spalling occurs due to the buildup of very high pore pressures within the high strength concrete as a result of the liquid-vapor transition of the capillary pore water as well as that bound in the cement paste component of the concrete (so-called moisture clog spalling). The generation of pore pressure in high strength concrete is due to the fact that it possesses dense microstructure and segmented capillary pores. The dense microstructure and segmented capillary pores significantly prevent water vapor from free transport and escape in the matrix thereby building up the pore pressure when exposed to elevated temperatures. The generated pore pressure exerts tensile stress in the matrix, which accumulates. The explosive spalling takes place when the accumulated tensile stress in concrete exceeds the tensile strength of concrete [26]. According to a second hypothesis the explosive spalling is due to the buildup of strain energy within the concrete caused by the thermal incompatibility between the cement paste and the aggregates [24, 25].

The denser microstructures of UHPC due to use of increased cement and silica fume contents results into building up of internal water vapor pressure when UHPC is subjected to elevated temperatures. The increased water vapor pressure built-up in the microstructure of UHPC causes its explosive spalling. The risk of explosive spalling of UHPC increases

with the decrease in porosity of UHPC due to increase in cement content and silica fume/cement ratio [27]. This is due to interaction between the increase of the water vapor by the dehydration of several hydrates, including $Ca(OH)_2$, and the escalation of vapor pressure due to dense microstructure of (UHPC). With the increase of cement and silica fume, the pore-volume proportion of 0.1 to 100 mm decreases which causes explosive spalling when this proportion decreases to less than 50.5% of the total pore volume. More will be the spalling with the reduction of capillary porosity.

Explosive spalling was observed in RPC specimens (with compressive strength in the range of 100 to 150 MPa) at high temperatures between 400 and 500°C within the first 10 minutes of heating in fire [27].

2.2.3 Effect of Fibers on Performance of UHPC at Elevated Temperatures

Zheng et al. [28] conducted a study on the effect of elevated temperatures (in the range of 20 to 900°C, elevated at a very slow rate of 4°C/min) on RPC made with different dosages of steel fibers. The compressive strength and modulus of elasticity first increased with increase in temperature then these properties decreased at higher temperatures. They found that at any temperature level, the compressive strengths for RPC mixtures with 2 and 3% of steel fibers (by volume of RPC) were same but higher than the compressive strength of RPC mixture with 1% steel fiber (by volume of RPC), indicating that there was no beneficial effect of the fiber content beyond a dosage of 2%.

Zheng et al. [29] have reported a minimum dosage of steel fibers to be 2% (by volume of concrete) to prevent explosive spalling of RPC subjected to high temperatures. Zheng et al. [28] have observed the beneficial effect of increasing the dosage of steel fiber content of RPC on its tensile properties under exposure to the elevated temperatures. Zheng et al.

[30] studied tensile properties of steel fiber reinforced RPC having GGBS along with silica fume. They reported the increase of tensile properties until 200^{o}C then the reduction in the tensile properties beyond 200^{o}C.

The main concern for making UHPC fire-resistant is to enhance its resistance against explosive spalling by reinforcing the UHPC with a suitable type and dosage of fibers, particularly when temperature is elevated at a faster rate [31]. Canbaz [32] found that the addition of 2% steel fibers prevent the RPC from explosive spalling when temperature is elevated at a slow rate, for example @ 10^{o}C/min. However, the steel fibers fail to cease the explosive spalling when temperature is raised at a faster rate, for example @ 30^{o}C/min [27]. The use of polypropylene fibers along with steel fibers is found to be effective to prevent the explosive spalling of UHPC when subjected to elevated temperatures at slower as well as faster rates [24, 27].

Canbaz [32] investigated the performance of RPC (containing steel as well as polypropylene fibers) at elevated temperatures by keeping the heating rate as 10^{o}C/min. The strength increased by maximum of 100% at a maximum temperature of 400^{o}C after that compressive strength decreased. Although, addition of polypropylene fibers has reduced the strength by maximum of 35% due to reduction in flow and formation of the weakest part to concrete mass, but this addition showed positive effect at elevated temperature. The compressive strength of RPC with polypropylene fiber reduced by 50% at 900^{o}C. RPC with 1% polypropylene fiber was recommended as compared to that without fibers subjected to similar exposure. The increase in strength is due to hydration of un-hydrated constituents of concrete with the vapors. Cracks were terminated and their energy dissipated by the channels generated due to melting of fibers. Compressive strengths higher

than 200 MPa were achieved after water curing at 90^{o}C for three days and after applying a pre-setting pressure of 80 MPa to the RPC.

So et al. [27] also used steel as well as polypropylene fibers in RPC. They kept the steel fiber content constant and varied the polypropylene fiber content from 0 to 8 kg/m^3. The beneficial effect of using hybrid fiber system in preventing explosive failure was observed at elevated temperatures attained at faster rate of about 30^{o}C/min. They found that the explosive spalling is not prevented up to a polypropylene fiber content of 1 kg/m^3. The explosive spalling was partially prevented at a polypropylene fiber content of 2 kg/m^3 and fully prevented when the polypropylene fiber content was 4 kg/m^3 and above.

In another study, Zheng et al. [21] evaluated the performance of UHPC made with hybrid fibers (steel and polypropylene fibers) keeping steel fiber content constant and with different dosages of polypropylene fibers, subjected to elevated temperatures in the range of 20 to 900°C, elevated at a very slow rate of 4^{o}C/min. It was observed that the minimum dosage of polypropylene fibers should be 0.3% (by volume of UHPC) for preventing the explosive spalling. Like the case of RPC mixtures with steel fibers, the UHPC mixtures with polypropylene fibers also showed initially enhancement in the mechanical properties and then degradation with increase in the temperature. Zheng et al. [21] reported that the minimum dosages of steel and polypropylene fibers for preventing explosive spalling of RPC subjected to elevated temperatures should be 2% and 0.3% (by volume of concrete), respectively.

2.3 Performance of UHPC Subjected to Heat-Cool and Wet-Dry Cycles

Ahmad, et al [33] exposed the UHPC specimens made with 6.2% steel fibers to wetting-drying and heating-cooling cycles for 6 months (45 cycles) and found that these cyclic exposures for a short period of 6 months do not produce any adverse effect on the performance of UHPC. It was observed that the wet–dry cycles had no effect on the compressive strength and modulus of elasticity of UHPC. Furthermore, instead of negative impact, the heating–cooling cycles revamped these properties.

Hakeem et al. [34] have observed an enhancement of the fracture properties of UHPC with 6.2% fiber content after a six months exposure to the cycles heating and cooling (total about 45 cycles). Azad et al. [35] have reported that instead of degradation of the tensile properties, there was no effect of wet-dry cycles and there was increase in tensile properties after a six months exposure to the cycles heating and cooling (total about 45 cycles). This increase in properties of UHPC instead of decrease is due to a short exposure of 45 cycles only. During this short exposure, enhancement of the properties of UHPC is attributed to more complete hydration of the binders. Therefore, the performance of UHPC should be studied with a large number of heat-cool and wet-dry cycles or by providing more adverse exposures.

Wang et al. [36] have reported their study on the performance UHPC having 1 and 1.5% fiber contents and subjected to sulphate dry-wet cycles. They found that initially the compressive strength increases but after 50 cycles of wetting and drying there was decrease in the compressive strength. In the course of 60 cycles, the flexural strength was found first to decrease then increase and then decrease.

CHAPTER 3

RESEARCH METHODOLOGY

3.1 General

The focus of the present research was on evaluation of the performance of already developed UHPC mixtures exposed to elevated temperatures and alternate wet-dry and heat-cool cycles. Three UHPC mixtures developed through previous research work conducted at KFUPM [5] were suitably selected and different types of specimens were cast, cured, and exposed to elevated temperature and cyclic exposures before conducting various tests required to evaluate their performance in terms of mechanical performance and durability characteristics. In this chapter, materials utilized, preparation of specimens, curing, exposure conditions and experimental program are discussed in details.

3.2 Materials

3.2.1 Cementitious Materials

In all the UHPC mixtures, ASTM C 150 Type I cement having a specific gravity of 3.15 was used. Out of three selected mixtures of UHPC, only silica fume was used as mineral filler in the first mixture. The blend of silica fume and natural pozzolana was used as mineral filler in the second mixture, while in the third mixture a blend of silica fume and limestone powder was used as mineral filler. Silica fume with market name as Elkem micro silica, a byproduct of silicon and ferrosilicon alloys produced from the carbo-thermic reduction of quartz and quartzite in electric furnace with a specific gravity of 2.25 was

used. Natural pozzolana obtained from the western province of Saudi Arabia with a specific gravity of 3.00 was used. Limestone powder brought from Abu Hadriyah, Saudi Arabia, and having a specific gravity of 2.25 was used. While silica fume used in this study were imported, both natural pozzolana and limestone powder were acquired from the local sources.

The properties of cement and other cementitious materials are tabulated in the Table 3.1 and Table 3.2 respectively.

Table 3.1: Chemical composition of cement and silica fume

Constituent	% by mass	
	Type I Cement	Silica fume
CaO	64.35	0.48
SiO_2	22.0	92.5
Al_2O_3	5.64	0.72
K_2O	3.80	0.84
MgO	2.11	1.78
Na_2O	0.19	0.5
Equivalent alkalis ($Na_2O + 0.658K_2O$)	0.33	-
Loss on Ignition	0.7	1.55
C_3S	55	-
C_2S	19	-
C_3A	10	-
C_4AF	7	-

Table 3.2: Chemical composition of replacement materials

Replacement Materials	Constituents (% by mass)	
	CaO	SiO_2
Natural Pozzolana (NP)	8.06	42.13
Lime Stone Powder (LSP)	45.70	11.79

3.2.2 Aggregate

Locally available dune sand (characterized as fine quartz sand), with a specific gravity of 2.56 and 0.4 % water absorption, was used as fine aggregate. The grading of the dune sand used is presented in the Table 3.3:

Table 3.3: Sieve analysis of dune sand

ASTM sieve Number	Size (mm)	Percentage passing (%)
4	4.75	100
8	2.36	100
16	1.18	100
30	0.6	75
50	0.3	10
100	0.15	5

3.2.3 Superplasticizer

A polycarboxylic-based hyper-plasticizer, named as Glenium 51 in compliance with ASTM C495 Type A and F, was used for obtaining the required flow of the mixtures. Glenium 51 superplasticizer is available in the form of brownish liquid having specific gravity minutely higher than that of water. It is an imported brand however it available with the local suppliers. Properties of Glenium 51, as specified by the manufacturer, are shown in the Table 3.4:

Table 3.4: Properties of Glenium 51

Property	Description
Specific gravity	1.08 ± 0.02 g/cm^3
pH at 20^{o}C	7.0 ± 1.0
Alkali content, %	≤ 5.0
Chloride Content, %	0.6

3.2.4 Fibers

Two types of fibers were used; steel fibers and polypropylene fibers. Short copper-coated plain steel fibers were used in both types of specimens; the specimens subjected to elevated temperatures and those subjected to cyclic exposures. Whereas, wavy polypropylene fibers were only used in the specimens subjected to elevated temperatures. Steel fibers are shown in Figure 3.1 and polypropylene fibers are shown in Figure 3.2.

The properties of steel fibers and polypropylene fibers available from the manufacturers are shown in the Table 3.5 and Table 3.6, respectively.

Figure 3.1: Steel fibers

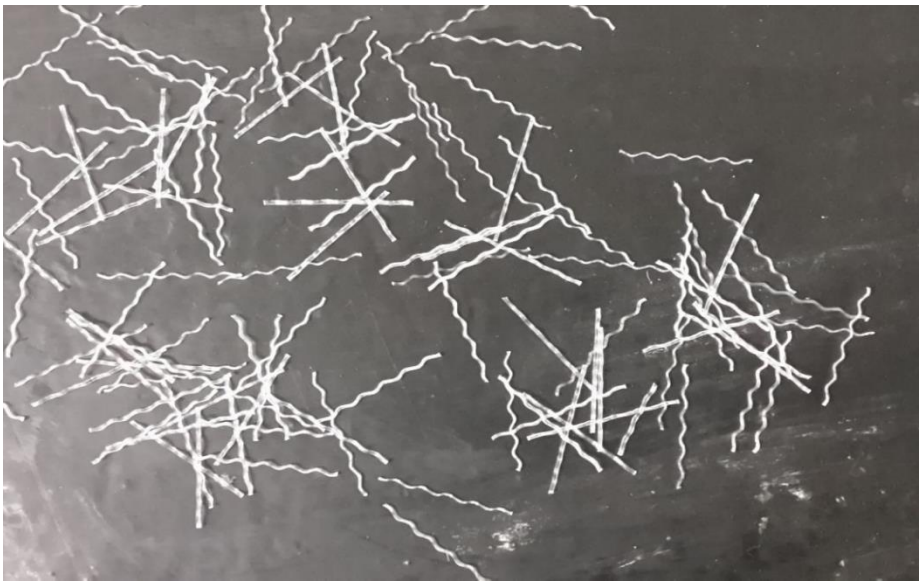

Figure 3.2: Polypropylene fibers

Table 3.5: Properties of steel fibers

Property	Description
Tensile Strength	2500 MPa
Length	12.7 mm
Diameter	0.15 mm
Aspect ratio	65

Table 3.6: Properties of polypropylene fibers

Property	Description
Tensile Strength	450 MPa
Length	20 mm
Width	1 mm
Thickness	0.8 mm
Specific Weight	910 kg/m^3
Modulus of Elasticity	3.5 kN/mm^2

3.3 Details of Selected UHPC Mixtures

For UHPC mixtures subjected to elevated temperatures, the mixture proportions of three already developed UHPC mixtures [5] were used by varying the fiber content. Three different UHPC mixtures × two types of fibers (steel and polypropylene) × four dosages of each type of fibers resulted into 24 mixtures for exposure to the elevated temperature. Another three mixtures of UHPC containing only steel fibers at a constant fiber content were used for the cyclic exposures (heat-cool and wet-dry). In all 27 mixtures a cement content of 900 kg/m^3 and a water to binder ratio of 0.145 (by mass) were kept constant. The UHPC mixtures containing silica fume alone as mineral filler contained 220 kg/m^3 of silica fume. The UHPC mixtures made with the blend of silica fume and natural pozzolana as mineral filler contained 132 kg/m^3 of silica fume and 88 kg/m^3 of natural pozzolana. The UHPC mixtures made with the blend of silica fume and limestone powder as mineral filler contained 176 kg/m^3 of silica fume and 44 kg/m^3 of limestone powder.

The details and IDs of all 27 mixtures are shown in Table 3.7.

Table 3.7: Description of 27 Mixtures of UHPC

Mixture ID	Description
12 UHPC mixtures containing steel fibers for exposure to elevated temperature	
MS02	UHPC mixtures containing *silica fume alone* as mineral filler and 2, 4, 6 and 8% of steel fibers (by mass), respectively.
MS04	
MS06	
MS08	
MSN2	UHPC mixtures containing *silica fume and natural pozzolana* as mineral filler and 2, 4, 6 and 8% of steel fibers (by mass), respectively.
MSN4	
MSN6	
MSN8	
MSL2	UHPC mixtures containing *silica fume and limestone powder* as mineral filler and 2, 4, 6 and 8% of steel fibers (by mass), respectively.
MSL4	
MSL6	
MSL8	
12 UHPC mixtures containing polypropylene fibers for exposure to elevated temperature	
MP01	UHPC mixtures containing *silica fume alone* as mineral filler and 0.1, 0.2, 0.3 and 0.4% of polypropylene fibers (by mass), respectively.
MP02	
MP03	
MP04	
MPN1	UHPC mixtures containing *silica fume and natural pozzolana* as mineral filler and 0.1, 0.2, 0.3 and 0.4% of polypropylene fibers (by mass), respectively.
MPN2	
MPN3	
MPN4	
MPL1	UHPC mixtures containing *silica fume and limestone powder* as mineral filler and 0.1, 0.2, 0.3 and 0.4% of polypropylene fibers (by mass), respectively.
MPL2	
MPL3	
MPL4	
3 UHPC mixtures containing 6% steel fibers (by mass) for cyclic exposures	
MS06	UHPC mixture containing *silica fume alone* as mineral filler
MSN6	UHPC mixtures containing *silica fume and natural pozzolana* as mineral filler
MSL6	UHPC mixtures containing *silica fume and limestone powder* as mineral filler

The weight of ingredients of first 12 UHPC mixtures containing steel fibers and prepared for exposure to the elevated temperature are given in Table 3.8. The weight of ingredients

of second 12 UHPC mixtures containing polypropylene fibers and prepared for exposure to the elevated temperature are given in Table 3.9. The weight of ingredients of last three UHPC mixtures containing a single optimum dosage of steel fibers (157 kg/m^3) and prepared for cyclic exposures are given in Table 3.10.

Table 3.8: Weight of ingredients for 1 m^3 of UHPC mixtures with steel fibers

Mixture ID	Cement kg	Sand kg	Water kg	MS kg	NP kg	LSP kg	Glenium 51 kg	Steel fiber kg
MS02	900	1040	162	220	0	0	40	50
MS04	900	1024	162	220	0	0	40	100
MS06	900	1005	162	220	0	0	40	157
MS08	900	991	162	220	0	0	40	200
MSN2	900	1064	162	132	88	0	40	50
MSN4	900	1048	162	132	88	0	40	100
MSN6	900	1030	162	132	88	0	40	157
MSN8	900	1016	162	132	88	0	40	200
MSL2	900	1020	162	176	0	44	40	50
MSL4	900	1003	162	176	0	44	40	100
MSL6	900	985	162	176	0	44	40	157
MSL8	900	971	162	176	0	44	40	200

Table 3.9: Weight of ingredients for 1 m^3 of UHPC mixtures with polypropylene (PP) fibers

Mixture ID	Cement kg	Sand kg	Water kg	MS kg	NP kg	LSP kg	Glenium 51, kg	PP fiber, kg
MP01	900	1055	162	220	0	0	40	2.4
MP02	900	1054	162	220	0	0	40	4.8
MP03	900	1053	162	220	0	0	40	7.2
MP04	900	1053	162	220	0	0	40	9.6
MPN1	900	1080	162	132	88	0	40	2.4
MPN2	900	1079	162	132	88	0	40	4.8
MPN3	900	1078	162	132	88	0	40	7.2
MPN4	900	1077	162	132	88	0	40	9.6
MPL1	900	1035	162	176	0	44	40	2.4
MPL2	900	1034	162	176	0	44	40	4.8
MPL3	900	1033	162	176	0	44	40	7.2
MPL4	900	1033	162	176	0	44	40	9.6

Table 3.10: Weight of ingredients for 1 m^3 of UHPC mixtures with steel fibers for cyclic exposures

Mixture ID	Cement kg	Sand kg	Water kg	MS kg	NP kg	LSP kg	Glenium 51 kg	Steel fiber kg
MS06	900	1005	162	220	0	0	40	157
MSN6	900	1030	162	132	88	0	40	157
MSL6	900	985	162	176	0	44	40	157

3.4 Mixing Procedure

Following steps were adopted for the preparation of UHPC mixtures:

- Weigh the water and super-plasticizer in the start and mix them. Leave this mixture for around 15 minutes.
- Start weighing the materials in the order of lighter material first followed by heavier materials. This precaution is taken in order to minimize the loss of material happens due to spilling of material in dry mixing.
- Put these materials one after the other into the mixing drum except fibers.
- Run the mixer for 2-3 minutes for dry mixing.
- Put 50% of water with small discharge so that water can be thoroughly mixed rather than being concentrated at locations and forming lumps.
- Note the time when water is mixed.
- Keep monitoring the mix for observing the signs of cohesiveness.
- After 7-9 minutes of first pouring of water add another 20% of water.
- While pouring the water in cylinder (through which water is poured into the mixing drum), use funnel and place your cylinder in a container so that the spilled water can also be used

- Around 13 minutes after first pour, signs of cohesive mix will be prominent and moisture traces will be visible in mix. Then pour the remaining water and mix for another 2 minutes. The mix will start to flow at this stage
- Dispense the steel fibers in the mixing drum and keep mixing for another 2-5 minutes until all fibers seems to be evenly mixed in the matrix
- The mix is ready to perform the flow test and start putting it in the molds.

Figure 3.3: Planetary mixer (Left), UHPC mixture (Center), Flow table test (Right)

3.5 Casting and Curing of Test Specimens

After completion of mixing and conducting flow test, the specimens were cast by pouring the mixture into the mould within first 30 minutes to avoid excessive loss of moisture. Filling the moulds by scooping and in layers is avoided to prevent creation of weak zones due to desperation of layers while vibrating. So, molds were filled in one layers then vibrated to remove air voids. Specimens were covered by plastic sheets and demolding was done after 24 hours. After removing the specimens from molds, specimens were put inside

the indoor curing tanks to moist-cure them for 28 days at room temperature. Aforementioned procedure was followed for all the specimens; specimens subjected to elevated temperature and specimens subjected to cyclic exposures before exposing them to the exposures. The details of tests and total number of specimens cast are mentioned in the Tables 3.11 through 3.14. The specimens prepared for exposures to elevated temperatures are shown in Figure 3.4 and those prepared for cyclic exposures are shown in Figure 3.5.

Table 3.11: Tests for specimens exposed to elevated temperatures

Property	**Specimen shape and size**	**Test method**
Compressive strength	75 × 150 mm cylinder	ASTM C 39
Modulus of elasticity	75 × 150 mm cylinder	ASTM C 469
Failure pattern for exposure to high temp.	During the test for comp. strength	Visual observation for detecting the failure patterns
Flexural tensile strength (using 3rd point load test)	40 × 40 × 160 mm prism	ASTM C 78
Splitting tensile strength	75 × 150 mm cylinder	ASTM C 496

Table 3.12: Details of specimens prepared for elevated temperatures exposures

Description	**Quantity**
Types of UHPC mixtures	3
Types of fibers (Steel & Polypropylene)	2
Dosage of each type of fibers	4
Types of specimens (cylinders for compressive strength and modulus of elasticity; cylinders for split-tensile strength; prisms for flexural tensile strength)	3
Exposure Durations (60 min, 120 min, 180 min, 240 min, 300 min)	5
Replicates	3
Elevated temperature level	1
Total No. of Samples	3×2×4×3×5×3×1 + 216 control =1296

Figure 3.4: Specimens for exposure to elevated temperatures

Table 3.13: Tests for specimens exposed to cyclic exposures

Property	**Specimen shape and size**	**Test method**
Compressive strength	75 × 150 mm cylinder	ASTM C 39
Modulus of elasticity	75 × 150 mm cylinder	ASTM C 469
Flexural tensile strength (using 3rd point load test)	40 × 40 × 160 mm prisms	ASTM C 78
Splitting tensile strength	75 × 150 mm cylinder	ASTM C 496
Fracture toughness	40 × 40 × 160 mm prisms (notched)	------
Water permeability	150 mm cube	DIN 1048
Chloride permeability	100 × 200 mm cylinder	ASTM C 1202
Corrosion current density	A centrally embedded rebar in 75 × 150 mm concrete cylinder	Linear polarization resistance method

Table 3.14: Total no. of specimens prepared for cyclic exposures

Description	Quantity
Types of UHPC mixtures	3
Types and dosage of fibers (6% steel fibers)	1
Number of tests	7
Cyclic stages	2
Replicates	3
Types of exposures (wet-dry, hot-cool)	2
Total No. of Samples	3×1×7×2×3×2 + 63 control=315

Figure 3.5: Specimens for exposure to cyclic exposures

3.6 Exposures

3.6.1 Exposures to Elevated Temperatures

After 28 days of moist-curing, the specimens were air dried for 15 days to reduce the moisture content to avoid early explosive spalling due to exposure to elevated temperatures. As the water vapor in pore generates the pressure inside the pore due to heating which causes spalling. For exposures to elevated temperatures, electric furnace having maximum temperature of 1200^{o}C and maximum heating rate of 30^{o}C/min was used, as shown in Figure 3.6. The specimens were placed at farthest possible place from the coil of the furnace to avoid intense local heating on the specimens' surface. A reasonable distance was maintained between the specimens to provide homogeneous heating environment all around the surfaces of the specimens. The specimens were heated at a high heating rate of 30^{o}C/min.

Figure 3.6: Lenton Electric Furnace, outside view (left), inside view (right)

First, maximum safe temperature, which UHPC mixtures could withstand, was measured. For this purpose, representative specimens were placed inside the furnace and the temperature was raised until sounds of explosive spalling of specimens were heard from inside the furnace. Explosive spalling took place when temperature exceeded 350^{o}C. The explosive spalled specimens are shown in Figure 3.7.

Figure 3.7: Spalled specimens undergone the exposure beyond 350^{o}C

Therefore, the temperatures below 350^{o}C were considered be safe against explosive spalling for the UHPC mixtures with strength around 150 MPa with steel fibers, considered in the present study. To eliminate even the margin of doubt and 100% safety against explosive spalling, an elevated constant temperature of 300^{o}C was chosen as safe maximum temperature. Five exposure durations were chosen; 60 min, 120 min, 180 min, 240 min and 300 min. Exposure duration was counted after the furnace reached to 300^{o}C. After completion of the exposure, the specimens were cooled down while keeping the

furnace door closed to avoid huge thermal gradient due to difference in outside and inside temperature of the furnace.

3.6.2 Exposures to Heat-Cool Cycles

After 28 days moist-curing, the specimens were exposed to heat-cool cycles by putting them inside an oven. One cycle of heat-cool consisted of heating the specimens for 5 hours at 70^{o}C and subsequently cooling them down during the next 19 hours. This heat-cool cycle was selected to simulate the daily variation of ambient temperature, prevalent locally during the summers. For this purpose, an automated oven having fan-heating system with timer was used. A sufficient space was maintained in between the specimens to allow the homogeneous flow of hot air movement during heating and easy dissipation of heat during cooling. The specimens were placed at sufficient distance from inlets of hot air to avoid generation of local heating zones on the specimens' surfaces. The setup is shown in the Figure 3.8.

Figure 3.8: Setup for heating-cooling cyclic exposure

The specimens were tested after exposing them to 90 and 180 cycles of heating and cooling.

3.6.3 Exposures to Wet-Dry Cycles

After 28 days of moist-curing, the specimens were exposed to wet-dry cycles. Each wet-dry cycle consisted of submerging the specimens in the water (containing 5% NaCl) for 6 hours and subsequently allowing them to dry for the next 18 hours at room temperature. This exposure of wet-dry cycles was selected to represent the splash zone conditions, in which concrete structures undergo alternate wetting and drying cycles. NaCl was added to produce adverse saline environment that could cause salt weathering due to very tiny pore structure of UHPC. For the wet-dry cycles, a tailor-made automated setup was used which had two water tanks, two electric motors and timers. In lower tank, specimens were placed, whereas, in the upper tank, water was stored during drying cycles. The setup is shown in the Figure 3.9.

Figure 3.9: Setup for wetting-drying cyclic exposure

The specimens were tested after exposing them to 90 and 180 cycles of wetting and drying.

3.7 Test Methods

3.7.1 Compressive Strength and Modulus of Elasticity

For measurement of compressive strength and modulus of elasticity, cylindrical specimens of 75 mm of diameter and 150 mm of height were tested in compression according to ASTM C 39. Sulphur capping is not suitable to use for UHPC due to ultra-high strength of UHPC which results into failure of capping prior to the failure of UHPC specimens. To achieve smoothness of top surface, rough portions of the top surfaces of specimens were cut which resulted into a length to diameter ratio of 1.92. For cutting purpose, high power cutter was used, as shown in Figure 3.10.

Figure 3.10: Smoothening of top surface of the specimens using high power cutter

A digital compression-testing machine having a maximum capacity of 3000 kN was used to record the load-deformation data. For this purpose, a frame of 87 mm gauge length containing two linear variable displacement transducers (LVDTs) was attached to the cylindrical specimen. A load cell of maximum capacity of 1000 kN was used. Load cell and LVDTs were attached to digital data logger to measure deflection corresponding to uniaxial compressive load applied at the interval of 2 kN. The setup used for compression testing is shown in Figure 3.10.

Figure 3.11: Typical compression test setup

Compressive strength was calculated by dividing load at failure to the cross-section area of the specimen.

Modulus of elasticity was calculated using the load-deformation data acquired during compression testing. Modulus of elasticity was calculated by following the formula given below (ASTM C 469):

$$E = \frac{(S_2 - S_1)}{(\epsilon_2 - 0.00005)}$$

Where

E = chord modulus of elasticity, MPa,

S_2 = stress corresponding to 40 % of ultimate load,

S_1 = stress corresponding to a longitudinal strain, ϵ_1, of 50 millionths, MPa, and

ϵ_2= longitudinal strain produced by stress S_2.

3.7.2 Energy Absorption Capacity (Modulus of Toughness)

Toughness in compression was calculated for all control specimens and specimens exposed to elevated temperatures to evaluate the overall effect of elevated temperature durations. Toughness was calculated by taking area under the stress-strain curve (acquired from compression testing) to a specific point such as point corresponding to the peak load [37, 38, 39]. It is also termed as strain-energy density or energy absorption capacity (kJ/m^3). This parameter indicates the total energy required to fracture the specimen in compression. In the present study, the toughness was calculated as the area under stress-strain curve between origin and the peak load point.

3.7.3 Flexural Strength

Modulus of rupture is the most commonly used parameter to represent the flexural strength of normal and high strength concrete as well. Four-point flexural loading was applied on prism specimens of 40×40×160 mm dimensions in accordance with ASTM C 78. For this purpose, INSTRON universal testing machine having a maximum capacity of 600 kN was used. LVDT was placed at mid-span to measure deflection corresponding to each loading interval, as shown in Figure 3.12. Loading rate was kept as 0.5 mm/min. Load-deflection

data was recorded by using digital data logger. Following equation was used to calculate modulus of rupture:

$$R = \frac{PL}{bd^2}$$

where:

R = modulus of rupture, MPa,

P = maximum applied load indicated by the testing machine, N,

L = span length, mm,

b = average width of specimen, mm, at the fracture,

d = average depth of specimen, mm, at the fracture.

Figure 3.12: Typical setup for flexural strength test (Left), Close up view of a prism under flexural load (Right)

3.7.4 Splitting Tensile Strength

Splitting-tensile strength was determined in according to ASTM C 496. For this test, cylindrical specimens of 75 mm diameter and 150 mm height were used. It is an indirect way to get tensile strength of the concrete specimens which is preferred as compared to direct tension test due to easiness and good approximation of tensile strength of concrete. For this test, compression-testing machine having a maximum capacity 3000 kN was used along with splitting tensile test assembly, as shown in Figure 3.13. Peak load at failure was

obtained from machine and the following formula was used to calculate splitting tensile strength:

$$T = \frac{2P}{\pi l d}$$

where:

T = splitting tensile strength, MPa,

P = maximum applied load, N,

l = length, mm, and

d = diameter, mm.

Figure 3.13: Typical test setup for splitting tensile strength

3.7.5 Fracture Toughness

Fracture toughness was calculated in terms of critical stress intensity factor, $K_{ic.}$ For this test, prism specimens of dimensions 40×40×160 mm with 13 mm deep and 4 mm wide notch at mid-span were used. Three-point bending test was performed and crack opening was measured using crack mouth opening device (extensometer). Mid span deflection was recorded using a LVDT and a digital data logger. Loading rate was kept as 0.5 mm/min.

First the specimen was loaded till peak was obtained then unloaded. The loading-unloading cycles were repeated until a significant reduction in residual peak load was observed. K_{ic} was calculated by using the formula given below[40, 41]:

$$K_{ic} = 3(P_c + \frac{0.5W_oS}{L})\frac{S\sqrt{\pi a_c g_1(\frac{a_c}{d})}}{2d^2b}$$

where P_c = peak load, W_o = weight of the specimen, L = length of the specimen, S = span, d = depth, b = width, and $g_1(a_c/d)$ = stress-intensity geometric function for a beam specimen defined as follows:

$$g_1\left(\frac{a_c}{d}\right) = \frac{1.99 - \left(\frac{a_c}{d}\right)\left(1 - \frac{a_c}{d}\right)\left[2.15 - 3.93\left(\frac{a_c}{d}\right) + 2.70\left(\frac{a_c}{d}\right)^2\right]}{\sqrt{\pi}\left[1 + 2\left(\frac{a_c}{d}\right)\right]\left[1 - \left(\frac{a_c}{d}\right)\right]^{\frac{3}{2}}}$$

Where, a_c = critical crack length, which is calculated by equating the concrete's modulus of elasticity from the loading and unloading curves ($E = E_i = E_u$)

$$E_i = \frac{6Sa_o g_2(\alpha_o)}{C_i d^2 b} \qquad and \qquad E_u = \frac{6Sa_c g_2(\alpha_c)}{C_u d^2 b}$$

$$\alpha_0 = \frac{(a_o + HO)}{(d + HO)} \qquad and \qquad \alpha_c = \frac{(a_c + HO)}{(d + HO)}$$

where α_o = initial notch/depth ratio, α_c = critical notch/depth ratio, a_o is the initial notch depth of the beam, HO = thickness of the clip gauge holder, C_i = loading compliance, C_u = unloading compliance, and $g_2(\alpha)$ = opening displacement geometric factor for the three-point bending (TPB) specimen given by:

$$g_2(\alpha) = 0.76 - 2.28\alpha + 3.87\alpha^2 - 2.04\alpha^3 + \frac{0.66}{(1-\alpha^2)}$$

The loading compliance (C_i) is the inverse of the slope of the point from 10% of the peak load to 50% of the peak load. Similarly, C_u is the inverse of slope of the unloading curve between 10% and 80% of the peak load [40], [41].

Figure 3.14: Typical specimen under fracture toughness test

3.7.6 Water Permeability

Water permeability was measured in terms of water penetration depth in accordance to DIN 1048. 100 mm cubes were used for this test. A 5-bar water pressure was applied to one side of the cube for 72 hours. Then the specimens were split into two halves just after the completion of test as shown in Figure 3.15. Maximum penetration was measured from the face facing the water pressure. The quality of concrete was assessed by comparing the water penetration depth with the standard depth values shown in Table 3.15.

Table 3.15: Standard criteria for water permeability

Water penetration depth (mm)	Permeability
< 30	Low
30 to 60	Moderate
> 60	High

Figure 3.15: Water permeability setup (Left), Typical split cube specimen (Right)

3.7.7 Rapid Chloride Ion Permeability

Rapid chloride ion permeability test gives the ability of concrete to resist penetration of chloride ions under the influence of applied current. ASTM C 1202 was followed for this test by using PROOVE IT instrument. 100 mm diameter cylinders were cast and disk specimens of 40 mm thickness were cut out from the center of each specimen. Slices were epoxy-coated at periphery and dried, as shown in Figure 3.16. Then, the slices were saturated with water for 24 hours after removing the air bubbles from water using vacuum pump. Slices were then clamped between two cells, one cell was filled with 0.3 % NaOH and connected to positive terminal and the other cell was filled with 3 % NaCl and

connected to negative terminal or electric connection, as shown in Figure 3.17. The test was run for 6 hours and the amount of charges (in Coulombs) passed through the splice samples was noted.

Figure 3.16: Epoxy coated slice specimen for rapid chloride ion permeability

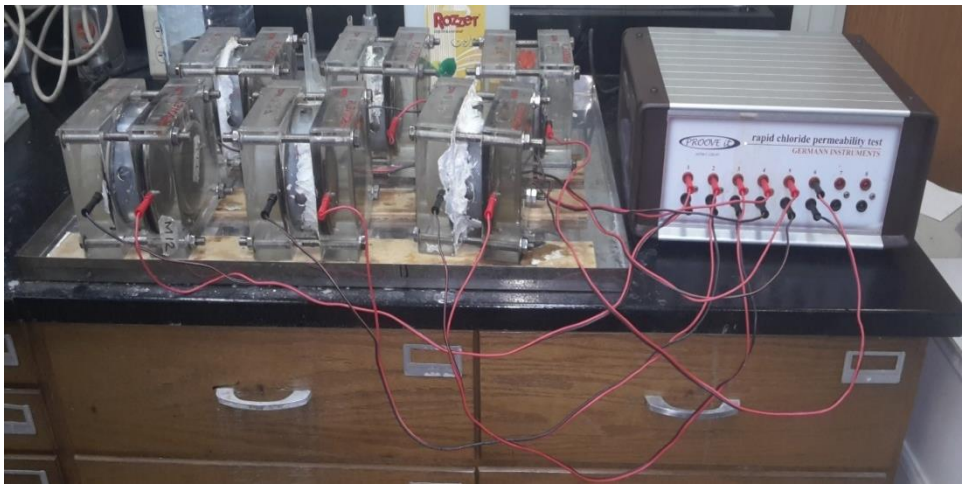

Figure 3.17: Setup for Rapid chloride ion permeability test

3.7.8 Corrosion Current Density

Corrosion current density was measured using the "Linear polarization resistance (LPR) method". UHPC specimens of diameter 75 mm and height 150 mm with centrally embedded 13 mm diameter rebar were used. Specimens were placed into 5 % NaCl solution up to 2/3rd of its height and corrosion current density was measured at regular intervals. In this experiment, Gamry instrument was used, as shown in Figure 3.18. Saturated Calomel electrode was used as reference electrode.

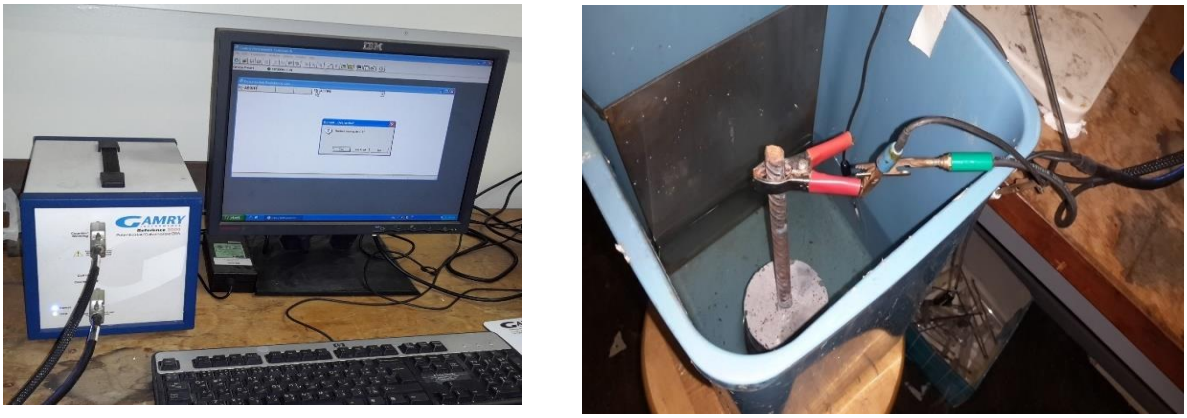

Figure 3.18: Gamry potentiostat for LPR measurement

CHAPTER 4

RESULTS AND DISCUSSIONS

In this chapter, test results obtained for the control specimens, the specimens subjected to elevated temperature, and cyclic exposures are presented. Important observations are noted pertaining to the performance of the selected UHPC mixtures against the aggressive exposure conditions considered in the present study. Discussions are made based on the scientific reasoning and comparison of the findings of the present work with the relevant information available in the literature.

Discussions for the specimens subjected to elevated temperatures were made on the results of compressive strength, modulus of elasticity, flexural strength and splitting-tensile strength tests. Whereas, discussions for the specimens subjected to cyclic exposures were about the results of compressive strength, modulus of elasticity, flexural and splitting tensile strength, fracture toughness, water permeability, chloride permeability and corrosion current density tests.

4.1 UHPC Mixtures with Steel Fibers Subjected to Elevated Temperatures

4.1.1 Compressive Strength

a) Failure modes in compression test

Figure 4.1 shows the failure modes in compression for control specimens, containing 2, 4, 6 and 8% steel fibers. It can be seen from Figure 4.1 that the failure mode is more ductile with more fiber content. All control specimens showed gentle failure and found to be intact

without explosive spalling due to presence of steel fibers and absence of elevated temperature.

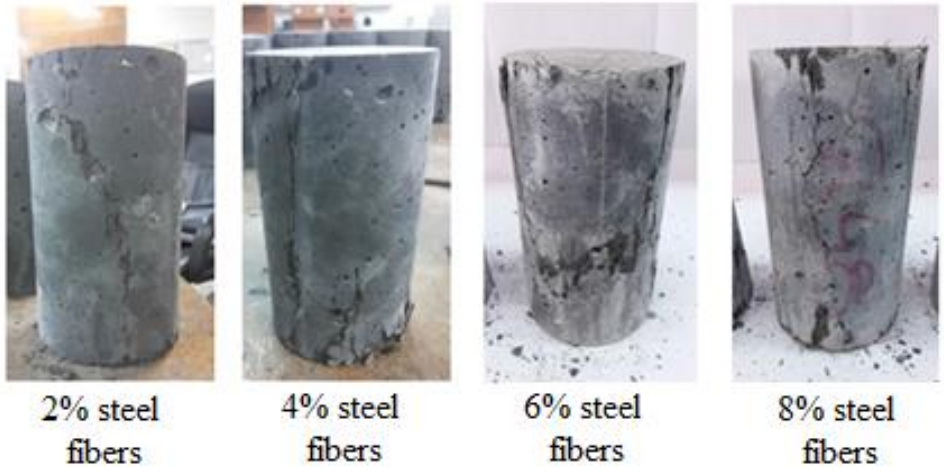

Figure 4.1: Typical failure modes in compression test for control specimens with different steel fiber contents

Figures 4.2 and 4.3 show the failure modes in compression for specimens containing 2, 4, 6 and 8% steel fibers and exposed to the elevated temperature of 300°C for 5-hour duration.

Figure 4.2: Typical failure modes in compression test of UHPC with 2% fibers after 5 hours of exposure to the elevated temperature

Figure 4.3: Typical failure modes in compression test of UHPC with 4, 6 and 8% after 5 hours of exposure to the elevated temperature

As evident from Figures 4.2 and 4.3, explosive failure took place when the UHPC specimens were tested in compression after exposing them to elevated temperature. However, the extent of damage and intensity of sound were more in case of specimens with lesser fiber content. The highest damage with loudest sound took place in case of specimens with lowest fiber content of 2%.

b) Compressive strength test results

Average compressive strength of the control specimens and specimens exposed to elevated temperature of 300ºC for 60 min, 120 min, 180 min, 240 min and 300 min are summarized in the Table 4.1. The ratios of the compressive strength after a particular exposure duration to the compressive strength of control specimens $(f'_c)_T/f'_c$ are summarized in Table 4.2. Based on the data presented in Tables 4.1 and 4.2, discussions were made regarding the effect of fiber content and duration of elevated temperature and the effect of type of UHPC on compressive strength.

Table 4.1: Compressive strength of UHPC mixtures containing steel fibers exposed to elevated temperatures

Mixture ID	Compressive Strength (MPa)					
	Control	60 min	120 min	180 min	240 min	300 min
MS02	142.8	173.6	190.7	191.3	201.3	195.1
MS04	143.1	188.1	196.2	210.8	214.5	202.4
MS06	147.7	191.1	202.8	215.0	215.5	204.5
MS08	157.1	206.2	210.7	215.7	221.8	217.0
MSN2	140.2	179.9	183.0	190.9	186.5	183.5
MSN4	142.2	182.1	188.0	196.4	194.6	192.0
MSN6	145.4	183.5	191.9	198.0	196.7	195.8
MSN8	152.6	187.5	193.6	204.5	200.7	199.6
MSL2	137.6	179.4	186.4	198.0	204.5	202.4
MSL4	140.9	180.7	195.2	200.8	206.7	206.4
MSL6	142.7	183.3	189.1	201.4	217.8	217.7
MSL8	153.2	185.7	197.9	204.6	217.9	215.9

Table 4.2: $(f'_c)_T/f'_c$ of UHPC mixtures containing steel fibers exposed to elevated temperatures

Mixture ID	$(f'_c)_T/f'_c$				
	60 min	120 min	160 min	240 min	300 min
MS02	1.22	1.34	1.34	1.41	1.37
MS04	1.31	1.37	1.47	1.50	1.41
MS06	1.29	1.37	1.46	1.46	1.38
MS08	1.31	1.34	1.37	1.41	1.38
MSN2	1.28	1.31	1.36	1.33	1.31
MSN4	1.28	1.32	1.38	1.37	1.35
MSN6	1.26	1.32	1.36	1.35	1.35
MSN8	1.23	1.27	1.34	1.31	1.31
MSL2	1.30	1.35	1.44	1.49	1.47
MSL4	1.28	1.39	1.43	1.47	1.46
MSL6	1.28	1.32	1.41	1.53	1.53
MSL8	1.21	1.29	1.34	1.42	1.41

i. Effect of fiber content and duration of elevated temperature on compressive strength

The plots of compressive strength versus exposure duration data corresponding to different fiber contents are shown in Figures 4.4 through 4.6 for UHPC mixture with silica fume alone, blend of silica fume and natural pozzolana, and blend of silica fume and limestone powder, respectively.

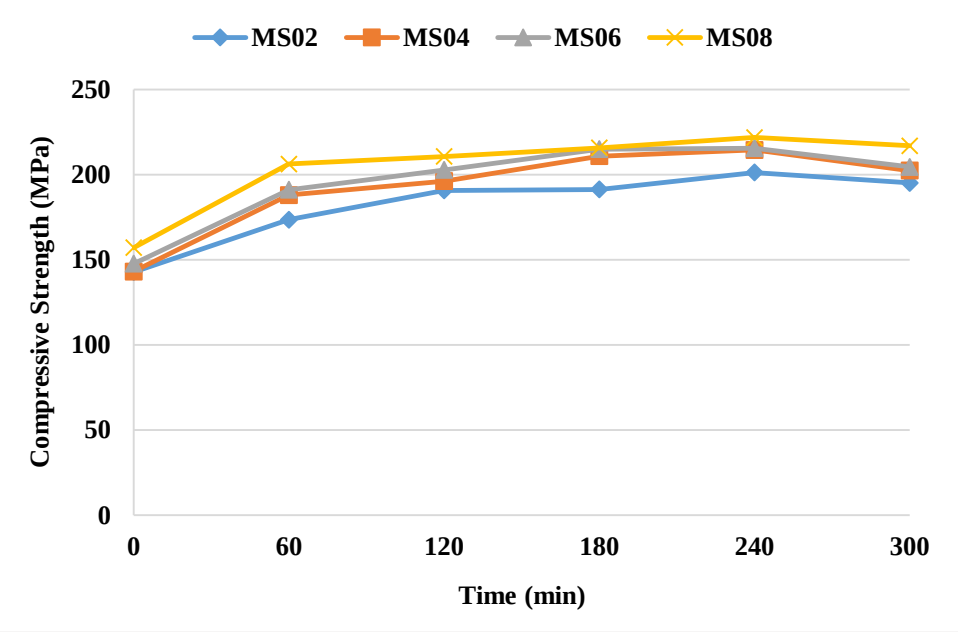

Figure 4.4: Variation of compressive strength with exposure duration for UHPC with silica fume and different steel fiber contents

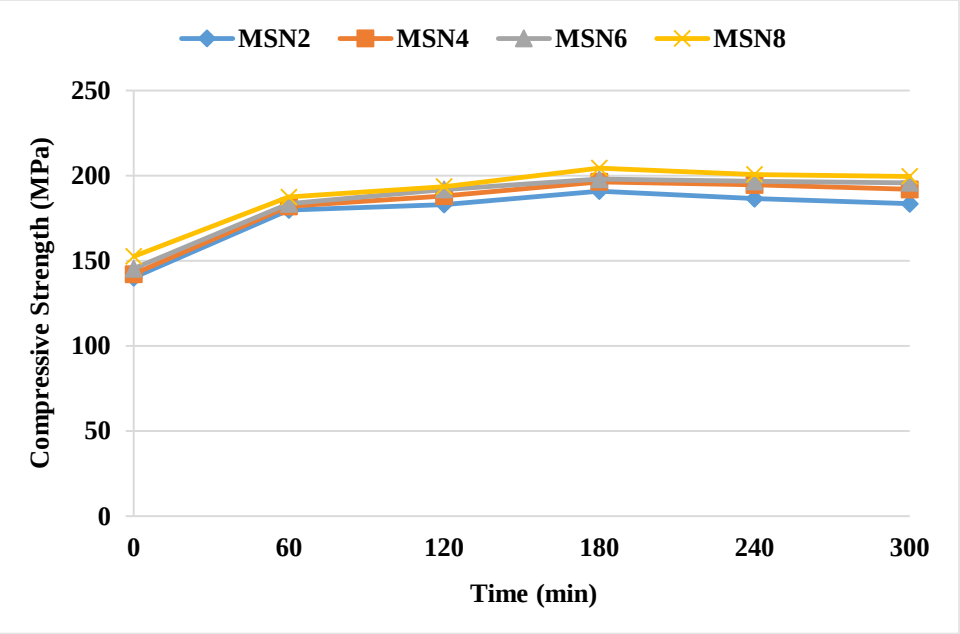

Figure 4.5: Variation of compressive strength with exposure duration for UHPC with blend of silica fume and natural pozzolana and different steel fiber contents

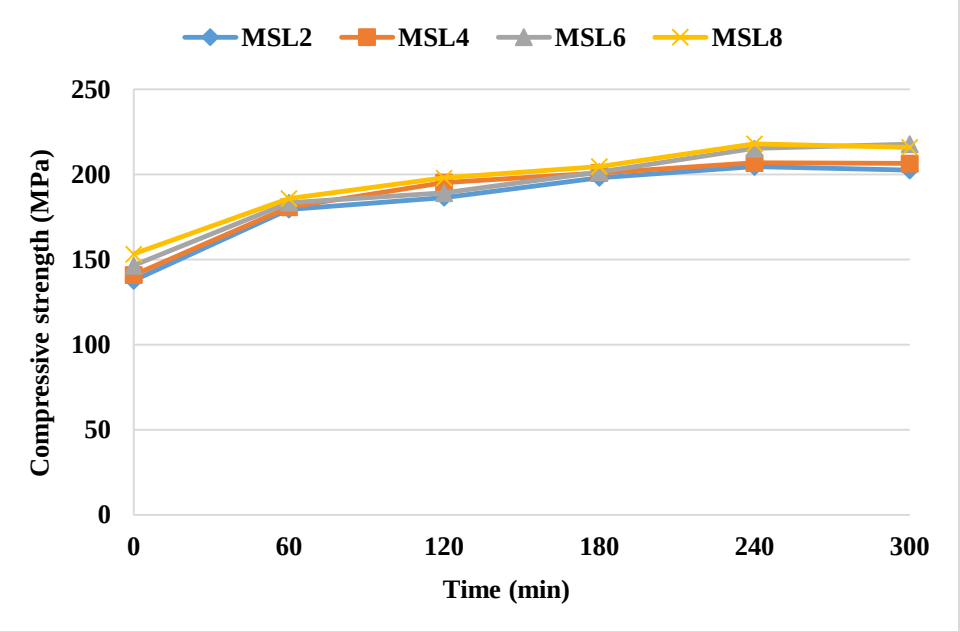

Figure 4.6: Variation of compressive strength with exposure duration for UHPC with blend of silica fume and limestone powder and different steel fiber contents

In case of each type of UHPC mixture, the compressive strength increases with an increase in the exposure duration and fiber content. However, the increasing trend is up to 240

minutes. After 240 minutes of exposure, the strength remained either unchanged or slightly decreased. It can be seen from Figures 4.4 through 4.6 that the increase in strength with exposure duration was more pronounced after 60 minutes of exposure. It is observed from Table 4.2 that an increase of 21 to 31% of strength took place in first 60 minutes of exposure at 300^{o}C. The increase in strength from 60 minutes to 240 minutes was found to be at slow rate. In 180 minutes of exposure (from 61st minute to 240th minute), the strength increased by 10 to 22%. The fiber content has a minor effect on compressive strength. The compressive strength is slightly higher at a higher fiber content.

It can be noted that even the reduced compressive strength after 5 hours of exposure to elevated temperature was lot more than the strength at room temperature. The reason behind strength higher at elevated temperature than the room temperature is attributed to the various beneficial developments leading to the denser microstructure such as enhanced pozzolanic reaction, dry hardening, and "self-steaming" or "internal autoclave" when the water present inside the capillary pores is heated by elevated temperature [19, 21, 22, 28]. As mentioned earlier, at a temperature of 250^{o}C, 95% of pozzolanic reactions is completed contributing to the strength [19]. dry hardening, and "self-steaming result into enhancement of the hydration process and pozzolanic reaction forming more amount of C-S-H gel and reducing the pore sizes [21, 22, 28]. The minor contribution of steel fibers to the strength is because of prevention of the propagation of cracks generated due to elevated temperatures [22].

The analysis of variance (ANOVA) of the compressive strength data presented in Table 4.1 for all three UHPC mixtures are presented in Tables 4.3 through 4.5.

Table 4.3: ANOVA table for compressive strength of steel fiber reinforced UHPC mixture with silica fume only

Source of variation	SS	DOF	MS	F	P	F_{cr}	Significance criteria P< 0.05 and F > F_{cr}
Exposure duration	11562.9	5	2312.6	151.9	2.7×10^{-12}	2.9	**Significant**
Fiber content	1532.6	3	510.9	33.6	6.8×10^{-7}	3.3	**Significant**
Error	228.3	15	15.2				
Total	13323.8	23					

Table 4.4: ANOVA table for compressive strength of steel fiber reinforced UHPC mixture with silica fume and natural pozzolana

Source of variation	SS	DOF	MS	F	P	F_{cr}	Significance criteria P< 0.05 and F > F_{cr}
Exposure duration	7644.1	5	1528.8	507.9	3.6×10^{-16}	2.9	**Significant**
Fiber content	484.9	3	161.6	53.7	2.9×10^{-8}	3.3	**Significant**
Error	45.2	15	3.0				
Total	8174.2	23					

Table 4.5: ANOVA table for compressive strength of steel fiber reinforced UHPC mixture with silica fume and limestone powder

Source of variation	SS	DOF	MS	F	P	F_{cr}	Significance criteria P< 0.05 and F > F_{cr}
Exposure duration	12507.7	5	2501.5	258.5	5.4×10^{-14}	2.9	**Significant**
Fiber content	415.9	3	138.6	14.3	1.1×10^{-4}	3.3	**Significant**
Error	145.2	15	9.7				
Total	13068.8	23					

From the ANOVA results, as presented in Tables 4.3 through 4.5, it can be observed that for all three UHPC mixtures, both exposure duration as well as fiber content have significant effect on compressive strength. However, the exposure duration, having a very high F-value and very low P-value as compared to that for fiber content, have stronger effect on the compressive strength.

Empirical model for compressive strength in terms of exposure duration and fiber content, as obtained through regression analysis, is given as:

$$f_c' = a + b(T) + c(T^2) + d(F) + e(F^2)$$

Where:

f_c' is compressive strength (MPa)

a, *b*, *c*, *d* and *e* are regression coefficients, as given in Table 4.6 for all three UHPC mixtures

T is exposure duration (0, 60, 120, 180, 240, and 360 minutes)

F is fiber content (2, 4, 6, and 8% by mass of mixture)

Table 4.6: Values of regression coefficients for compressive strength of UHPC mixtures with steel fibers

UHPC mixture	***a***	***b***	***c***	***d***	***e***	R^2
Mixture with silica fume only	132.3	0.5813	-0.0014	4.3939	-0.0870	0.95
Mixture with silica fume and natural pozzolana	138.4	0.4733	-0.0011	2.9442	-0.0856	0.97
Mixture with silica fume and limestone powder	139.1	0.4875	-0.0009	1.9055	-0.0044	0.96

A very high value of regression coefficient, R^2, for each of the UHPC mixtures, as shown in Table 4.6, indicate a high degree of fit of the data. These derived models can be used to

predict the compressive strength for a given set of exposure duration and fiber content. Alternatively, these models can be utilized to calculate the exposure duration required to achieve a give strength at a given fiber content.

ii. Effect of type of UHPC mixture on compressive strength

The plots of compressive strength of three UHPC mixtures at different exposure durations are shown in Figures 4.7 through 4.10, for 2, 4, 6, and 8%, respectively. It can be observed from Figures 4.7 through 4.10 that at any exposure duration and fiber content, there is not much difference between the compressive strengths of the three mixtures. Therefore, it can be concluded that the performance of all three UHPC is comparable.

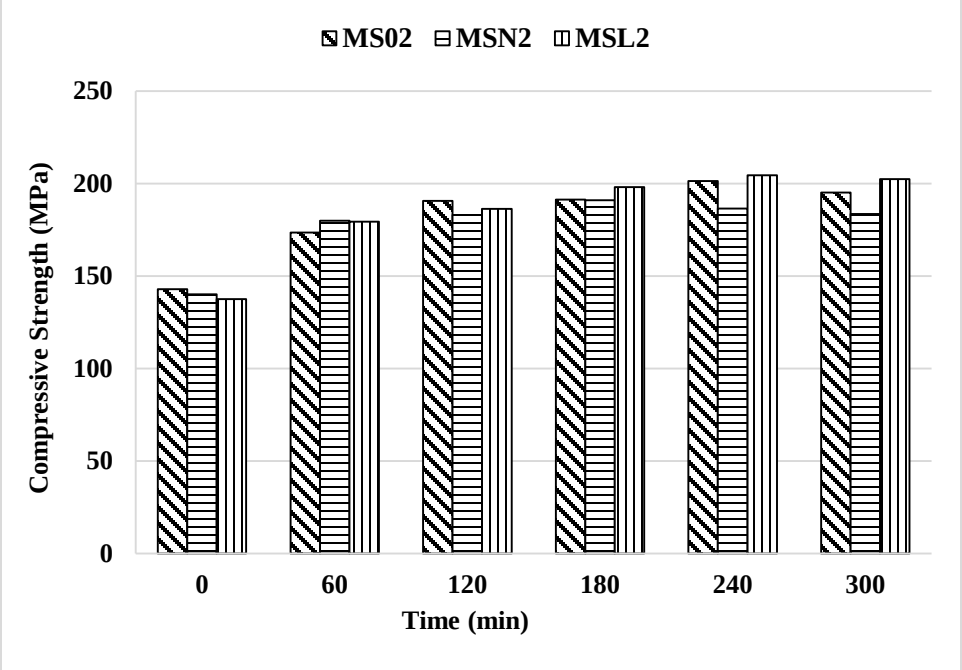

Figure 4.7: Compressive strength vs exposure duration for UHPC mixtures with 2% steel fibers

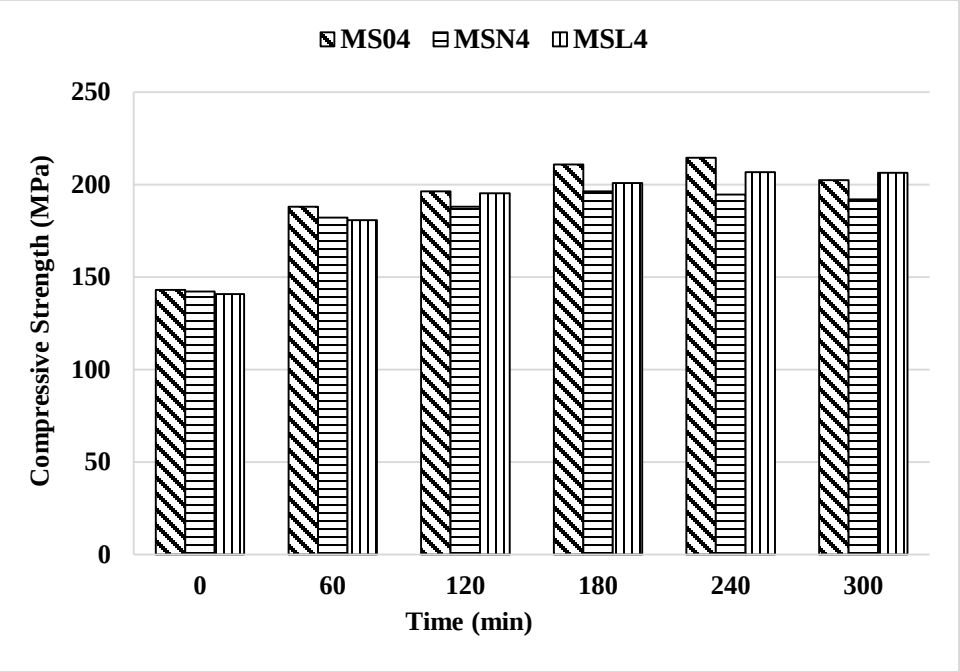

Figure 4.8: Compressive strength vs exposure duration for UHPC mixtures with 4% steel fibers

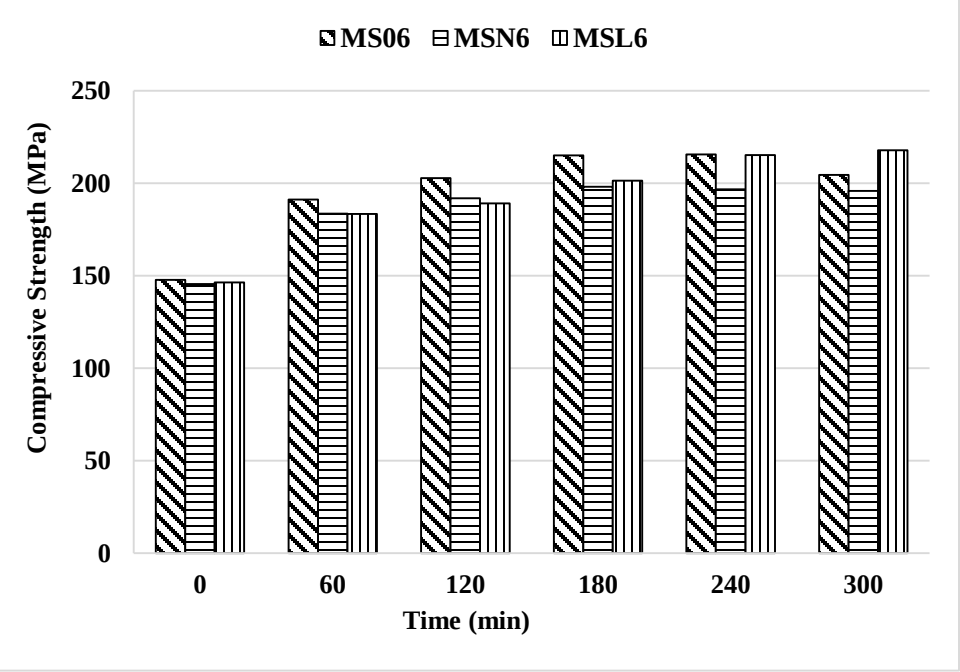

Figure 4.9: Compressive strength vs exposure duration for UHPC mixtures with 6% steel fibers

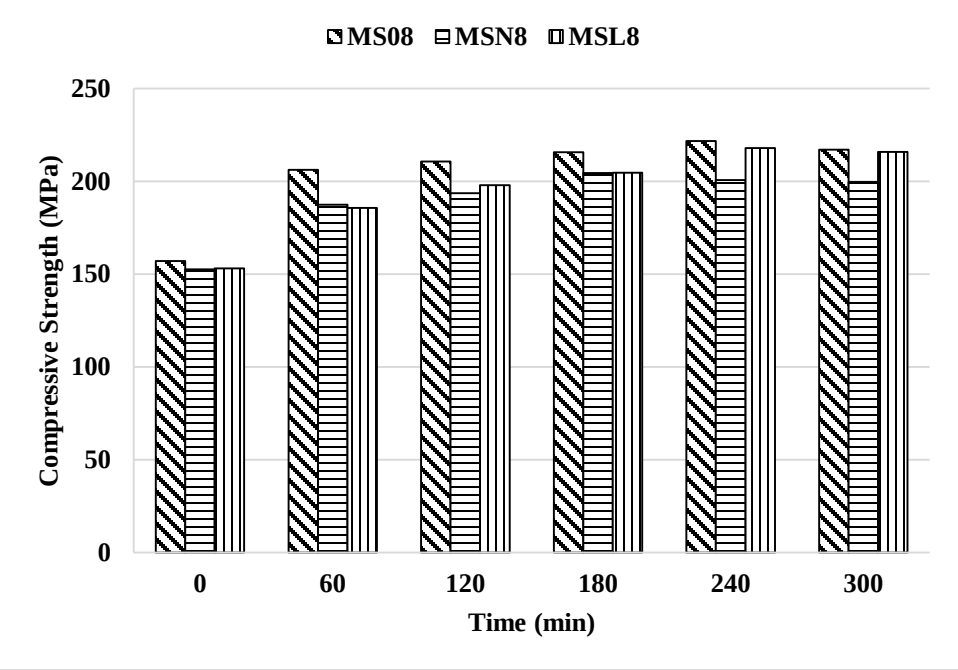

Figure 4.10: Compressive strength vs exposure duration for UHPC mixtures with 8% steel fibers

4.1.2 Modulus of Elasticity

The modulus of elasticity values of the control specimens and specimens subjected to elevated temperature of 300^{o}C for 60 min, 120 min, 180 min, 240 min and 300 min for all three UHPC mixtures were calculated from the respective stress-strain curves. The stress-strain curves up to the failure for MS02 to MS08 are shown typically in Figures 4.11 through 4.14.

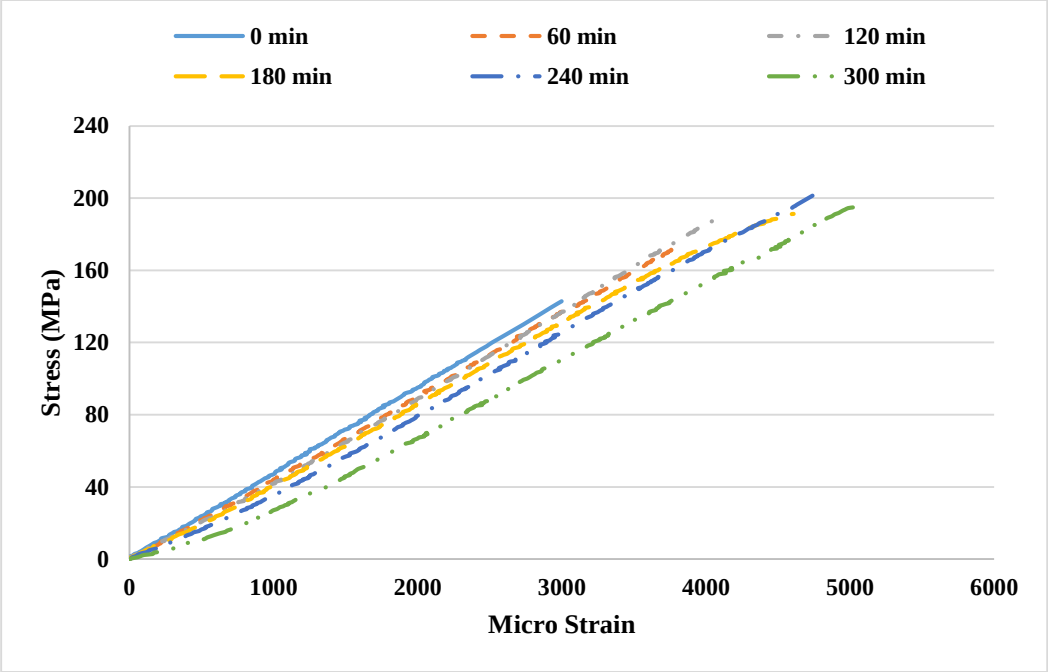

Figure 4.11: Stress-strain curves for MS02 for all exposure durations

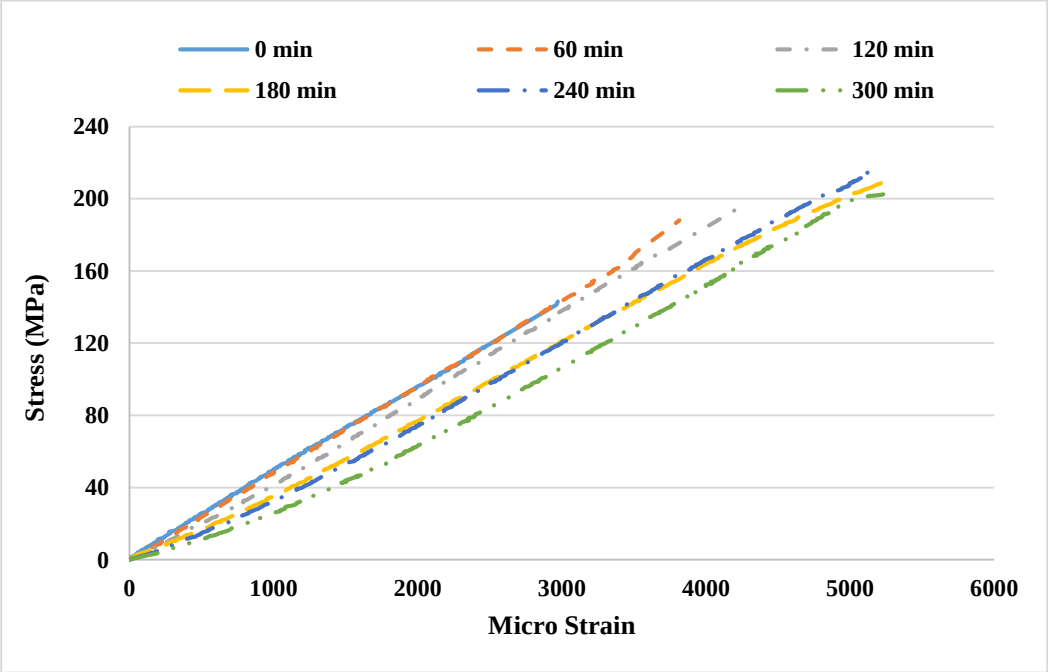

Figure 4.12: Stress-strain curves for MS04 for all exposure durations

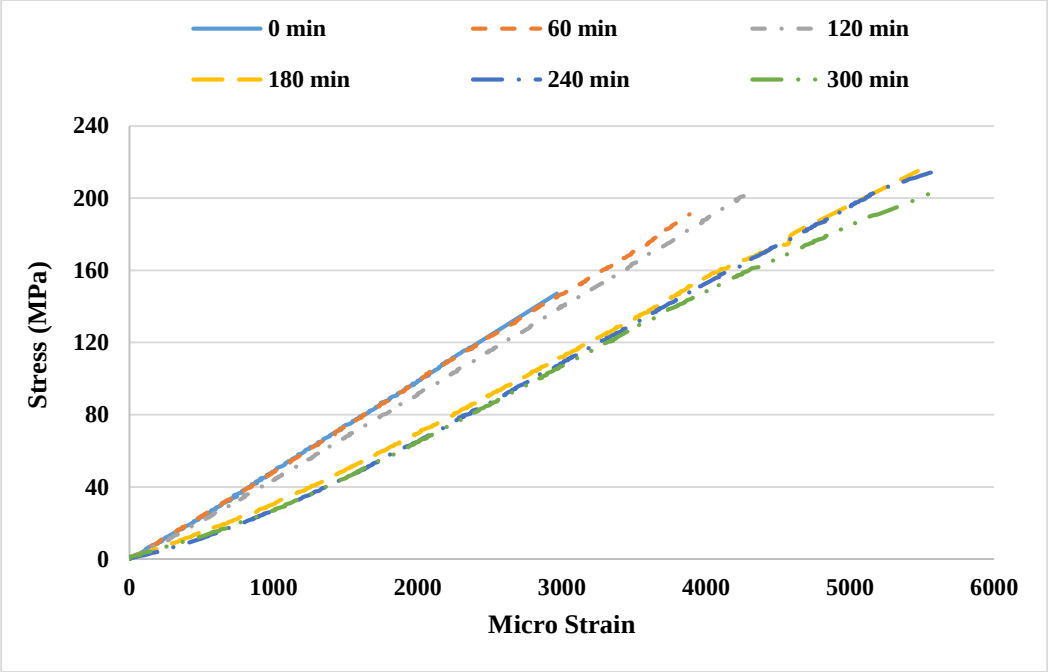

Figure 4.13: Stress-strain curves for MS06 for all exposure durations

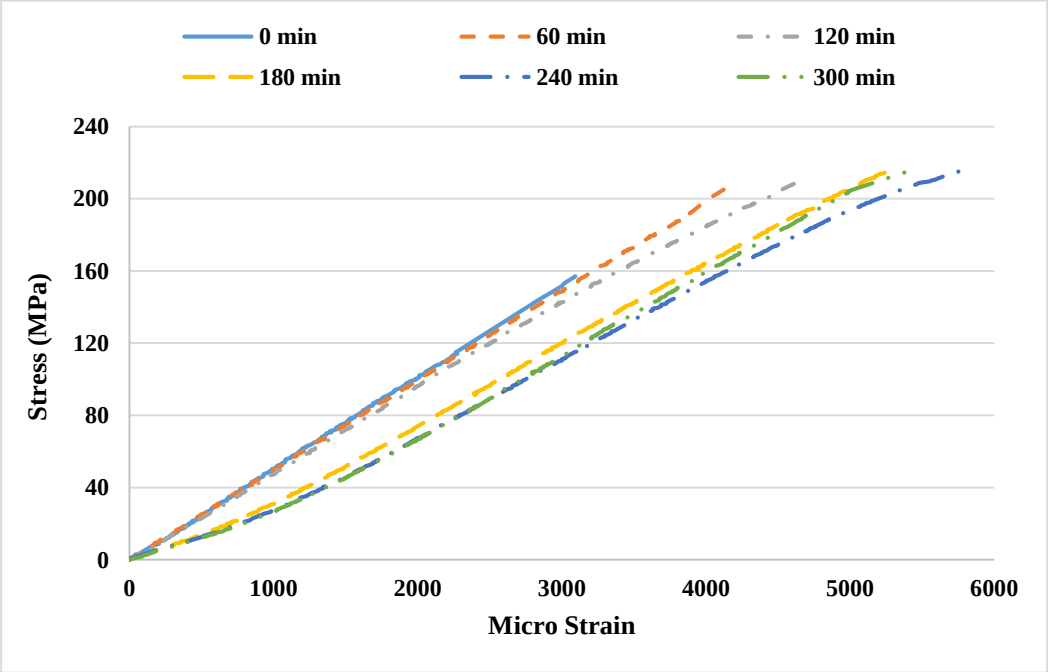

Figure 4.14: Stress-strain curves for MS08 for all exposure durations

It is observed from Figures 4.11 through 4.14 that the stress-strain curves shifted downward with the increase of exposure duration, indicating that more deformation occurs at the same stress level when the exposure duration is increased. Slope of the stress-strain curves also reduced with an increase in the exposure duration. Peak strains also increased with the increase of exposure durations. All of the above mentioned factors caused the reduction in the modulus of elasticity. The shifting effect of stress-strain curves was more prominent for higher fiber content as compared to less fiber content. The behavior was approximately similar for other two UHPC mixtures as well. The reason behind higher strain (at the same stress level) with increase in exposure duration may be attributed to the increase in ductility of steel fibers with increase in exposure duration.

Average modulus of elasticity (MOE) of the control specimens and specimens subjected to elevated temperature of 300^{o}C for 60 min, 120 min, 180 min, 240 min and 300 min are summarized in the Table 4.7. The ratios of the modulus of elasticity after a particular exposure duration to the modulus of elasticity of control specimens (MOE_T/MOE) are summarized in Table 4.8. Based on the data presented in Tables 4.7 and 4.8, discussions were made regarding the effect of fiber content and duration of elevated temperature and the effect of type of UHPC on modulus of elasticity.

Table 4.7: MOE of UHPC mixtures containing steel fibers exposed to elevated temperatures

Mixture ID	MOE (GPa)					
	control	60 min	120 min	180 min	240 min	300 min
MS02	46.73	44.24	43.33	42.27	39.55	34.26
MS04	48.49	48.24	43.44	38.22	37.87	34.02
MS06	48.86	48.55	45.10	34.98	34.76	33.97
MS08	50.43	49.57	47.42	37.88	35.37	34.79
MSN2	47.27	46.93	43.16	38.16	35.35	35.35
MSN4	49.27	46.54	43.30	43.01	36.70	35.70
MSN6	51.21	49.83	45.30	41.65	37.50	36.70
MSN8	51.64	50.21	45.74	41.80	37.80	36.73
MSL2	47.58	46.54	43.86	38.70	37.63	36.37
MSL4	48.20	48.20	43.70	40.11	36.69	34.47
MSL6	51.18	47.64	40.96	37.90	36.80	32.30
MSL8	51.30	50.75	41.98	40.03	36.80	33.70

Table 4.8: MOE_T/MOE of UHPC mixtures containing steel fibers exposed to elevated temperatures

Mixture ID	MOE_T/MOE				
	60 min	120 min	180 min	240 min	300 min
MS02	0.95	0.93	0.90	0.85	0.73
MS04	0.99	0.90	0.79	0.78	0.70
MS06	0.99	0.92	0.72	0.71	0.70
MS08	0.98	0.94	0.75	0.70	0.69
MSN2	0.99	0.91	0.81	0.75	0.75
MSN4	0.94	0.88	0.87	0.74	0.72
MSN6	0.97	0.88	0.81	0.73	0.72
MSN8	0.97	0.89	0.81	0.73	0.71
MSL2	0.98	0.92	0.81	0.79	0.76
MSL4	1.00	0.91	0.83	0.76	0.72
MSL6	0.93	0.80	0.74	0.72	0.63
MSL8	0.99	0.82	0.78	0.72	0.66

i. Effect of fiber content and duration of elevated temperature on MOE

The plots of MOE versus exposure duration data corresponding to different fiber contents are shown in Figures 4.15 through 4.17 for UHPC mixtures with silica fume alone, blend of silica fume and natural pozzolana, and blend of silica fume and limestone powder, respectively.

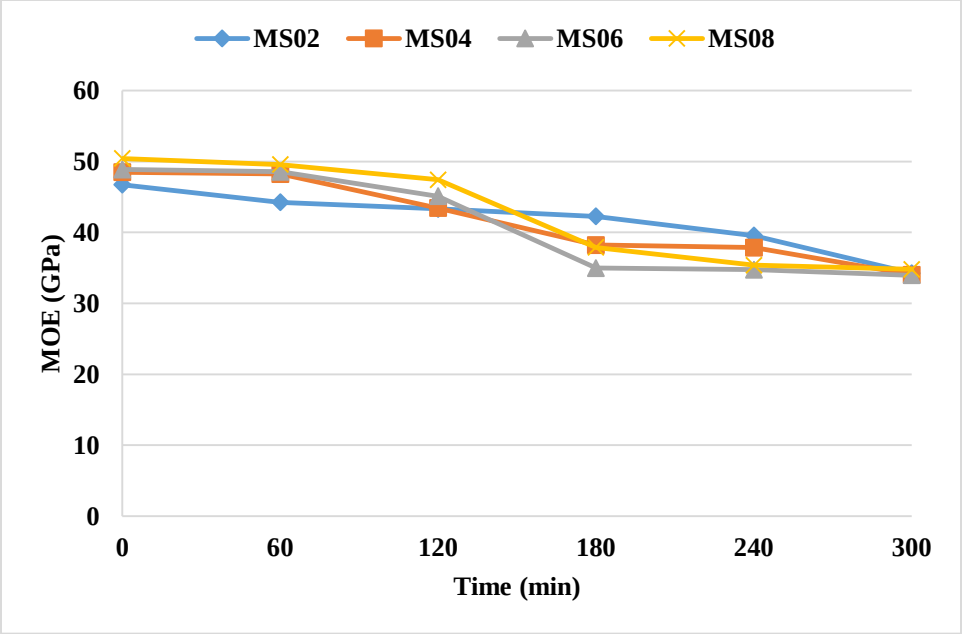

Figure 4.15: Variation of MOE with exposure duration for UHPC with silica fume and different steel fiber contents

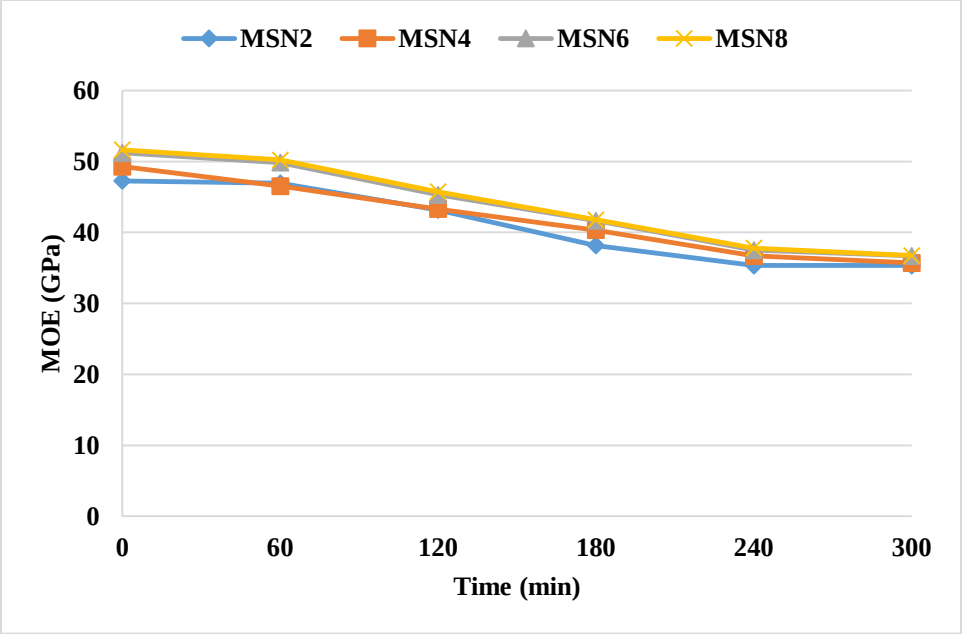

Figure 4.16: Variation of MOE with exposure duration for UHPC with blend of silica fume and natural pozzolana and different steel fiber contents

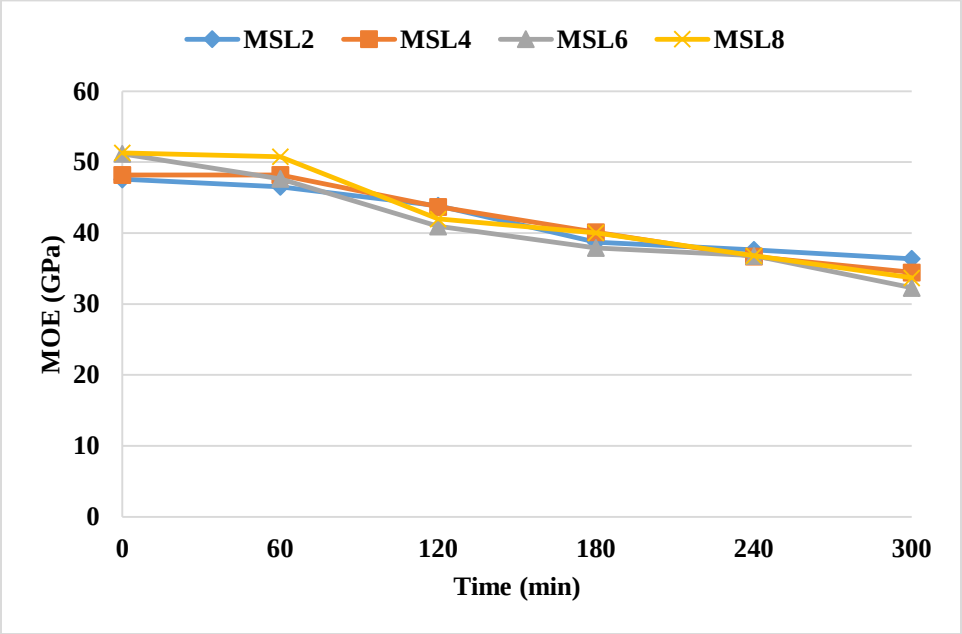

Figure 4.17: Variation of MOE with exposure duration for UHPC with blend of silica fume and limestone powder and different steel fiber contents

It can be observed from Figures 4.15 through 4.17 that in case of each type of UHPC mixture, unlike compressive strength that increased with increase in exposure duration,

MOE decreases with an increase in exposure duration. This observation is in contradiction with the normal correlation between compressive strength and MOE, according to which MOE increases with the increase of strength. The decrease in MOE with increase in exposure duration for concrete subjected to elevated temperatures may be due to the increased ductility of steel fibers at elevated temperature for longer duration. The decrease in MOE up to 60 minutes of exposure is very little, after that, a sharp decrease in MOE is observed with increase in the exposure duration. It is observed from Table 4.4 that a decrease of only 0 to 7% of MOE took place in first 60 minutes of exposure at 300^{o}C. The total decrease in MOE in 300 minutes of exposure is found to be in the range of 24 to 37%. For all fiber content, the trend was similar. Zheng et al. and S. Adyin et al. also reported the increase in strength but decrease in modulus of elasticity after exposing the RPC and HPC to 300^{o}C, respectively [28, 42]. Chang et al. reported the reduction in modulus of elasticity for normal concrete after exposures to 300^{o}C by around 35% [43]. The fiber content has negligible effect on MOE.

The analysis of variance (ANOVA) of the MOE data presented in Table 4.7 for all three UHPC mixtures are presented in Tables 4.9 through 4.11. From the ANOVA results, as presented in Tables 4.9 through 4.11, it can be observed that for all three UHPC mixtures, exposure duration has significant effect on MOE as it is having a very high F-value and very low P-value. The effect of fiber content is clearly insignificant in case two UHPC mixtures. However, some marginal effect of fiber content is observed in one mixture (UHPC mixture with silica fume and natural pozzolana).

Table 4.9: ANOVA table for MOE of steel fiber reinforced UHPC mixture with silica fume only

Source of variation	SS	DOF	MS	F	P	F_{cr}	Significance criteria P< 0.05 and F > F_{cr}
Exposure duration	731.7	5	146.3	31.6	1.8×10^{-07}	2.9	**Significant**
Fiber content	7.2	3	2.4	0.5	6.8×10^{-1}	3.3	**Insignificant**
Error	69.4	15	4.6				
Total	808.3	23					

Table 4.10: ANOVA table for MOE of steel fiber reinforced UHPC mixture with silica fume and natural pozzolana

Source of variation	SS	DOF	MS	F	P	F_{cr}	Significance criteria P< 0.05 and F > F_{cr}
Exposure duration	674.8	5	134.9	324.2	1.0×10^{-14}	2.9	**Significant**
Fiber content	35.7	3	11.9	28.6	1.9×10^{-06}	3.3	**Significant**
Error	6.2	15	0.4				
Total	716.8	23					

Table 4.11: ANOVA table for MOE of steel fiber reinforced UHPC mixture with silica fume and limestone powder

Source of variation	SS	DOF	MS	F	P	F_{cr}	Significance criteria P< 0.05 and F > F_{cr}
Exposure duration	762.7	5	152.6	66.5	1.1×10^{-09}	2.9	**Significant**
Fiber content	5.1	3	1.7	0.7	5.4×10^{-1}	3.3	**Insignificant**
Error	34.4	15	2.3				
Total	802.3	23					

Empirical model for MOE in terms of exposure duration and fiber content, as obtained through regression analysis, is given as:

$$MOE = a + b(T) + c(F)$$

Where:

MOE is modulus of elasticity (GPa)

a, *b* and *c* are regression coefficients, as given in Table 4.12 for all three UHPC mixtures

T is exposure duration (0, 60, 120, 180, 240, and 360 minutes)

F is fiber content (2, 4, 6, and 8% by mass of mixture)

Table 4.12: Values of regression coefficients for MOE of UHPC mixtures with steel fibers

UHPC mixture	***a***	***b***	***c***	R^2
Mixture with silica fume only	49.2	-0.05267	0.09333	0.87
Mixture with silica fume and natural pozzolana	47.7	-0.05102	0.52950	0.96
Mixture with silica fume and limestone powder	49.7	-0.05435	0.05893	0.93

High values of regression coefficient, R^2, for each of the UHPC mixtures, as shown in Table 4.12, indicate a high degree of fit of the data. These derived models can be used to predict the MOE for a given set of exposure duration and fiber content.

ii. Effect of type of UHPC mixture on MOE

Figures 4.18 through 4.21 show the plots of MOE of three UHPC mixtures at different exposure durations separately for 2, 4, 6, and 8% of fibers, respectively. It can be seen from Figures 4.18 through 4.21 that at any exposure duration and fiber content, all the UHPC

mixtures showed more or less identical MOE. Therefore, it can be concluded that the MOE of all three UHPC mixture is comparable without any major difference.

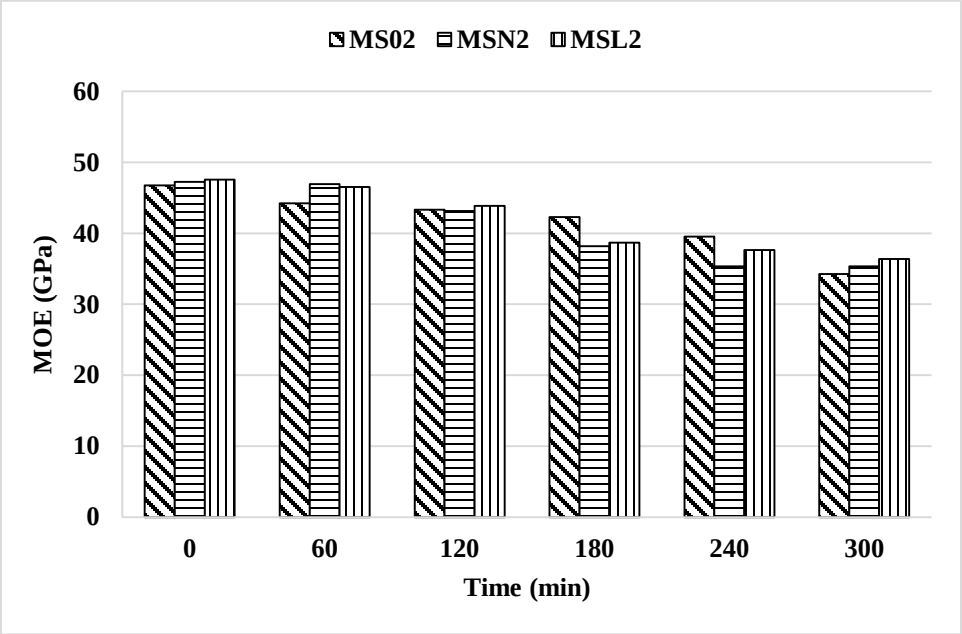

Figure 4.18: MOE vs exposure duration for UHPC mixtures with 2% steel fibers

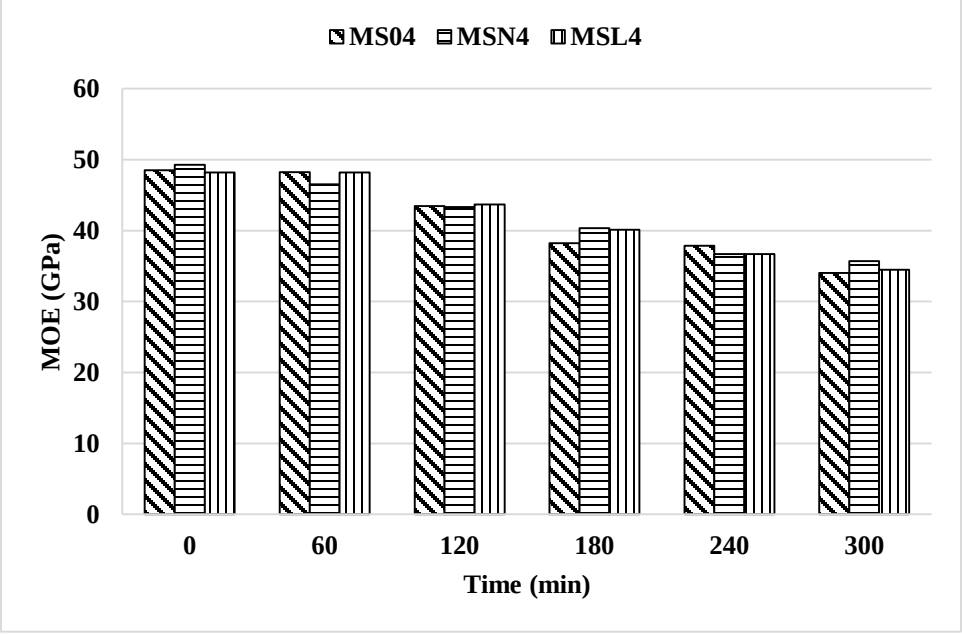

Figure 4.19: MOE vs exposure duration for UHPC mixtures with 4% steel fibers

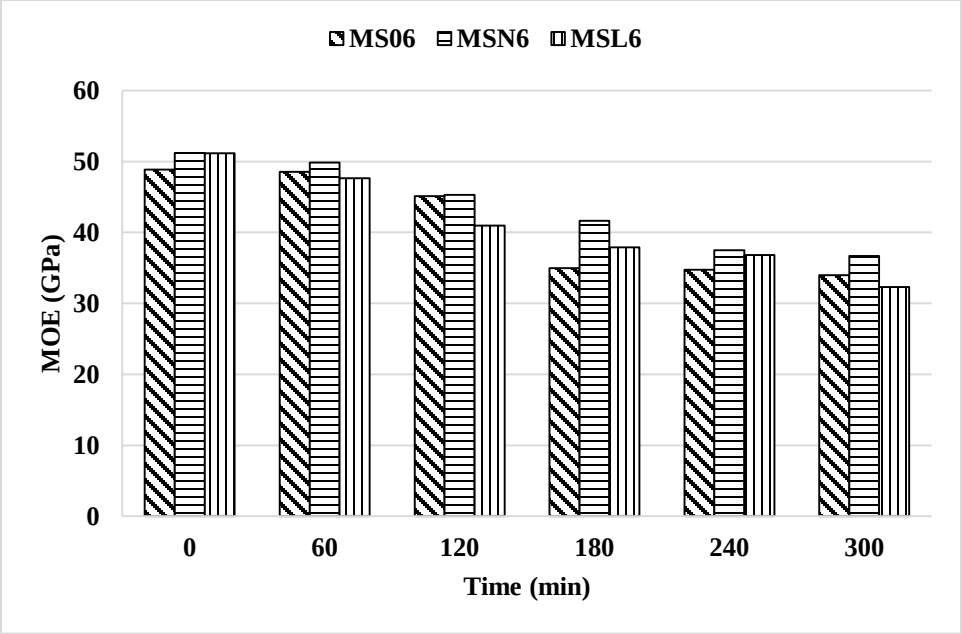

Figure 4.20: MOE vs exposure duration for UHPC mixtures with 6% steel fibers

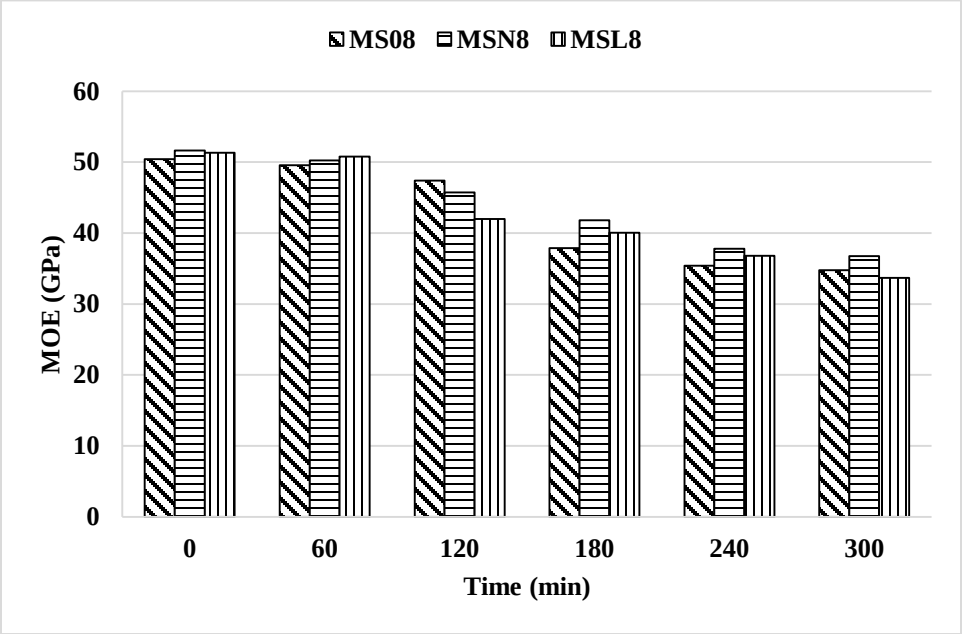

Figure 4.21: MOE vs exposure duration for UHPC mixtures with 8% steel fibers

4.1.3 Energy Absorption Capacity (Modulus of Toughness)

Since the increase in exposure duration increases compressive strength on one hand and decreases the MOE on the other hand, as observed in the previous sections, it would be a better option to evaluate the performance of UHPC mixtures in terms of energy absorption capacity (modulus of toughness in compression), MOT. The MOT calculated as the area under stress-strain diagram, as described in the previous chapter, can be used to indicate the overall performance of the concrete mixtures against exposure to elevated temperature. Higher MOT (i.e., higher energy required to cause failure of the specimen) indicates higher performance of the mixture.

Average values of MOT of the control specimens and specimens subjected to elevated temperature of 300^{o}C for 60 min, 120 min, 180 min, 240 min and 300 min are presented in Table 4.13. The ratios of the energy absorption capacity after a particular exposure duration to the energy absorption capacity of control specimens (MOT_T/MOT) are summarized in Table 4.14. Based on the data presented in Tables 4.13 and 4.14, discussions were made regarding the effect of fiber content and duration of elevated temperature on energy absorption capacity.

Table 4.13: MOT of UHPC mixtures containing steel fibers exposed to elevated temperatures

Mixture ID	MOT (kJ/m^3)					
	control	60 min	120 min	180 min	240 min	300 min
MS02	223	348	402	478	476	493
MS04	223	359	418	566	549	549
MS06	226	378	446	566	596	564
MS08	252	442	520	573	630	572
MSN2	216	300	303	360	347	342
MSN4	217	349	439	475	489	469
MSN6	218	422	446	523	507	467
MSN8	244	471	520	598	555	544
MSL2	211	370	450	463	500	489
MSL4	212	373	477	495	542	518
MSL6	257	375	480	500	568	618
MSL8	293	378	488	606	679	661

Table 4.14: MOT_T/MOT of UHPC mixtures containing steel fibers exposed to elevated temperatures

Mixture ID	MOT_T/MOT				
	60 min	120 min	180 min	240 min	300 min
MS02	1.56	1.80	2.14	2.13	2.21
MS04	1.61	1.87	2.54	2.46	2.46
MS06	1.67	1.97	2.50	2.64	2.49
MS08	1.75	2.06	2.27	2.50	2.27
MSN2	1.39	1.40	1.66	1.60	1.58
MSN4	1.61	2.02	2.18	2.25	2.16
MSN6	1.93	2.05	2.40	2.33	2.14
MSN8	1.93	2.13	2.45	2.28	2.23
MSL2	1.75	2.13	2.19	2.37	2.31
MSL4	1.76	2.25	2.34	2.56	2.45
MSL6	1.46	1.87	1.95	2.21	2.41
MSL8	1.29	1.66	2.07	2.31	2.26

i. Effect of fiber content and duration of elevated temperature on MOT

The plots of MOT versus exposure duration data corresponding to different fiber contents are shown in Figures 4.22 through 4.24 for UHPC mixture with silica fume alone, blend of silica fume and natural pozzolana, and blend of silica fume and limestone powder, respectively.

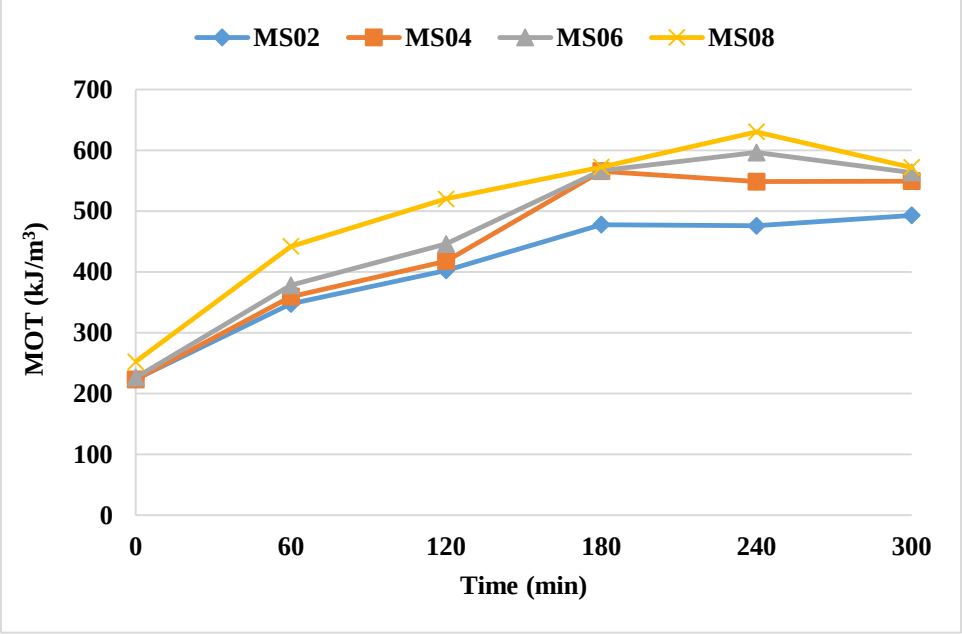

Figure 4.22: Variation of MOT with exposure duration for UHPC with silica fume and different steel fiber contents

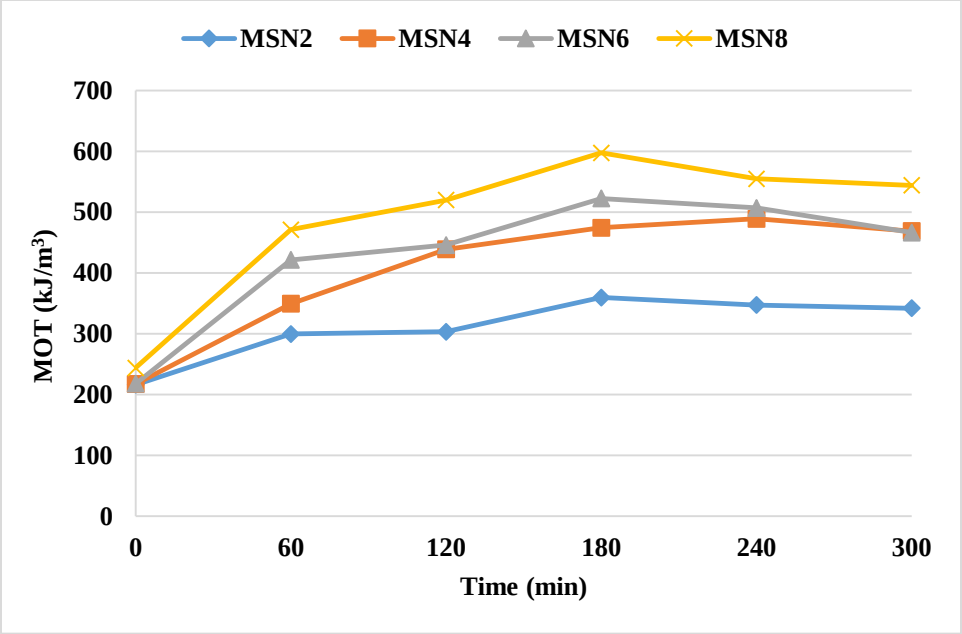

Figure 4.23: Variation of MOT with exposure duration for UHPC with blend of silica fume and natural pozzolana and different steel fiber contents

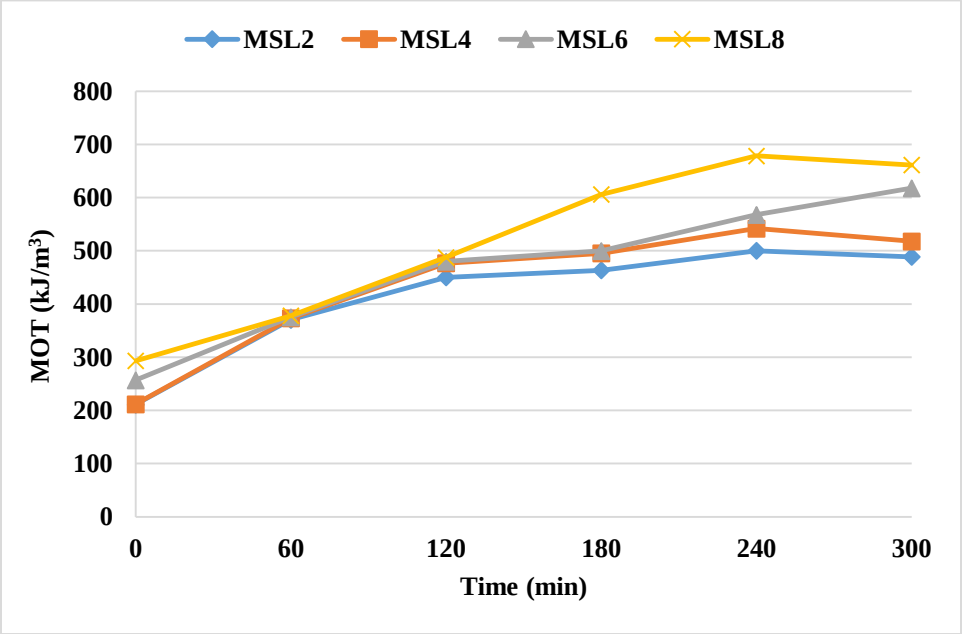

Figure 4.24: Variation of MOT with exposure duration for UHPC with blend of silica fume and limestone powder and different steel fiber contents

From Figures 4.11 through 4.14, it can be seen that for each type of UHPC mixture, although the slope of stress-strain curves (i.e., modulus of elasticity) decreased with

exposure duration, stress and stain at failure increased with the increase of exposure durations increasing the area under stress-strain curves. This resulted into an increase in MOT in compression with the increase in exposure duration and fiber content, as can be observed from Figures 4.22 through 4.24. It can be noted from Figures 4.22 through 4.24 that for all three UHPC mixtures, there is a sharp increase in MOT with exposure duration after 60 minutes of exposure. From Table 4.14 it can be seen that the MOT increased by 29 to 93% in first 60 minutes of exposure at 300^{o}C. The increase in MOT from 60 minutes to 240 minutes was found to be mostly at slow rate. In 180 minutes of exposure (from 61st minute to 240th minute), the MOT increased by 60 to 164%. MOT is found to be slightly higher at a higher fiber content. Zheng et al. [28] reported the similar behavior that with the increase of fiber content area under the stress-strain also increases, resulting into increase in toughness.

It is interesting to note that even after 300 minutes of exposures, the MOT was found to be more than two times of the MOT of control specimens in case of almost all the three UHPC mixtures. All three UHPC mixtures showed comparable MOT in compression at each exposure duration indicating no major effect of the type of UHPC mixture.

The analysis of variance (ANOVA) of MOT data presented in Table 4.13 for all three UHPC mixtures are presented in Tables 4.15 through 4.17.

Table 4.15: ANOVA table for MOT of steel fiber reinforced UHPC mixture with silica fume only

Source of variation	SS	DOF	MS	F	P	F_{cr}	Significance criteria P< 0.05 and F > F_{cr}
Exposure duration	333203.5	5	66640.7	106.3	3.6×10^{-11}	2.9	**Significant**
Fiber content	28123.7	3	9374.6	15.0	8.9×10^{-05}	3.3	**Significant**
Error	9401.4	15	626.8				
Total	370728.7	23					

Table 4.16: ANOVA table for MOT of steel fiber reinforced UHPC mixture with silica fume and natural pozzolana

Source of variation	SS	DOF	MS	F	P	F_{cr}	Significance criteria P< 0.05 and F > F_{cr}
Exposure duration	191716.1	5	38343.2	30.0	2.6×10^{-7}	2.9	**Significant**
Fiber content	97938.2	3	32646.1	25.6	3.8×10^{-6}	3.3	**Significant**
Error	19146.2	15	1276.4				
Total	308800.5	23					

Table 4.17: ANOVA table for MOT of steel fiber reinforced UHPC mixture with silica fume and limestone powder

Source of variation	SS	DOF	MS	F	P	F_{cr}	Significance criteria P< 0.05 and F > F_{cr}
Exposure duration	330595.2	5	66119.0	54.0	4.6×10^{-9}	2.9	**Significant**
Fiber content	36069.7	3	12023.2	9.8	7.8×10^{-4}	3.3	**Significant**
Error	18351.4	15	1223.4				
Total	385016.4	23					

From the ANOVA results, as presented in Tables 4.15 through 4.17, it can be observed that for all three UHPC mixtures, both exposure duration as well as fiber content have significant effect on MOT. However, the exposure duration, having a very high F-value and very low P-value as compared to that for fiber content, have more significant effect on MOT than the effect of fiber content.

Empirical model for MOT in terms of exposure duration and fiber content, as obtained through regression analysis, is given as:

$$MOT = a + b(T) + c(T^2) + d(F) + e(F^2)$$

Where:

MOT is modulus of toughness in compression (kJ/m^3)

a, b, c, d and *e* are regression coefficients, as given in Table 4.18 for all three UHPC mixtures

T is exposure duration (0, 60, 120, 180, 240, and 360 minutes)

F is fiber content (2, 4, 6, and 8% by mass of mixture)

Table 4.18: Values of regression coefficients for MOT of UHPC mixtures with steel fibers

UHPC mixture	***a***	***b***	***c***	***d***	***e***	R^2
Mixture with silica fume only	150.4	2.59	-0.0051	18.38	-0.3207	0.98
Mixture with silica fume and natural pozzolana	51.3	2.38	-0.0056	50.64	-2.2869	0.91
Mixture with silica fume and limestone powder	197.5	2.32	-0.0041	-1.17	1.8190	0.94

Very high value of regression coefficient, R^2, for each of the UHPC mixtures, as shown in Table 4.18, indicate a high degree of fit of the data. These derived models can be used to predict the MOT for a given set of exposure duration and fiber content.

4.1.4 Flexural Strength

a) Failure modes in flexural test

Figures 4.25 through 4.28 show the failure modes developed when control specimens were tested in flexure. It was observed that for all UHPC mixtures, the failure was more ductile at higher fiber contents. In case of 2% fiber content, normally one cracked in the middle one-third portion appeared and the same crack propagated. However, with increase in fiber content, multiple cracks distributed along the length of prism appeared and normally one of these multiple cracks propagated**.** Similar failure modes were observed for specimens tested in flexural after exposing to the elevated temperature (Figure 4.29).

Figure 4.25: Typical flexural failure of control specimen with 2% steel fibers

Figure 4.26: Typical flexural failure of control specimen with 4% steel fibers

Figure 4.27: Typical flexural failure of control specimen with 6% steel fibers

Figure 4.28: Typical Flexural failure of control specimen with 8% steel fibers

Figure 4.29: Typical flexural failure of a specimen with steel fibers exposed to elevated temperature

Typical load-deflection curves at different fiber contents are shown in Figure 4.30. These load-deflection curves confirm the ductile failure of specimens under flexure.

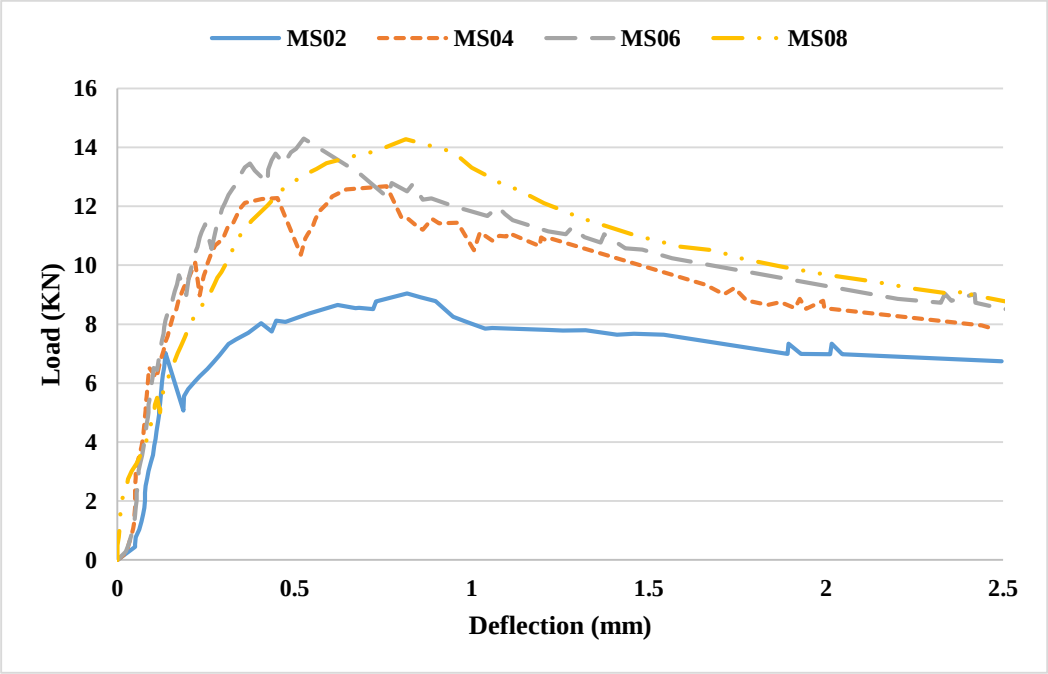

Figure 4.30: Typical load-deflection curves

b) Flexural test results

Flexural strength was calculated in terms of modulus of rupture (MOR) using the peak load taken from load-deflection curves. Average MOR of the control specimens and specimens subjected to elevated temperature of 300^{o}C for 60 min, 120 min, 180 min, 240 min and 300 min are given in the Table 4.19. The ratios of the MOR after a particular exposure duration to the MOR of control specimens (MOR_T/MOR) are presented in Table 4.20. Based on the data presented in Tables 4.19 and 4.20, discussions were made regarding the effect of fiber content and duration of elevated temperature and the effect of type of UHPC on MOR.

Table 4.19: MOR of UHPC mixtures containing steel fibers exposed to elevated temperatures

Mixture ID	MOR (MPa)					
	control	60 min	120 min	180 min	240 min	300 min
MS02	22.62	20.44	18.63	16.91	16.69	16.55
MS04	31.69	29.48	27.49	25.2	23.3	23.21
MS06	35.74	33.14	32.9	32.18	32.07	30.51
MS08	34.97	34.59	33.44	32.23	32.12	30.49
MSN2	19.44	17.93	17.75	16.9	14.88	14.48
MSN4	28.5	26.25	25.43	25.32	24.24	22.51
MSN6	34.79	34.37	33.54	32.51	31.83	30.47
MSN8	35.7	33.91	33.75	33	32.63	31.52
MSL2	20.12	18.89	18.21	16.9	15.84	15.24
MSL4	25.12	23.57	22.71	22.14	21.44	21.15
MSL6	33.45	32.07	31.79	30.91	29.52	28.53
MSL8	33.15	32.05	31.8	30.1	30	29.26

Table 4.20: MOR_T/ MOR of UHPC mixtures containing steel fibers exposed to elevated temperatures

Mixture ID	MOR_T/ MOR				
	60 min	120 min	180 min	240 min	300 min
MS02	0.90	0.82	0.75	0.74	0.73
MS04	0.93	0.87	0.80	0.74	0.73
MS06	0.93	0.92	0.90	0.90	0.85
MS08	0.99	0.96	0.92	0.92	0.87
MSN2	0.92	0.91	0.87	0.77	0.74
MSN4	0.92	0.89	0.89	0.85	0.79
MSN6	0.99	0.96	0.93	0.91	0.88
MSN8	0.95	0.95	0.92	0.91	0.88
MSL2	0.94	0.91	0.84	0.79	0.76
MSL4	0.94	0.90	0.88	0.85	0.84
MSL6	0.96	0.95	0.92	0.88	0.85
MSL8	0.97	0.96	0.91	0.90	0.88

i. Effect of fiber content and duration of elevated temperature on MOR

The plots of MOR versus exposure duration data corresponding to different fiber contents are shown in Figures 4.31 through 4.33 for UHPC mixture with silica fume alone, blend of silica fume and natural pozzolana, and blend of silica fume and limestone powder, respectively.

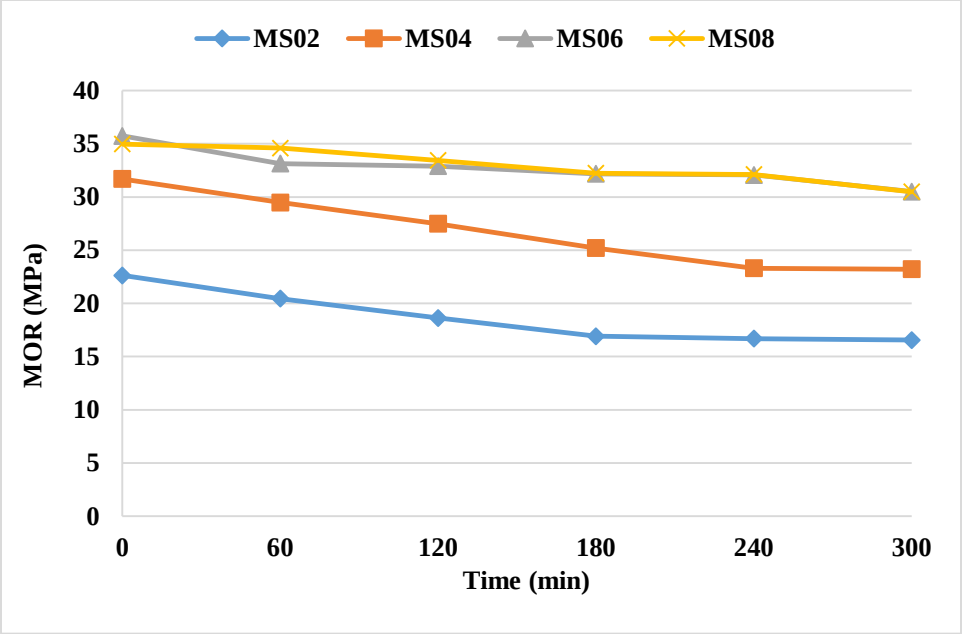

Figure 4.31: Variation of MOR with exposure duration for UHPC with silica fume and different steel fiber contents

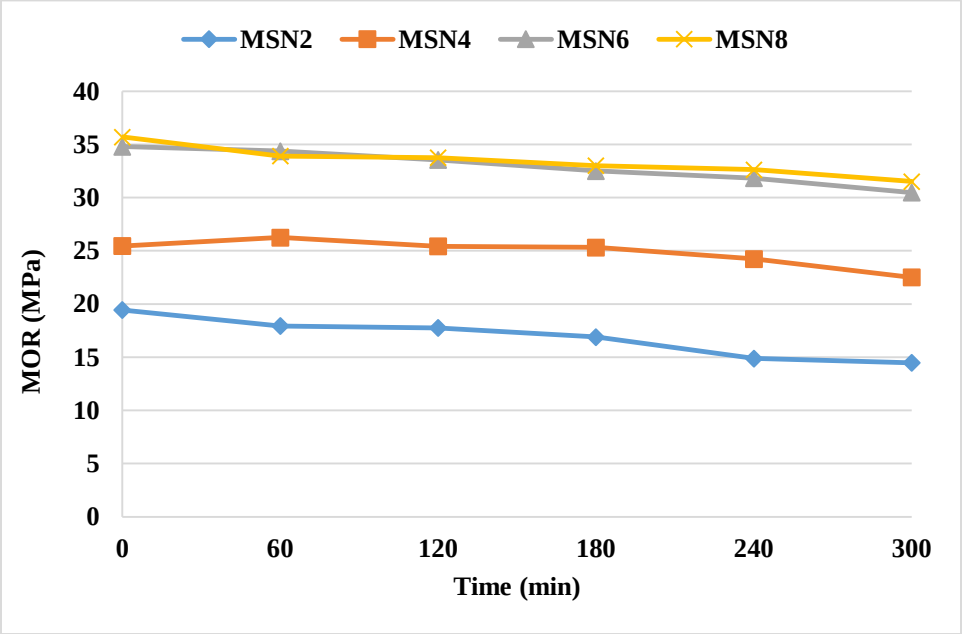

Figure 4.32: Variation of MOR with exposure duration for UHPC with blend of silica fume and natural pozzolana and different steel fiber contents

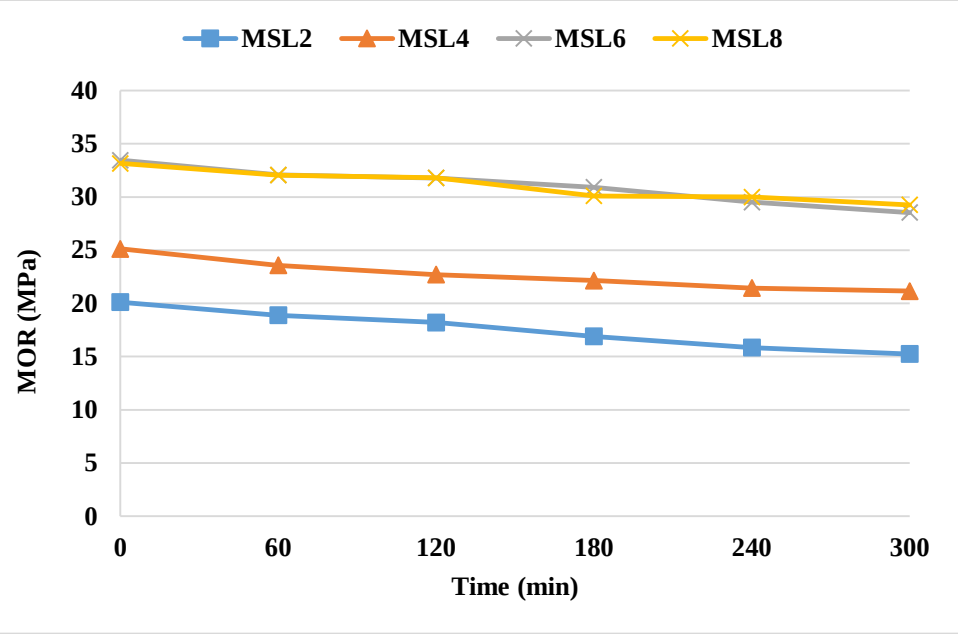

Figure 4.33: Variation of MOR with exposure duration for UHPC with blend of silica fume and limestone powder and different steel fiber contents

From the data in Figures 4.31 through 4.33, it is observed that for control specimens the flexural strength increased with the increase of fiber content until 6%. The effect of fiber content on flexural strength beyond 6% of fibers was not significant in both control specimens as well as specimens exposed to the elevated temperature.

The MOR decreases with an increase of exposure duration. The mixtures with less fiber contents were more affected by the elevated temperature exposures as compared to the mixtures with more fiber content. From Table 4.20, reductions in MOR was noted to be in the range of 1 to 10% and 12 to 27% after 60 and 300 minutes of exposure, respectively. The reduction in MOR due to exposure to the elevated temperature may be attributed to the development of micro cracks inside the concrete mass [30]. Zheng et al. [30] reported that the reduction in flexural strength occurred because temperature beyond 200^{o}C caused deterioration in the bond between concrete and steel fibers.

The analysis of variance (ANOVA) of the MOR data presented in Table 4.19 for all three UHPC mixtures are presented in Tables 4.21 through 4.23.

Table 4.21: ANOVA table for MOR of steel fiber reinforced UHPC mixture with silica fume only

Source of variation	SS	DOF	MS	F	P	F_{cr}	Significance criteria P< 0.05 and F > F_{cr}
Exposure duration	103.6	5	20.7	20.6	3.12×10^{-06}	2.9	**Significant**
Fiber content	818.3	3	272.7	271.1	2.76×10^{-13}	3.3	**Significant**
Error	145.2	15	9.7				
Total	1067	23					

Table 4.22: ANOVA table for MOR of steel fiber reinforced UHPC mixture with silica fume and natural pozzolana

Source of variation	SS	DOF	MS	F	P	F_{cr}	Significance criteria P< 0.05 and F > F_{cr}
Exposure duration	45.3	5	9.07	28.02	4.18×10^{-07}	2.9	**Significant**
Fiber content	1097	3	365.7	1130.1	6.91×10^{-18}	3.3	**Significant**
Error	4.9	15	0.32				
Total	1147	23					

Table 4.23: ANOVA table for MOR of steel fiber reinforced UHPC mixture with silica fume and limestone powder

Source of variation	SS	DOF	MS	F	P	F_{cr}	Significance criteria $P< 0.05$ and $F > F_{cr}$
Exposure duration	53.8	5	10.8	89.3	1.28×10^{-10}	2.90	**Significant**
Fiber content	798.0	3	266.0	2205.8	4.66×10^{-20}	3.29	**Significant**
Error	1.8	15	0.12				
Total	853.7	23					

From the ANOVA results, as presented in Tables 4.21 through 4.23, it can be observed that for all three UHPC mixtures, both exposure duration as well as fiber content have significant effect on MOR. However, the fiber content, having a very high F-value and very low P-value as compared to that for exposure duration, have stronger effect on the MOR.

Empirical model for MOR in terms of exposure duration and fiber content, as obtained through regression analysis, is given as:

$$MOR = a + b(T) + c(T^2) + d(F) + e(F^2)$$

Where:

MOR is modulus of rupture (MPa)

a, b, c, d and *e* are regression coefficients, as given in Table 4.24 for all three UHPC mixtures

T is exposure duration (0, 60, 120, 180, 240, and 360 minutes)

F is fiber content (2, 4, 6, and 8% by mass of mixture)

Table 4.24: Values of regression coefficients for MOR of UHPC mixtures with steel fibers

UHPC mixture	*a*	*b*	*c*	*d*	*e*	R^2
Mixture with silica fume only	9.1	-0.03155	0.000039	7.37	-0.49198	0.98
Mixture with silica fume and natural pozzolana	5.0	-0.00692	-0.000021	7.55	-0.46688	0.98
Mixture with silica fume and limestone powder	9.2	-0.01769	0.000011	5.66	-0.32125	0.95

A very high value of regression coefficient, R^2, for each of the UHPC mixtures, as shown in Table 4.24, indicate a high degree of fit of the data. These derived models can be used to predict the MOR for a given set of exposure duration and fiber content. Alternatively, these models can be utilized to calculate the exposure duration required to achieve a give MOR at a given fiber content.

ii. Effect of type of UHPC mixture on MOR

The plots of MOR of three UHPC mixtures at different exposure durations are shown in Figures 4.34 through 4.36, for 2, 4, 6, and 8%, respectively. It can be observed from Figures 4.34 through 4.36 that at any exposure duration and fiber content, there is not much difference between the MOR of the three mixtures. Therefore, it can be concluded that the performance of all three UHPC mixtures is comparable without major difference.

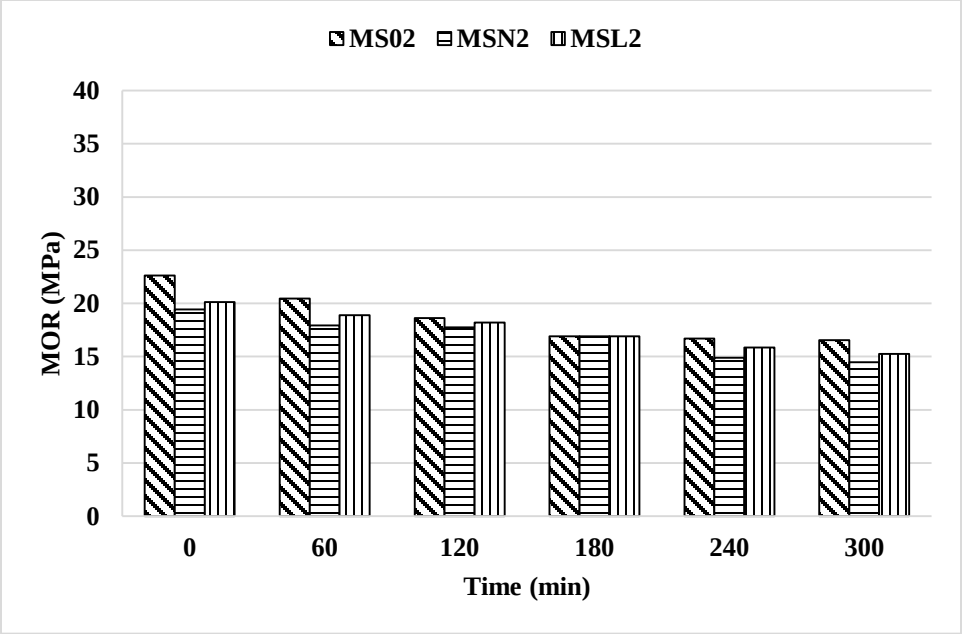

Figure 4.34: MOR vs exposure duration for UHPC mixtures with 2% steel fibers

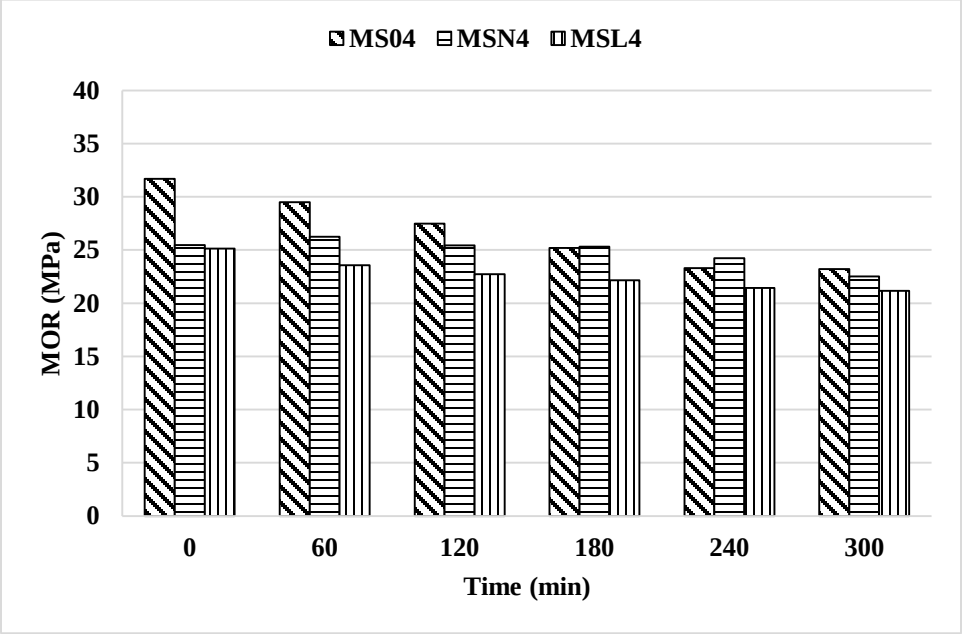

Figure 4.35: MOR vs exposure duration for UHPC mixtures with 4% steel fibers

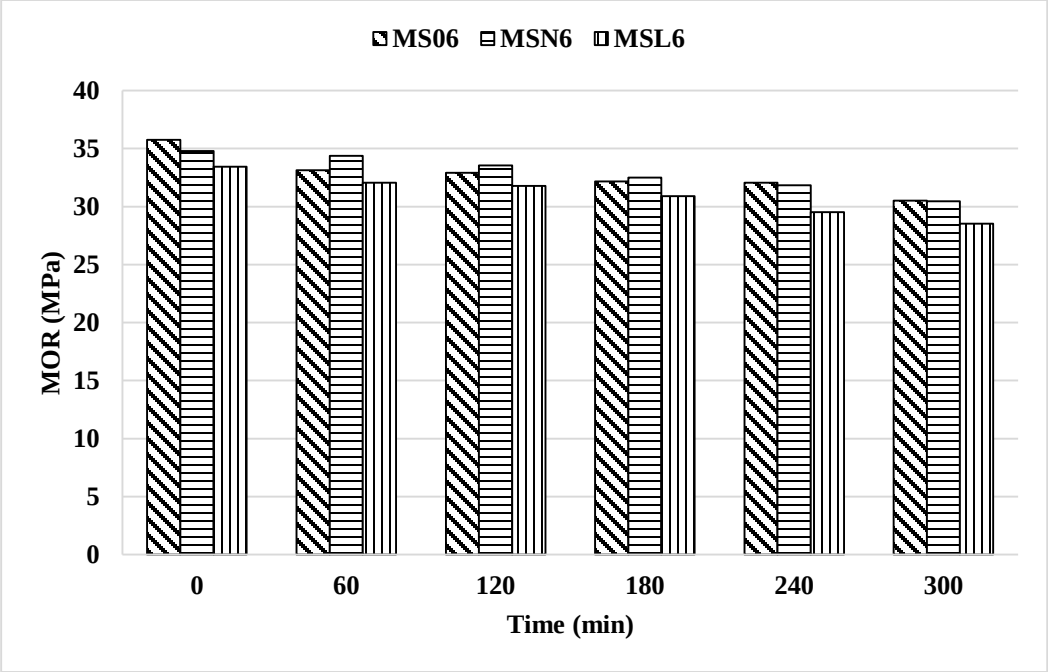

Figure 4.36: MOR vs exposure duration for UHPC mixtures with 6% steel fibers

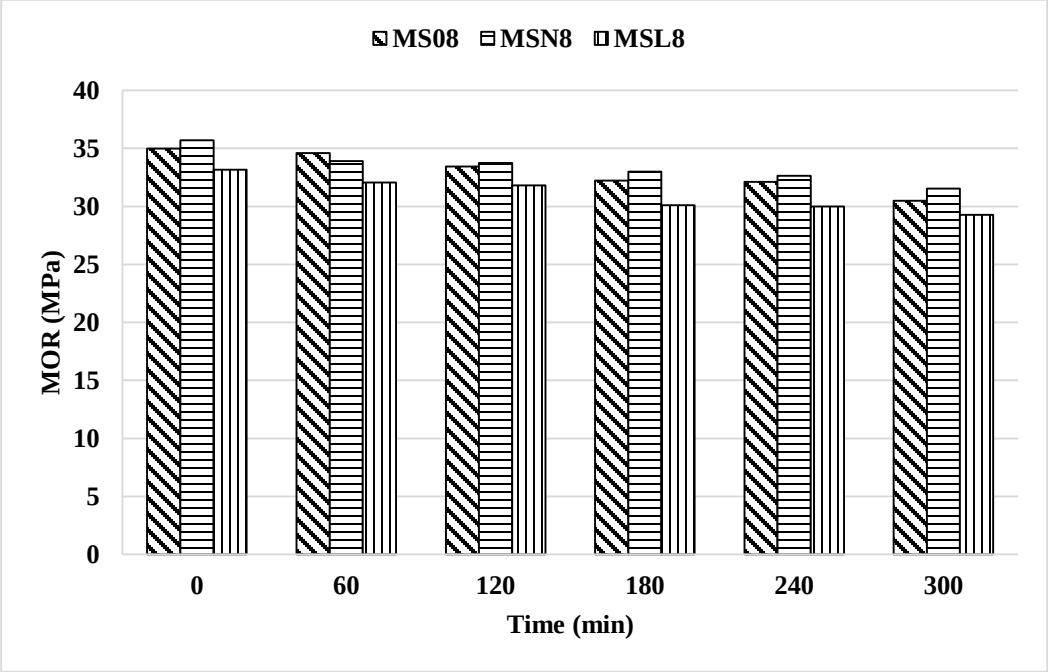

Figure 4.37: MOR vs exposure duration for UHPC mixtures with 8% steel fibers

4.1.5 Splitting Tensile Strength

a) Failure modes in splitting tensile strength test

Figures 4.38 and 4.39 show failure modes of control specimens and specimens exposed to elevated temperatures, respectively, when they were subjected to splitting tensile strength test. From Figures 4.38 and 4.39 it can be seen that the failure of specimens was ductile for all mixtures at all fiber contents.

Figure 4.38: Typical splitting failure of control specimens

Figure 4.39: Typical splitting failure of exposed specimens

b) Splitting tensile strength test results

Average splitting tensile strength of the control specimens and specimens subjected to elevated temperature of 300^{o}C for 60 min, 120 min, 180 min, 240 min and 300 min are presented in the Table 4.25. The ratios of the splitting tensile strength after a particular exposure duration to the splitting tensile strength of control specimens $(f_{st})_T/f_{st}$ are summarized in Table 4.26. Based on the data presented in Tables 4.25 and 4.26, discussions were made regarding the effect of fiber content and duration of elevated temperature and the effect of type of UHPC on splitting tensile strength.

Table 4.25: Splitting tensile strength of UHPC mixtures containing steel fibers exposed to elevated temperatures

Mixture ID	Splitting tensile strength, f_{st}, (MPa)					
	control	60 min	120 min	180 min	240 min	300 min
MS02	13.17	14.01	14.18	14.13	13.53	13.49
MS04	16.31	17.78	17.87	17.80	17.68	17.04
MS06	22.34	23.00	23.06	22.93	22.77	22.61
MS08	23.07	24.90	24.00	23.11	23.09	23.00
MSN2	12.96	13.70	13.81	12.70	12.64	12.47
MSN4	15.30	16.83	16.42	16.35	15.28	13.97
MSN6	19.50	21.40	19.63	19.18	18.48	18.40
MSN8	21.46	21.92	21.19	20.76	20.40	20.25
MSL2	12.53	13.82	14.01	13.89	13.77	13.72
MSL4	15.29	15.67	15.69	15.69	15.65	15.41
MSL6	18.45	18.93	18.86	18.85	18.79	18.79
MSL8	18.74	21.79	21.75	21.53	21.49	20.87

Table 4.26: $(f_{st})_T/f_{st}$ of UHPC mixtures with steel fibers exposed to elevated temperatures

Mixture ID	$(f_{st})_T/f_{st}$				
	60 min	120 min	160 min	240 min	300 min
MS02	1.06	1.08	1.07	1.03	1.02
MS04	1.09	1.10	1.09	1.08	1.04
MS06	1.03	1.03	1.03	1.02	1.01
MS08	1.08	1.04	1.00	1.00	1.00
MSN2	1.06	1.07	0.98	0.98	0.96
MSN4	1.10	1.07	1.07	1.00	0.91
MSN6	1.10	1.01	0.98	0.95	0.94
MSN8	1.02	0.99	0.97	0.95	0.94
MSL2	1.10	1.12	1.11	1.10	1.09
MSL4	1.02	1.03	1.03	1.02	1.01
MSL6	1.03	1.02	1.02	1.02	1.02
MSL8	1.16	1.16	1.15	1.15	1.11

i. Effect of fiber content and duration of elevated temperature on splitting tensile strength

The plots of splitting tensile strength versus exposure duration data corresponding to different fiber contents are shown in Figures 4.40 through 4.42 for UHPC mixture with silica fume alone, blend of silica fume and natural pozzolana, and blend of silica fume and limestone powder, respectively.

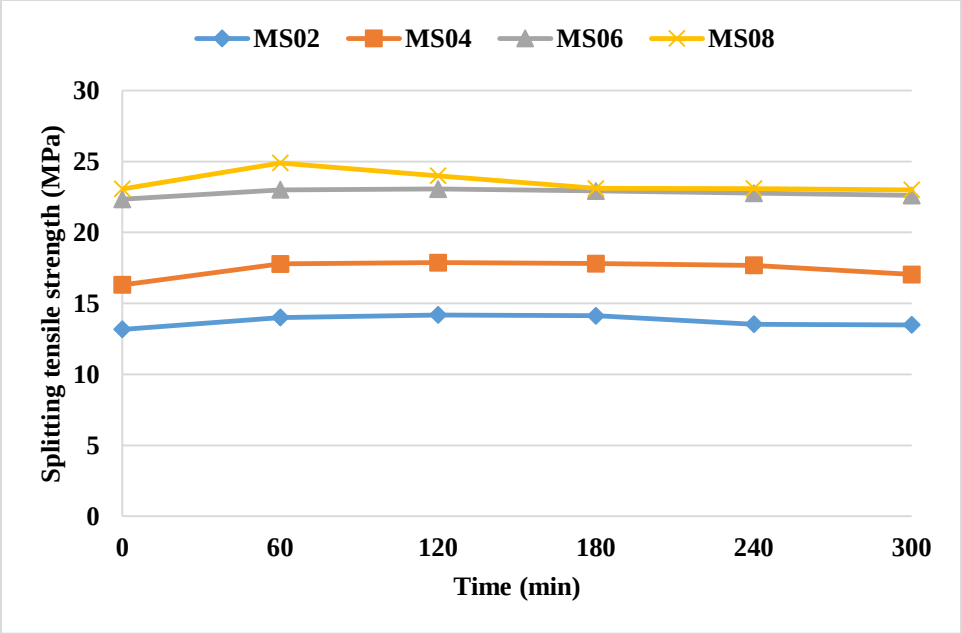

Figure 4.40: Variation of splitting tensile strength with exposure duration for UHPC with silica fume and different steel fiber contents

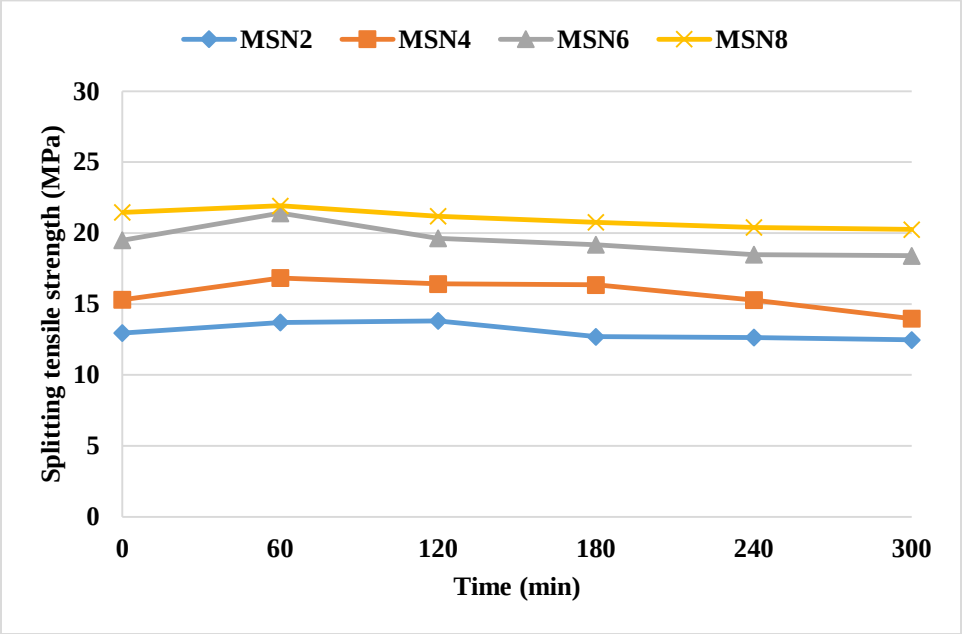

Figure 4.41: Variation of splitting tensile strength with exposure duration for UHPC with blend of silica fume and natural pozzolana and different steel fiber contents

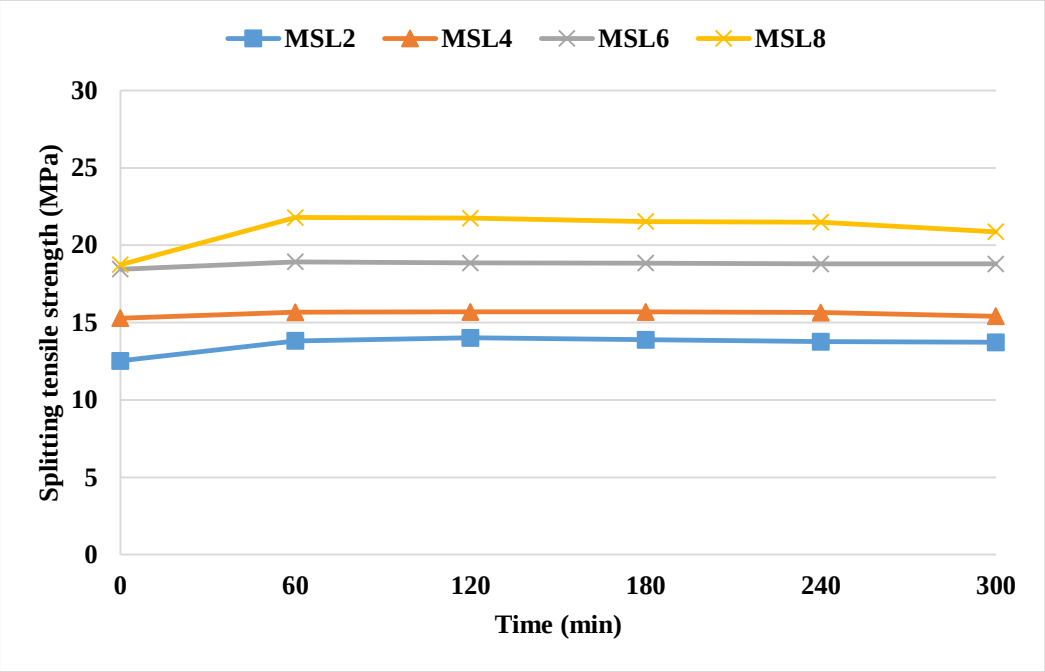

Figure 4.42: Variation of splitting tensile strength with exposure duration for UHPC with blend of silica fume and limestone powder and different steel fiber contents

From the data in Figures 4.40 through 4.42, it is observed that splitting tensile strength for each type of UHPC mixture increases with an increase of fiber content. There is a very little effect of the duration of elevated temperature exposure on splitting tensile strength, particularly a considerable increase in splitting tensile strength after 60 minutes of exposure. It is observed from Table 4.26 that an increase of 2 to 16% of strength took place in first 60 minutes of exposure. During next 240 minutes of exposure (from 61st minute to 300th minute), the strength reached almost to the level of that of control specimens.

The analysis of variance (ANOVA) of the splitting tensile strength, f_{st}, data presented in Table 4.25 for all three UHPC mixtures are presented in Tables 4.27 through 4.29.

Table 4.27: ANOVA table for splitting tensile strength of steel fiber reinforced UHPC mixture with silica fume only

Source of variation	SS	DOF	MS	F	P	F_{cr}	Significance criteria P< 0.05 and F > F_{cr}
Exposure duration	4.11	5	0.82	6.2	0.002609	2.9	**Significant**
Fiber content	386.1	3	128.7	970.8	2.2×10^{-17}	3.3	**Significant**
Error	2.0	15	0.13				
Total	392.2	23					

Table 4.28: ANOVA table for splitting tensile strength of steel fiber reinforced UHPC mixture with silica fume and natural pozzolana

Source of variation	SS	DOF	MS	F	P	F_{cr}	Significance criteria P< 0.05 and F > F_{cr}
Exposure duration	11.9	5	2.4	10.9	1.4×10^{-4}	2.9	**Significant**
Fiber content	233.3	3	77.8	356.3	3.7×10^{-14}	3.3	**Significant**
Error	3.27	15	0.2				
Total	248.5	23					

Table 4.29: ANOVA table for splitting tensile strength of steel fiber reinforced UHPC mixture with silica fume and limestone powder

Source of variation	SS	DOF	MS	F	P	F_{cr}	Significance criteria P< 0.05 and F > F_{cr}
Exposure duration	5.1	5	1.0	4.45	1.1×10^{-2}	2.9	**Significant**
Fiber content	195.6	3	65.2	282.2	2.1×10^{-13}	3.3	**Significant**
Error	3.5	15	0.2				
Total	204.2	23					

From the ANOVA results, as presented in Tables 4.27 through 4.29, it can be seen that for all three UHPC mixtures, both exposure duration as well as fiber content have significant effect on splitting tensile strength. However, the fiber content, having a very high F-value and very low P-value as compared to that for exposure duration, have much stronger effect on the splitting tensile strength.

Empirical model for splitting tensile strength in terms of exposure duration and fiber content, as obtained through regression analysis, is given as:

$$f_{st} = a + b(T) + c(T^2) + d(F) + e(F^2)$$

Where:

f_{st} is splitting tensile strength (MPa)

a, b, c, d and *e* are regression coefficients, as given in Table 4.30 for all three UHPC mixtures

T is exposure duration (0, 60, 120, 180, 240, and 360 minutes)

F is fiber content (2, 4, 6, and 8% by mass of mixture)

Table 4.30: Values of regression coefficients for splitting tensile strength of UHPC mixtures with steel fibers

UHPC mixture	*a*	*b*	*c*	*d*	*e*	R^2
Mixture with silica fume only	6.6	0.010807	-0.00004	3.56	-0.18239	0.96
Mixture with silica fume and natural pozzolana	9.4	0.005664	-0.00004	2.05	-0.06750	0.96
Mixture with silica fume and limestone powder	10.5	0.01393	-0.00004	1.08	0.01917	0.97

A very high value of regression coefficient, R^2, for each of the UHPC mixtures, as shown in Table 4.30, indicate a high degree of fit of the data. These derived models can be used to predict the splitting tensile strength for a given set of exposure duration and fiber content. Alternatively, these models can be utilized to calculate the exposure duration required to achieve a give strength at a given fiber content.

ii. Effect of type of UHPC mixture on splitting tensile strength

The plots of splitting tensile strength of three UHPC mixtures at different exposure durations are shown in Figures 4.43 through 4.46, for 2, 4, 6, and 8%, respectively. It can be observed from Figures 4.43 through 4.46 that at any exposure duration and fiber content, there is not much difference between the splitting tensile strengths of the three mixtures. Therefore, it can be concluded that the performance of all three UHPC is comparable.

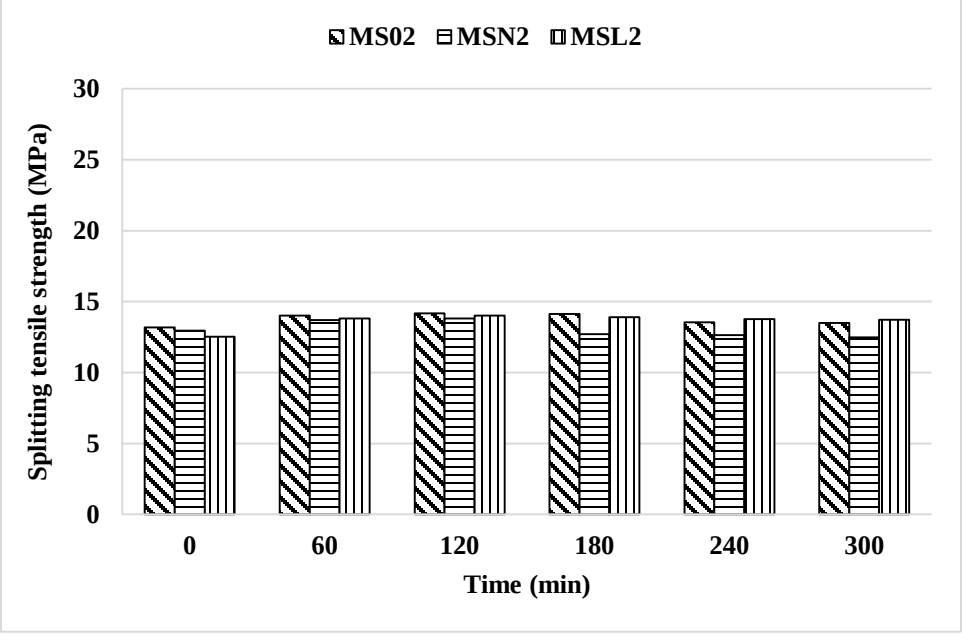

Figure 4.43: Splitting tensile strength vs exposure duration for UHPC mixtures with 2% steel fibers

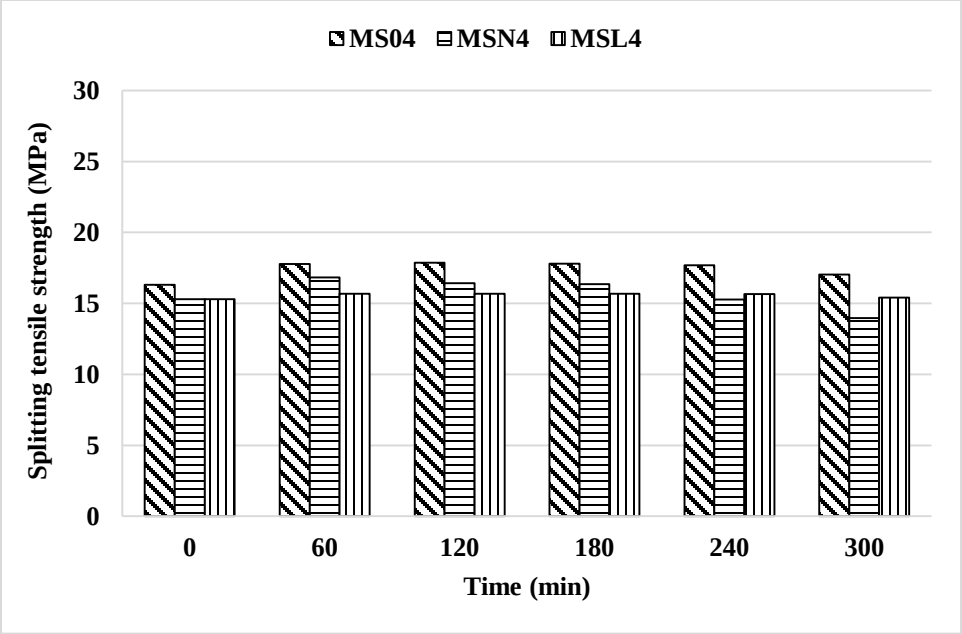

Figure 4.44: Splitting tensile strength vs exposure duration for UHPC mixtures with 4% steel fibers

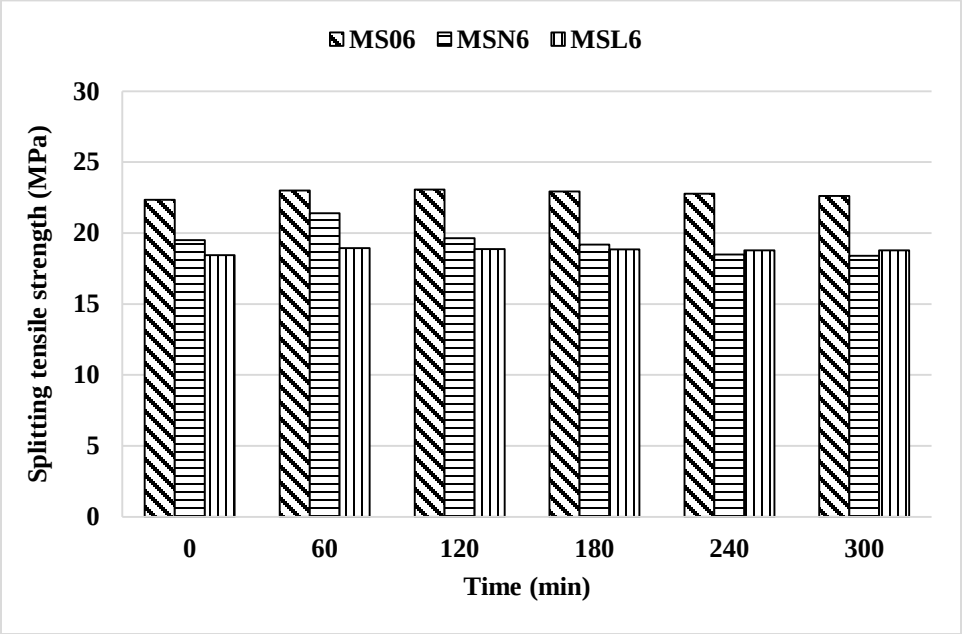

Figure 4.45: Splitting tensile strength vs exposure duration for UHPC mixtures with 6% steel fibers

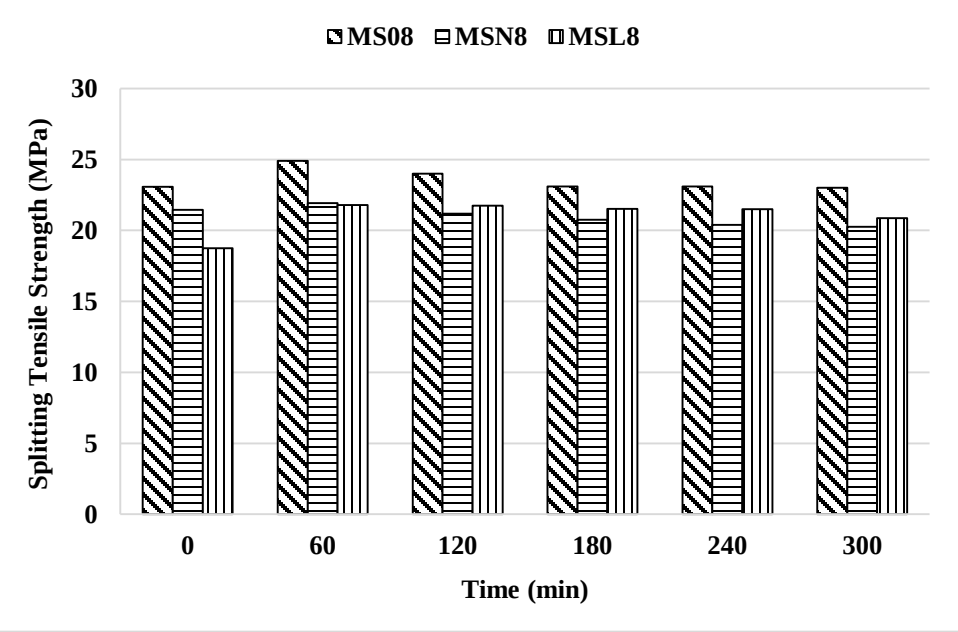

Figure 4.46: Splitting tensile strength vs exposure duration for UHPC mixtures with 8% steel fibers

4.2 UHPC Mixtures with Polypropylene Fibers Subjected to Elevated Temperatures

4.2.1 Compressive Strength

a) Failure modes in compression test

Figure 4.47 shows the failure modes in compression for control specimens, containing polypropylene fibers. It can be seen from Figure 4.47 that the failure mode for control specimens was gentle and ductile with minor damage of surface concrete due to the presence of fibers. The failure mode was still ductile but with little bit more damage on the surface of specimens when the specimens were tested in compression after 60 minutes of exposure to the elevated temperature (Figure 4.48). However, the failure mode became explosive and specimens were almost completed damaged (Figure 4.49) when they were tested in compression after an exposure for more than 60 minutes. The change in the behavior of the UHPC mixtures containing polypropylene fibers and exposed to elevated

temperature is because of the loss of ductility with increase in the temperature duration causing melting of polypropylene fibers.

Figure 4.47: Typical failure modes in compression for control specimens with polypropylene fiber

Figure 4.48: Typical failure modes in compression for specimens with polypropylene fiber after 60 minutes of exposures

Figure 4.49: Typical failure modes in compression for specimens with polypropylene fiber after more than 60 minutes of exposures

b) Compressive strength test results

Table 4.31 shows the average compressive strength of the control specimens and specimens subjected to elevated temperature of 300ºC for 60 min, 120 min, 180 min, 240 min and 300 min. The ratios of the compressive strength after a particular exposure duration to the compressive strength of control specimens $(f'_c)_T/f'_c$ are presented in Table 4.32. Based on the data presented in Tables 4.31 and 4.32, discussions were made regarding the effect of fiber content and duration of elevated temperature and the effect of type of UHPC on compressive strength.

Table 4.31: Compressive strength of UHPC mixtures containing polypropylene fibers exposed to elevated temperatures

Mixture ID	Compressive Strength (MPa)					
	control	60 min	120 min	180 min	240 min	300 min
MP01	126.4	147.8	152.2	154.5	158.0	165.6
MP02	132.3	135.1	141.2	142.4	149.9	156.0
MP03	118.1	128.1	129.7	130.0	136.4	136.1
MP04	118.5	121.8	124.1	125.2	128.6	135.6
MPN1	120.9	135.8	138.7	145.0	150.2	156.1
MPN2	121.9	131.8	132.3	140.2	141.8	144.0
MPN3	113.0	114.7	120.7	122.9	126.8	130.7
MPN4	104.8	112.0	112.0	117.5	119.1	120.6
MPL1	123.5	141.8	142.8	153.4	154.9	164.8
MPL2	129.0	133.5	134.2	138.6	147.6	152.4
MPL3	118.5	121.8	124.1	125.2	128.6	135.6
MPL4	107.0	108.7	114.7	116.9	120.8	124.7

Table 4.32: $(f'_c)_T/f'_c$ of UHPC mixtures with polypropylene fibers exposed to elevated temperatures

Mixture ID	$(f'_c)_T/f'_c$				
	60 min	120 min	160 min	240 min	300 min
MP01	1.17	1.20	1.22	1.25	1.31
MP02	1.02	1.07	1.08	1.13	1.18
MP03	1.08	1.10	1.10	1.16	1.15
MP04	1.03	1.05	1.06	1.09	1.14
MPN1	1.12	1.15	1.20	1.24	1.29
MPN2	1.08	1.08	1.15	1.16	1.18
MPN3	1.01	1.07	1.09	1.12	1.16
MPN4	1.07	1.07	1.12	1.14	1.15
MPL1	1.15	1.16	1.24	1.25	1.33
MPL2	1.04	1.04	1.07	1.14	1.18
MPL3	1.03	1.05	1.06	1.09	1.14
MPL4	1.02	1.07	1.09	1.13	1.17

i. Effect of fiber content and duration of elevated temperature on compressive strength

The plots of compressive strength versus exposure duration data corresponding to different fiber contents are shown in Figures 4.50 through 4.52 for UHPC mixture with silica fume alone, blend of silica fume and natural pozzolana, and blend of silica fume and limestone powder, respectively.

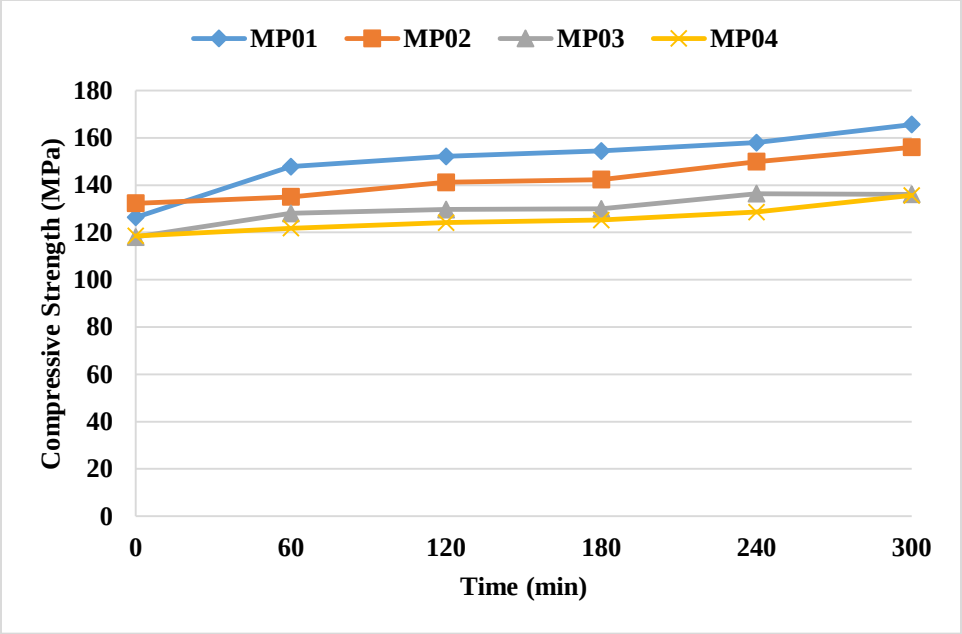

Figure 4.50: Variation of compressive strength with exposure duration for UHPC with silica fume and different polypropylene fiber contents

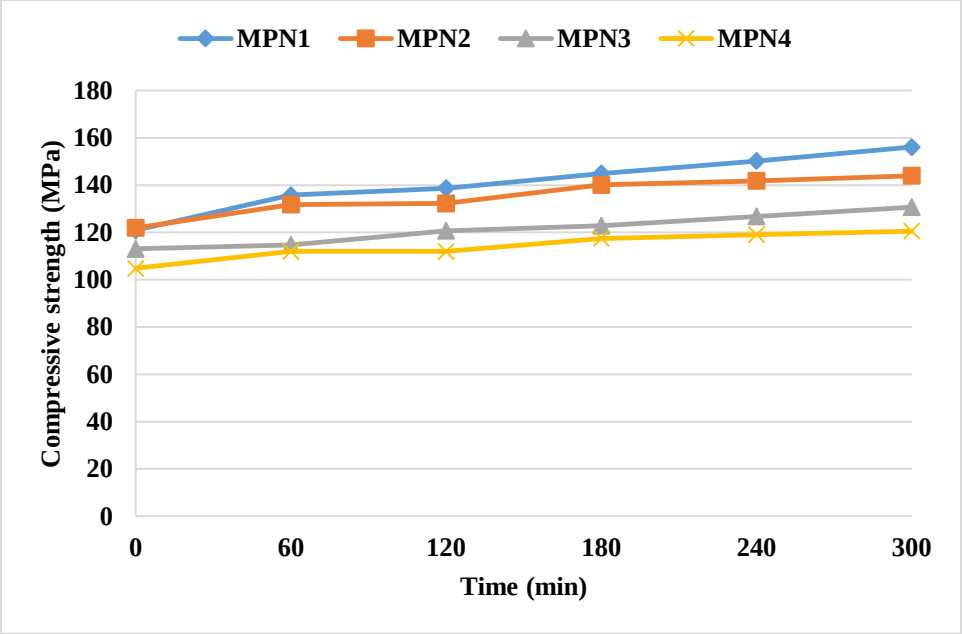

Figure 4.51: Variation of compressive strength with exposure duration for UHPC with blend of silica fume and natural pozzolana and different polypropylene fiber contents

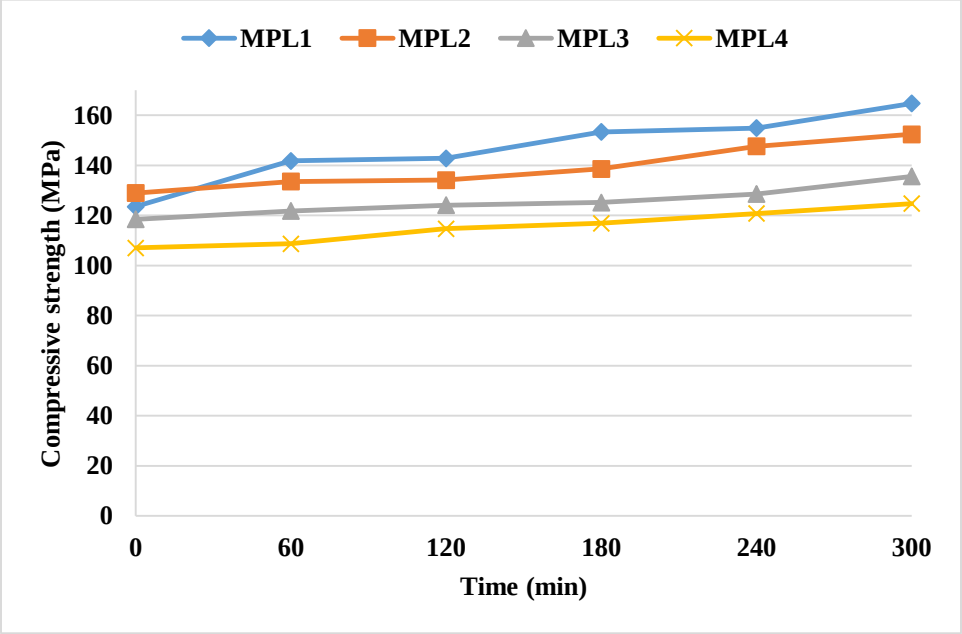

Figure 4.52: Variation of compressive strength with exposure duration for UHPC with blend of silica fume and limestone powder and different polypropylene fiber contents

The data in Figures 4.50 through 4.52 show clearly the effect of polypropylene fiber content on compressive strength. For control specimens of all three UHPC mixtures,

strength increased when fiber content increased from 0.1 to 0.2%. A significant decrease in strength of control specimens was observed when fiber content increased beyond 0.2%. For the specimens subjected to elevated temperature, the strength decreased with the increase in the fiber content at all exposure durations. Each of three UHPC mixtures had an average reduction of about 20% when fiber content increased from 0.1 to 0.4%. The reduction of compressive strength with increase in fiber content of control specimens may be attributed to the fact that the polypropylene fibers in quantity more than 0.2% might have created weaker zones in the mixtures. Further, in case of specimens subjected to elevated temperature, the lower strength at higher fiber content is due to melting of the polypropylene fibers creating soft zones and pores in the concrete matrix.

Although there is a reduction in compressive strength with increase in the quantity of polypropylene fibers, a considerable increase in compressive strength for longer exposure duration can be noticed from Figures 4.50 through 4.52. This increase in compressive strength is due to the net effect of two opposing factors: (i) decrease due to melting of polypropylene fibers and (ii) increase in strength due to densification of the matrix of mixtures at elevated temperature [19, 21, 22, 28]. It is observed from Table 4.32 that an increase of strength in the range of 1 to 17% took place in first 60 minutes of exposure. The total increase in strength is found to be in the range of 14 to 31% after exposure to the elevated temperature for a duration of 300 minutes.

The analysis of variance (ANOVA) of the compressive strength data presented in Table 4.31 for all three UHPC mixtures are presented in Tables 4.33 through 4.35.

Table 4.33: ANOVA table for compressive strength of polypropylene fibers reinforced UHPC mixture with silica fume only

Source of variation	SS	DOF	MS	F	P	F_{cr}	Significance criteria P< 0.05 and F > F_{cr}
Exposure duration	1424.8	5	285.0	16.2	1.38×10^{-05}	2.9	**Significant**
Fiber content	2425.1	3	808.4	46.1	8.38×10^{-08}	3.3	**Significant**
Error	263.3	15	17.6				
Total	4113.1	23					

Table 4.34: ANOVA table for compressive strength of polypropylene fibers reinforced UHPC mixture with silica fume and natural pozzolana

Source of variation	SS	DOF	MS	F	P	F_{cr}	Significance criteria P< 0.05 and F > F_{cr}
Exposure duration	1356.7	5	271.3	25.7	7.40×10^{-07}	2.9	**Significant**
Fiber content	2731.5	3	910.5	86.3	1.10×10^{-09}	3.3	**Significant**
Error	158.3	15	10.6				
Total	4246.5	23					

Table 4.35: ANOVA table for compressive strength of polypropylene fibers reinforced UHPC mixture with silica fume and limestone powder

Source of variation	SS	DOF	MS	F	P	F_{cr}	Significance criteria P< 0.05 and F > F_{cr}
Exposure duration	1546.4	5	309.3	16.4	1.31×10^{-05}	2.9	**Significant**
Fiber content	3518.9	3	1173.0	62.1	1.09×10^{-08}	3.3	**Significant**
Error	283.2	15	18.9				
Total	5348.5	23					

From the ANOVA results, as presented in Tables 4.33 through 4.35, it can be observed that for all three UHPC mixtures, both exposure duration as well as fiber content have significant effect on compressive strength. However, the fiber content, having a very high F-value and very low P-value as compared to that for exposure duration, have stronger effect on the compressive strength.

Empirical model for compressive strength in terms of exposure duration and fiber content, as obtained through regression analysis, is given as:

$$f_c' = a + b(T) + c(T^2) + d(F) + e(F^2)$$

Where:

f_c' is compressive strength (MPa)

a, b, c, d and *e* are regression coefficients, as given in Table 4.36 for all three UHPC mixtures

T is exposure duration (0, 60, 120, 180, 240, and 360 minutes)

F is fiber content (0.1, 0.2, 0.3, and 0.4% by mass of mixture)

Table 4.36: Values of regression coefficients for compressive strength of UHPC mixtures with polypropylene fibers

UHPC mixture	***a***	***b***	***c***	***d***	***e***	R^2
Mixture with silica fume only	152.3	0.09	-0.000074	-136.777	96.8	0.91
Mixture with silica fume and natural pozzolana	137.7	0.11	-0.0001	-77.0452	-34.4	0.94
Mixture with silica fume and limestone powder	144.2	0.07	0.0000	-76.1925	-63.1	0.94

A very high value of regression coefficient, R^2, for each of the UHPC mixtures, as shown in Table 4.36, indicate a high degree of fit of the data. These derived models can be used to predict the compressive strength for a given set of exposure duration and fiber content. Alternatively, these models can be utilized to calculate the exposure duration required to achieve a give strength at a given fiber content.

ii. Effect of type of UHPC mixture on compressive strength

The plots of compressive strength of three UHPC mixtures at different exposure durations are shown in Figures 4.53 through 4.56, for 0.1, 0.2, 0.3, and 0.4%, respectively. It can be observed from Figures 4.53 through 4.56 that at any exposure duration and fiber content, there is not much difference between the compressive strengths of the three mixtures. Therefore, it can be concluded that the performance of all three UHPC is comparable.

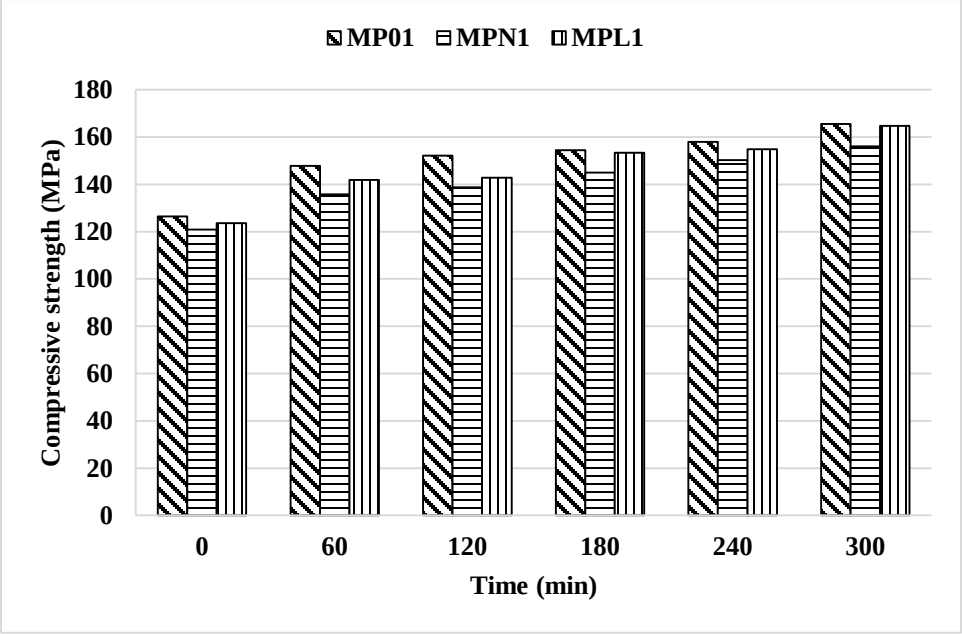

Figure 4.53: Compressive strength vs exposure duration for UHPC mixtures with 0.1% polypropylene fibers

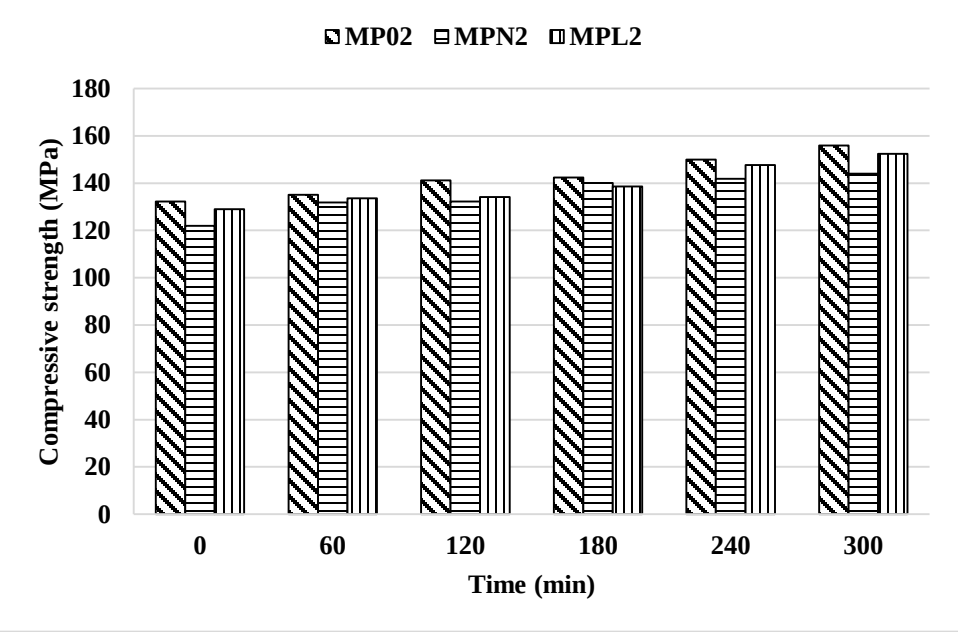

Figure 4.54: Compressive strength vs exposure duration for UHPC mixtures with 0.2% polypropylene fibers

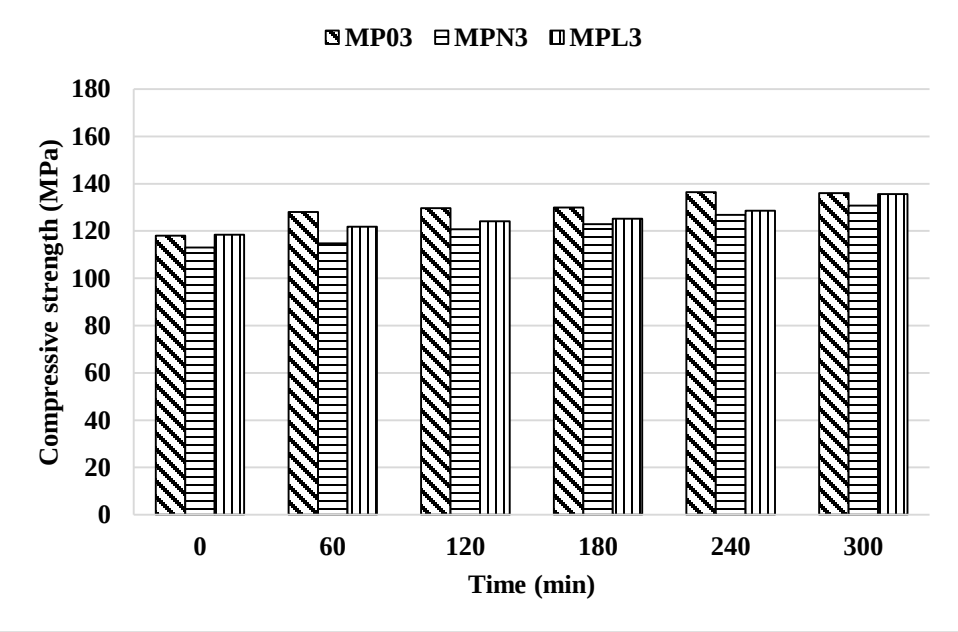

Figure 4.55: Compressive strength vs exposure duration for UHPC mixtures with 0.3% polypropylene fibers

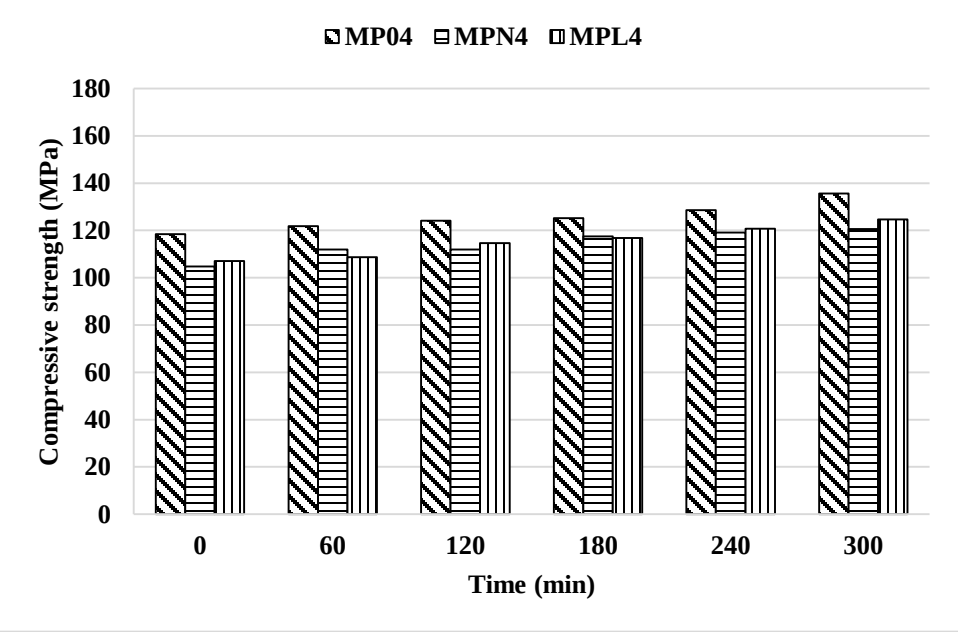

Figure 4.56: Compressive strength vs exposure duration for UHPC mixtures with 0.4% polypropylene fibers

4.2.2 Modulus of Elasticity

The modulus of elasticity of the control specimens and specimens exposed to elevated temperature of 300^{o}C for 60 min, 120 min, 180 min, 240 min and 300 min for all three UHPC mixtures were calculated from the respective stress-strain curves. The stress-strain curves up to the failure for MP01 to MP04 are shown typically in Figures 4.57 through 4.60.

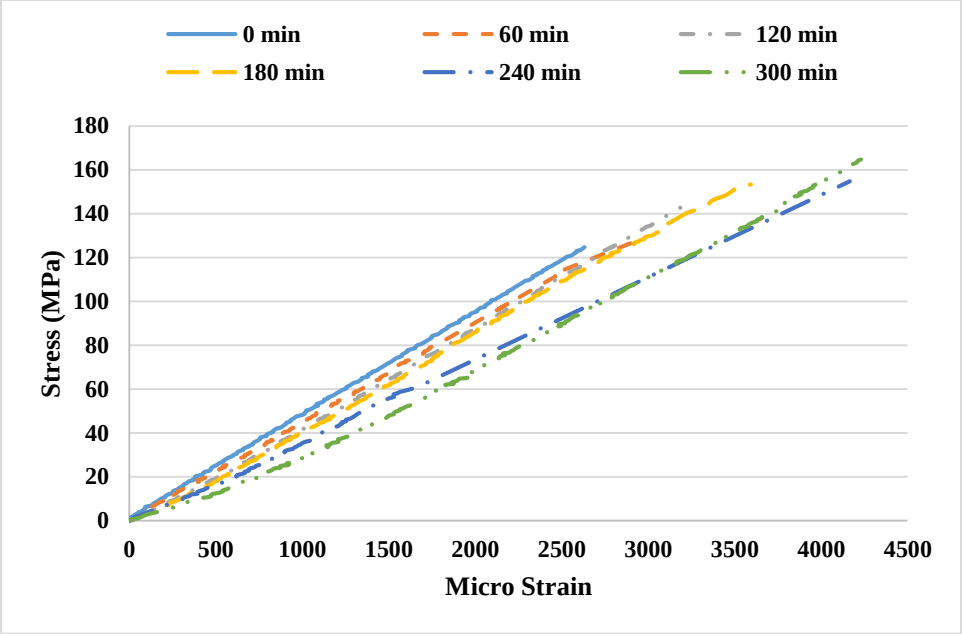

Figure 4.57: Stress-strain curves for MP01 for all exposure durations

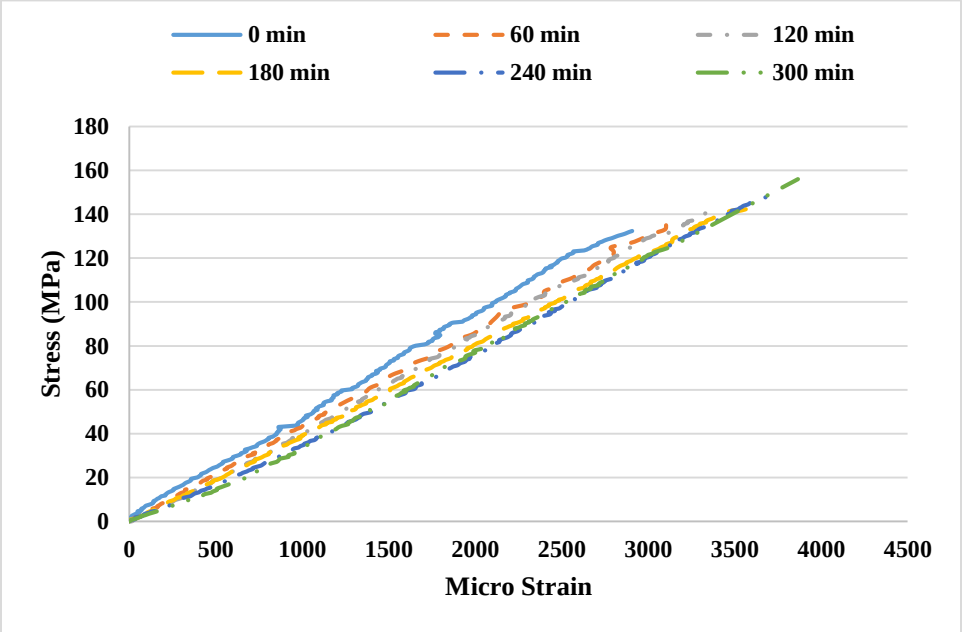

Figure 4.58: Stress-strain curves for MP02 for all exposure durations

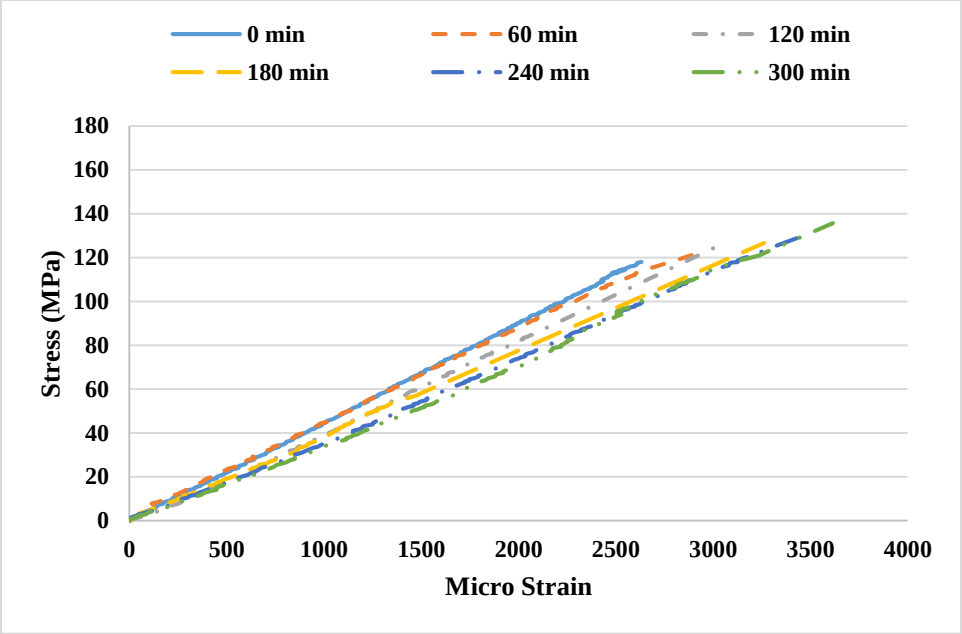

Figure 4.59: Stress-strain curves for MP03 for all exposure durations

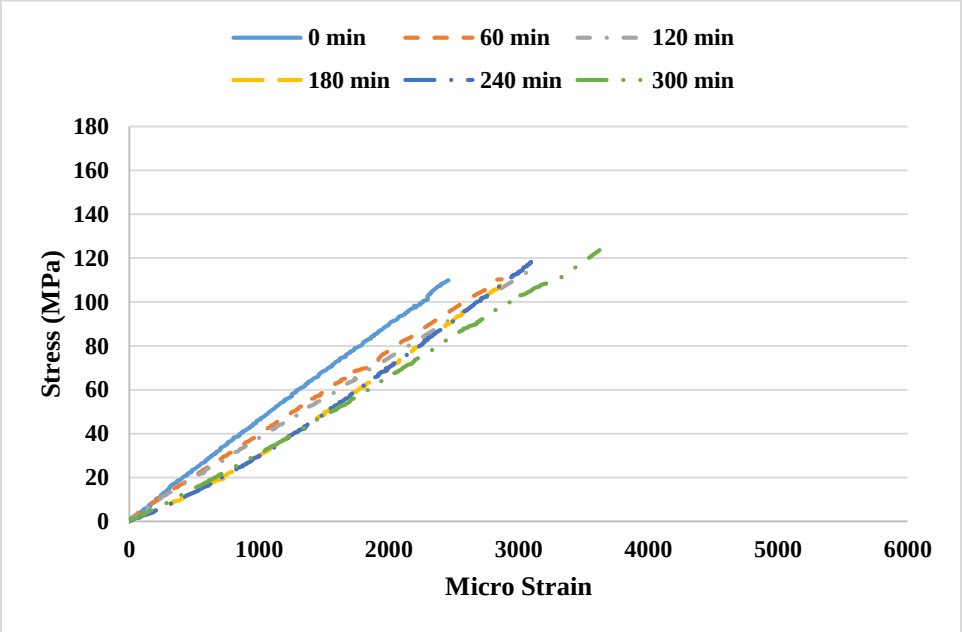

Figure 4.60: Stress-strain curves for MP04 for all exposure durations

It is observed from the data in Figures 4.57 through 4.60 that the stress-strain curves shifted downward with the increase of exposure duration, indicating that more deformation occurs

at the same stress level when the exposure duration is increased. With the increase of exposure durations, while slope of the stress-strain curves reduced, the peak strains increased. Therefore, reduction in modulus of elasticity took place with increase in the duration of exposure to elevated temperature. The stress-strain behavior was approximately similar for other two UHPC mixtures as well.

Average MOE of the control specimens and specimens subjected to elevated temperature of 300^{o}C for 60 min, 120 min, 180 min, 240 min and 300 min are summarized in the Table 4.37. The ratios of the MOE after a particular exposure duration to the MOE of control specimens (MOE_T/MOE) are summarized in Table 4.38. Based on the data presented in Tables 4.37 and 4.38, discussions were made regarding the effect of fiber content and duration of elevated temperature and the effect of type of UHPC on MOE.

Table 4.37: MOE of UHPC mixtures containing polypropylene fibers exposed to elevated temperatures

Mixture ID	MOE (GPa)					
	control	60 min	120 min	180 min	240 min	300 min
MP01	47.68	44.91	42.50	41.04	35.80	33.70
MP02	47.72	43.10	41.14	39.52	36.90	35.90
MP03	43.85	43.70	38.16	37.86	35.25	33.84
MP04	46.60	37.83	37.28	34.10	33.86	31.16
MPN1	45.74	43.41	42.13	40.53	40.99	34.27
MPN2	45.20	43.41	42.13	40.53	40.50	34.30
MPN3	45.29	40.41	36.68	36.55	36.37	33.02
MPN4	45.77	38.71	33.19	32.86	31.81	27.31
MPL1	43.65	43.39	42.77	41.91	36.47	31.71
MPL2	45.41	40.50	39.67	37.70	34.30	31.50
MPL3	45.17	40.74	37.43	35.51	31.48	29.14
MPL4	43.58	39.75	36.67	35.04	31.51	28.99

Table 4.38: MOE_T/MOE of UHPC mixtures containing polypropylene fibers exposed to elevated temperatures

Mixture ID	MOE_T/MOE				
	60 min	120 min	160 min	240 min	300 min
MP01	0.94	0.89	0.86	0.75	0.71
MP02	0.90	0.86	0.83	0.77	0.75
MP03	1.00	0.87	0.86	0.80	0.77
MP04	0.81	0.80	0.73	0.73	0.67
MPN1	0.95	0.92	0.89	0.90	0.75
MPN2	0.96	0.93	0.90	0.90	0.76
MPN3	0.89	0.81	0.81	0.80	0.73
MPN4	0.85	0.73	0.72	0.69	0.60
MPL1	0.99	0.98	0.96	0.84	0.73
MPL2	0.89	0.87	0.83	0.76	0.69
MPL3	0.90	0.83	0.79	0.70	0.65
MPL4	0.91	0.84	0.80	0.72	0.67

i. Effect of fiber content and duration of elevated temperature on MOE

The plots of MOE versus exposure duration data corresponding to different fiber contents are shown in Figures 4.61 through 4.63 for UHPC mixture with silica fume alone, blend of silica fume and natural pozzolana, and blend of silica fume and limestone powder, respectively.

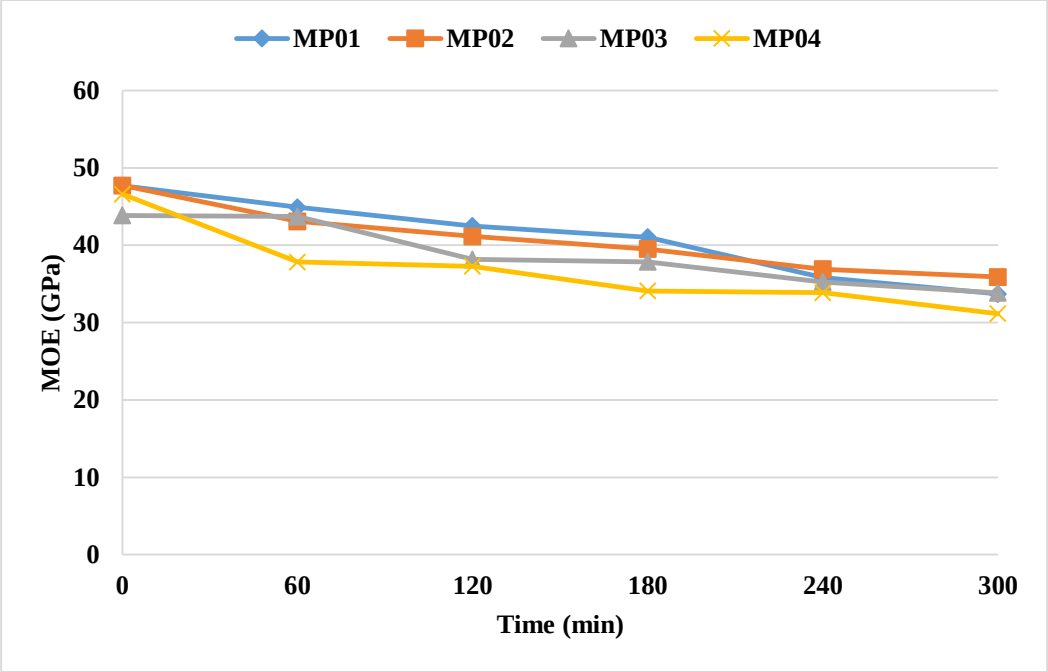

Figure 4.61: Variation of MOE with exposure duration for UHPC with silica fume and different polypropylene fiber contents

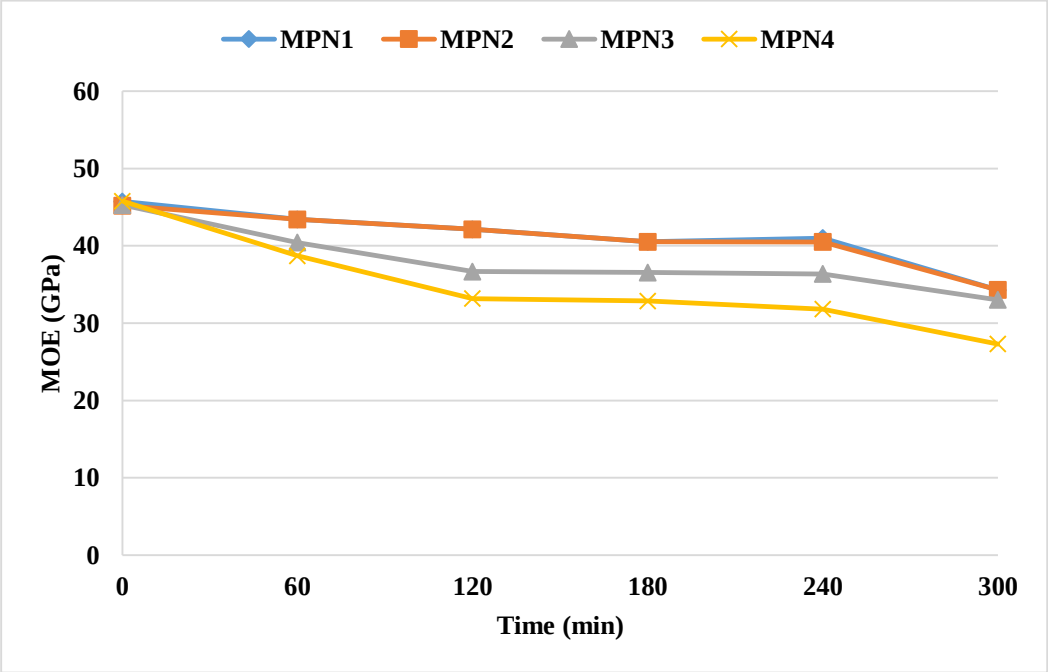

Figure 4.62: Variation of MOE with exposure duration for UHPC with blend of silica fume and natural pozzolana and different polypropylene fiber contents

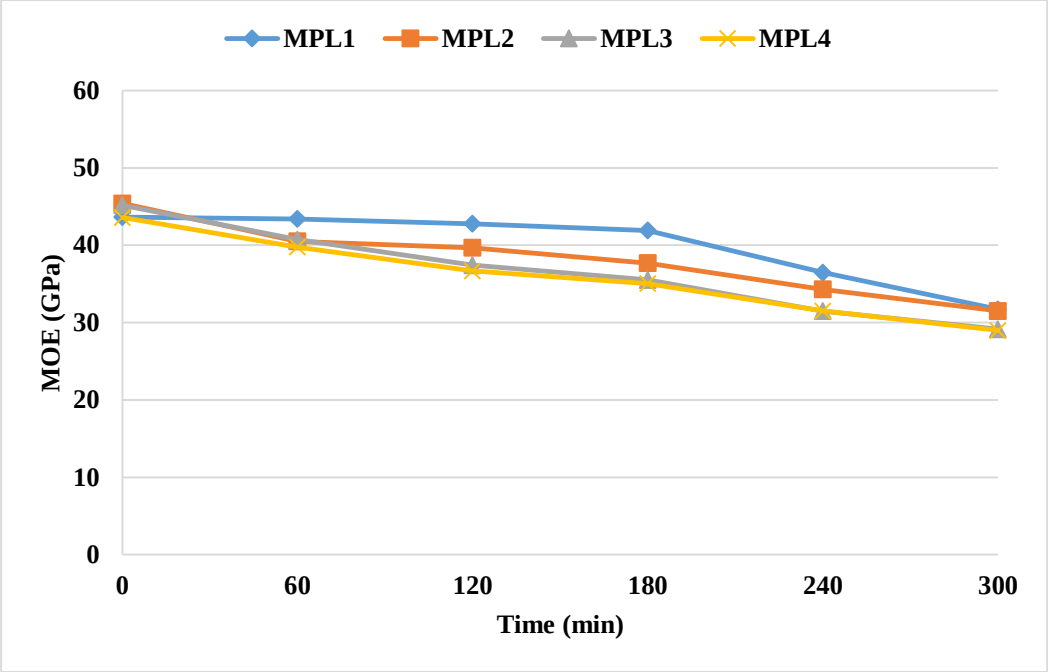

Figure 4.63: Variation of MOE with exposure duration for UHPC with blend of silica fume and limestone powder and different polypropylene fiber contents

It can be seen from the data in Figures 4.61 through 4.63 that in case of each type of UHPC mixture, the MOE is decreasing with the increase in exposure duration. It is observed from Table 4.38 that a decrease of 0 to 19% of MOE took place in first 60 minutes of exposure. The total decrease in MOE in 300 minutes of exposure is found to be in the range of 23 to 40%. The mixtures with more PP fiber content are losing the MOE more significantly as compared to the mixtures with less fiber content.

The analysis of variance (ANOVA) of the MOE data presented in Table 4.37 for all three UHPC mixtures are presented in Tables 4.39 through 4.41.

Table 4.39: ANOVA table for MOE of polypropylene fibers reinforced UHPC mixture with silica fume only

Source of variation	SS	DOF	MS	F	P	F_{cr}	Significance criteria P< 0.05 and F > F_{cr}
Exposure duration	436.5	5	87.3	39.5	4.07×10^{-08}	2.9	**Significant**
Fiber content	67.1	3	22.4	10.1	6.77×10^{-04}	3.3	**Significant**
Error	33.1	15	2.2				
Total	536.7	23					

Table 4.40: ANOVA table for MOE of polypropylene fibers reinforced UHPC mixture with silica fume and natural pozzolana

Source of variation	SS	DOF	MS	F	P	F_{cr}	Significance criteria P< 0.05 and F > F_{cr}
Exposure duration	394.8	5	79.0	25.1	8.74×10^{-07}	2.9	**Significant**
Fiber content	156.0	3	52.0	16.5	5.13×10^{-05}	3.3	**Significant**
Error	47.3	15	3.2				
Total	598.1	23					

Table 4.41: ANOVA table for MOE of polypropylene fibers reinforced UHPC mixture with silica fume and limestone powder

Source of variation	SS	DOF	MS	F	P	F_{cr}	Significance criteria P< 0.05 and F > F_{cr}
Exposure duration	526.4	5	105.3	58.0	2.80×10^{-09}	2.9	**Significant**
Fiber content	59.1	3	19.7	10.9	4.78×10^{-04}	3.3	**Significant**
Error	27.2	15	1.8				
Total	612.7	23					

From the ANOVA results, as presented in Tables 4.39 through 4.41, it can be observed that for all three UHPC mixtures, both exposure duration as well as fiber content have significant effect on MOE. However, the exposure duration, having a very high F-value and very low P-value as compared to that for fiber content, has stronger effect on the MOE.

Empirical model for MOE in terms of exposure duration and fiber content, as obtained through regression analysis, is given as:

$$MOE = a + b(T) + c(T^2) + d(F) + e(F^2)$$

Where:

MOE is modulus of elasticity (GPa)

a, b, c, d and *e* are regression coefficients, as given in Table 4.42 for all three UHPC mixtures

T is exposure duration (0, 60, 120, 180, 240, and 360 minutes)

F is fiber content (0.1, 0.2, 0.3, and 0.4% by mass of mixture)

Table 4.42: Values of regression coefficients for MOE of UHPC mixtures with polypropylene fibers

UHPC mixture	***a***	***b***	***c***	***d***	***e***	R^2
Mixture with silica fume only	47.5	-0.0577	0.0001	7.5	-43.7	0.93
Mixture with silica fume and natural pozzolana	46.5	-0.0455	0.0000	15.1	-73.6	0.86
Mixture with silica fume and limestone powder	48.9	-0.0344	-0.0000	-28.1	28.7	0.95

High value of regression coefficient, R^2, for each of the UHPC mixtures, as shown in Table 4.42, indicate a high degree of fit of the data. These derived models can be used to predict the MOE for a given set of exposure duration and fiber content.

ii. Effect of type of UHPC mixture on MOE

The plots of MOE of three UHPC mixtures at different exposure durations are shown in Figures 4.64 through 4.67, for 0.1, 0.2, 0.3, and 0.4%, respectively. It can be observed from Figures 4.64 through 4.67 that at any exposure duration and fiber content, there is not much difference between the MOE of the three mixtures. Therefore, it can be concluded that the performance of all three UHPC is comparable.

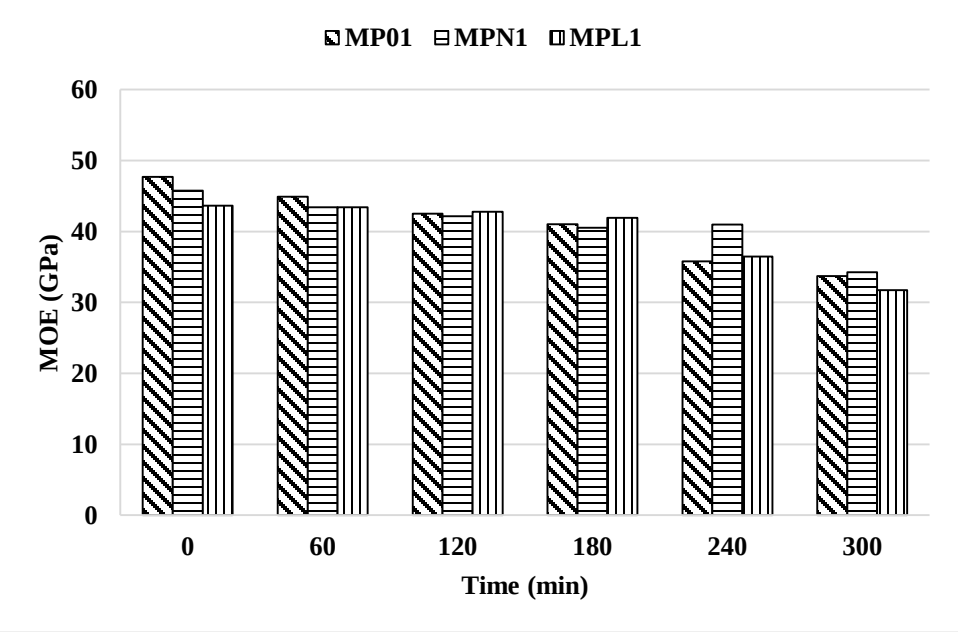

Figure 4.64: MOE vs exposure duration for UHPC mixtures with 0.1% polypropylene fibers

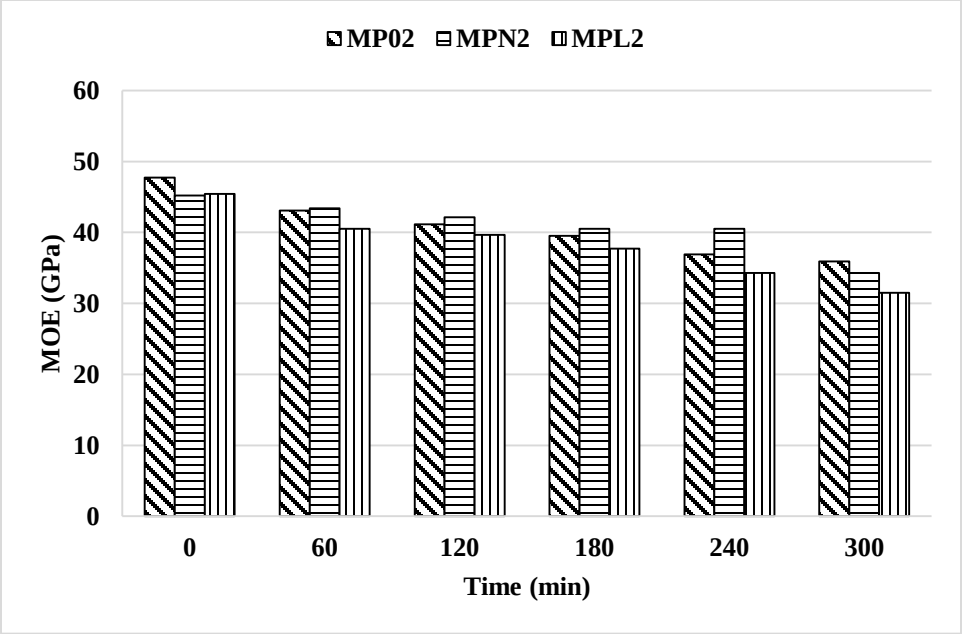

Figure 4.65: MOE vs exposure duration for UHPC mixtures with 0.2% polypropylene fibers

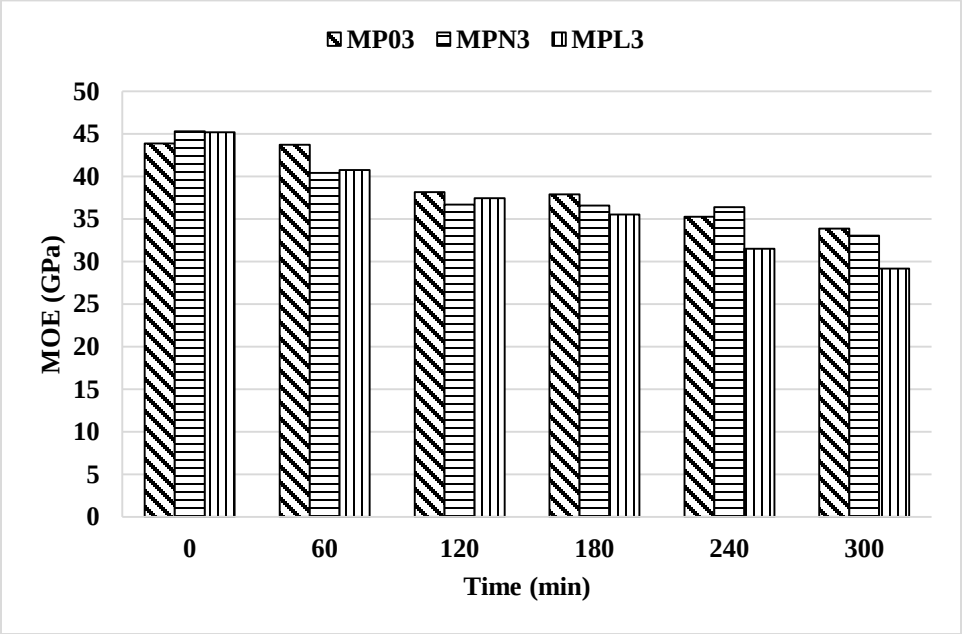

Figure 4.66: MOE vs exposure duration for UHPC mixtures with 0.3% polypropylene fibers

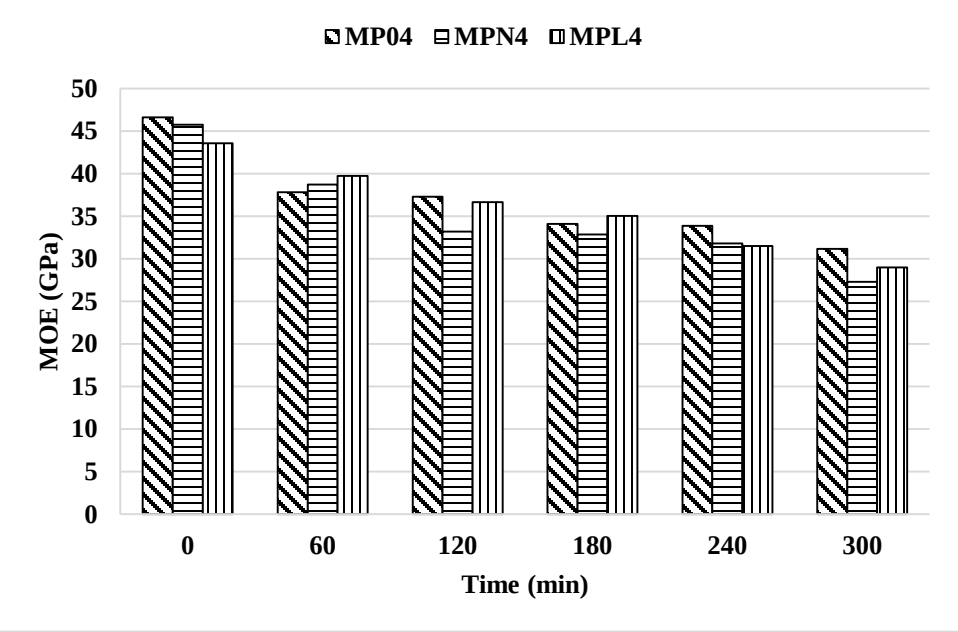

Figure 4.67: MOE vs exposure duration for UHPC mixtures with 0.4% polypropylene fibers

4.2.3 Energy Absorption Capacity (Modulus of Toughness)

Average energy absorption capacity (modulus of toughness in compression) of the control specimens and specimens subjected to elevated temperature of 300^{o}C for 60 min, 120 min, 180 min, 240 min and 300 min are summarized in the Table 4.43. The ratios of the modulus of toughness after a particular exposure duration to the modulus of toughness of control specimens (MOT_T/MOT) are summarized in Table 4.44. Based on the data presented in Tables 4.43 and 4.44, discussions were made regarding the effect of fiber content and duration of elevated temperature and the effect of type of UHPC on energy absorption capacity.

Table 4.43: MOT of UHPC mixtures containing polypropylene fibers exposed to elevated temperatures

Mixture ID	MOT (kJ/m^3)					
	control	60 min	120 min	180 min	240 min	300 min
MP01	149	210	223	280	319	357
MP02	216	216	245	258	292	297
MP03	170	190	183	207	221	242
MP04	138	164	180	166	174	220
MPN1	142	183	187	250	252	275
MPN2	173	182	190	224	218	228
MPN3	151	165	175	191	185	199
MPN4	120	145	174	161	169	188
MPL1	144	212	239	281	329	350
MPL2	183	203	227	255	285	295
MPL3	155	182	206	221	263	274
MPL4	132	149	179	195	232	218

Table 4.44: MOT_T/MOT of UHPC mixtures containing polypropylene fibers exposed to elevated temperatures

Mixture ID	MOT_T/MOT				
	60 min	120 min	180 min	240 min	300 min
MP01	1.41	1.50	1.88	2.14	2.40
MP02	1.00	1.14	1.20	1.35	1.38
MP03	1.12	1.08	1.22	1.30	1.43
MP04	1.19	1.30	1.20	1.26	1.59
MPN1	1.29	1.32	1.76	1.78	1.93
MPN2	1.05	1.10	1.29	1.26	1.31
MPN3	1.09	1.16	1.27	1.23	1.32
MPN4	1.21	1.45	1.35	1.41	1.57
MPL1	1.47	1.65	1.94	2.28	2.43
MPL2	1.11	1.24	1.39	1.55	1.61
MPL3	1.17	1.32	1.42	1.69	1.77
MPL4	1.13	1.36	1.48	1.76	1.65

i. Effect of fiber content and duration of elevated temperature on MOT

The plots of MOT versus exposure duration data corresponding to different fiber contents are shown in Figures 4.68 through 4.70 for UHPC mixture with silica fume alone, blend of silica fume and natural pozzolana, and blend of silica fume and limestone powder, respectively.

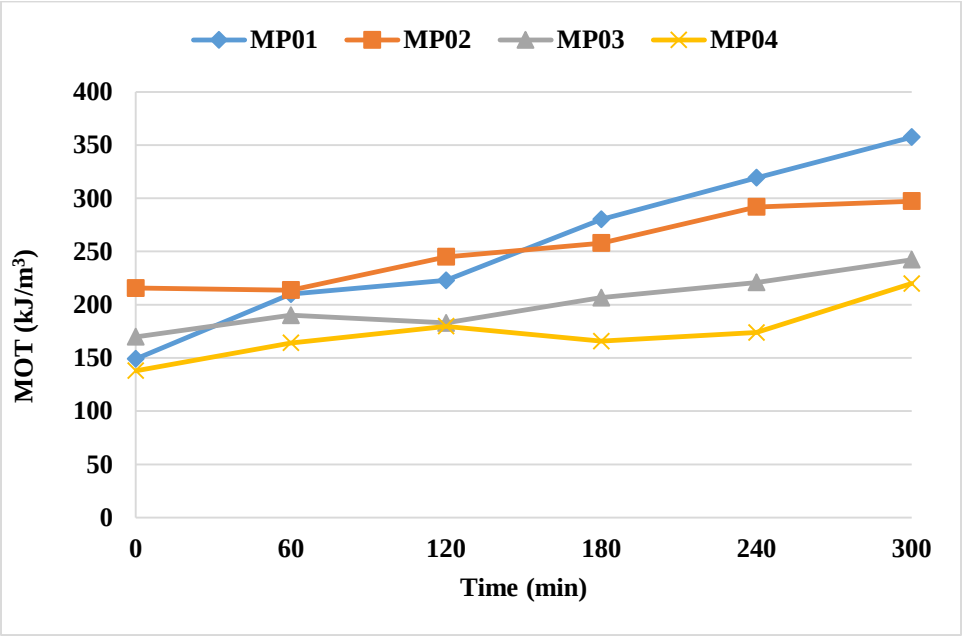

Figure 4.68: Variation of MOT with exposure duration for UHPC with silica fume and different polypropylene fiber contents

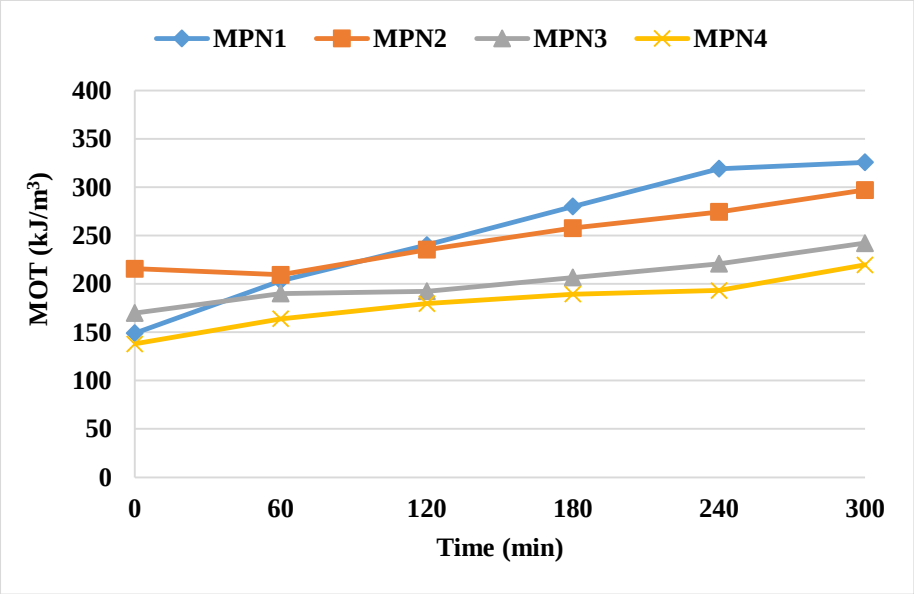

Figure 4.69: Variation of MOT with exposure duration for UHPC with blend of silica fume and natural pozzolana and different polypropylene fiber contents

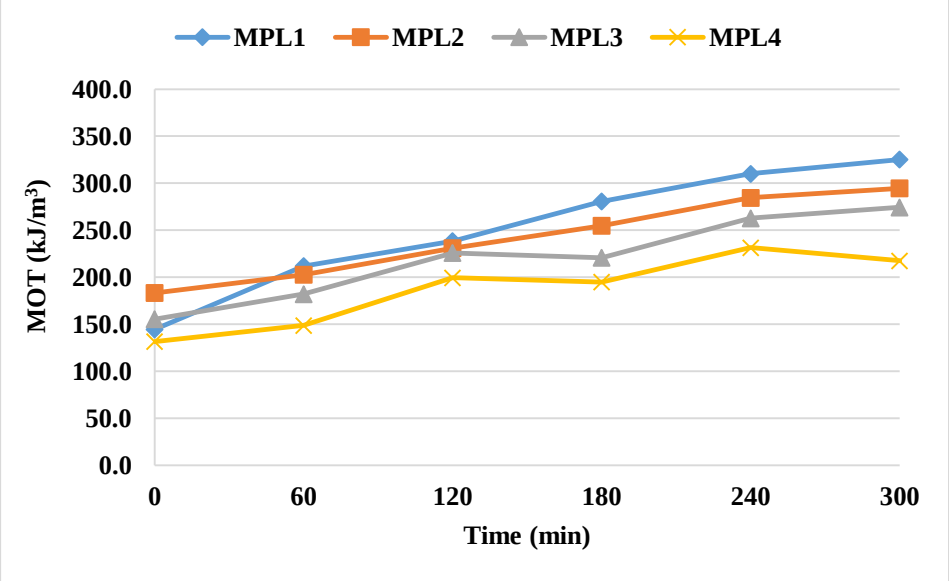

Figure 4.70: Variation of MOT with exposure duration for UHPC with blend of silica fume and limestone powder and different polypropylene fiber contents

It can be seen from the data in Figures 4.68 through 4.70 that in case of each type of UHPC mixture, the MOT is increasing with the increase in exposure duration. It is observed from Table 4.44 that an increase of 0 to 47% of MOT took place in first 60 minutes of exposure.

The total increase in MOT in 300 minutes of exposure is found to be in the range of 31 to 143%.

The analysis of variance (ANOVA) of the energy absorption capacity data presented in Table 4.43 for all three UHPC mixtures are presented in Tables 4.45 through 4.47.

Table 4.45: ANOVA table for MOT of polypropylene fibers reinforced UHPC mixture with silica fume only

Source of variation	SS	DOF	MS	F	P	F_{cr}	Significance criteria P< 0.05 and F > F_{cr}
Exposure duration	32140.1	5	6428.0	8.7	4.7×10^{-04}	2.9	**Significant**
Fiber content	29571.6	3	9857.2	13.4	1.6×10^{-04}	3.3	**Significant**
Error	11020.8	15	734.7				
Total	72732.4	23					

Table 4.46: ANOVA table for MOT of polypropylene fibers reinforced UHPC mixture with silica fume and natural pozzolana

Source of variation	SS	DOF	MS	F	P	F_{cr}	Significance criteria P< 0.05 and F > F_{cr}
Exposure duration	15905.1	5	3181.0	10.4	1.9×10^{-04}	2.9	**Significant**
Fiber content	10996.1	3	3665.4	12.0	2.9×10^{-04}	3.3	**Significant**
Error	4594.5	15	306.3				
Total	31495.7	23					

Table 4.47: ANOVA table for MOT of polypropylene fibers reinforced UHPC mixture with silica fume and limestone powder

Source of variation	SS	DOF	MS	F	P	F_{cr}	Significance criteria P< 0.05 and F > F_{cr}
Exposure duration	52407.1	5	10481.4	31.0	2.1×10^{-07}	2.9	**Significant**
Fiber content	19046.4	3	6348.8	18.8	2.4×10^{-05}	3.3	**Significant**
Error	5072.8	15	338.2				
Total	76526.3	23					

From the ANOVA results, as presented in Tables 4.45 through 4.47, it can be observed that for all three UHPC mixtures, both exposure duration as well as fiber content have significant effect on MOT

Empirical model for MOT in terms of exposure duration and fiber content, as obtained through regression analysis, is given as:

$$MOT = a + b(T) + c(T^2) + d(F) + e(F^2)$$

Where:

MOT is modulus of toughness (kJ/m^3)

a, b, c, d and *e* are regression coefficients, as given in Table 4.48 for all three UHPC mixtures

T is exposure duration (0, 60, 120, 180, 240, and 360 minutes)

F is fiber content (0.1, 0.2, 0.3, and 0.4% by mass of mixture)

Table 4.48: Values of regression coefficients for MOT of UHPC mixtures with polypropylene fibers

UHPC mixture	*a*	*b*	*c*	*d*	*e*	R^2
Mixture with silica fume only	214.0	0.281	0.000247	20.5	-641.7	0.82
Mixture with silica fume and natural pozzolana	187.4	0.368	-0.00041	-119.8	-140.4	0.84
Mixture with silica fume and limestone powder	196.6	0.565	-0.00038	-63.1	-373.3	0.93

A high value of regression coefficient, R^2, for each of the UHPC mixtures, as shown in Table 4.48, indicate a high degree of fit of the data. These derived models can be used to predict the energy absorption capacity for a given set of exposure duration and fiber content.

4.2.4 Flexural Strength

a) Failure modes in flexural strength test

Figures 4.71 and 4.72 show failure modes of control specimens with 0.1 and 0.4% polypropylene fibers, respectively, when subjected to flexural testing. It was observed that the failure was ductile for control specimens of all mixtures with different fiber contents. Normally, a single crack developed and the same crack propagated with the increase in load.

Figure 4.71: Typical ductile flexural failure of control specimen with 0.1% polypropylene fibers

Figure 4.72: Typical ductile flexural failure of control specimen with 0.4% polypropylene fibers

Figure 4.73 shows failure mode of a typical polypropylene-reinforced UHPC specimen subjected to flexural testing after exposure to the elevated temperature. Unlike the control specimens, the specimens of all polypropylene-reinforced UHPC mixtures subjected to elevated temperature showed a brittle failure, as typically seen from Figure 4.73, as a result of loss of fibers due to melting. It can be further noted from Figure 4.73 that there are no fibers visible confirming the melting of the polypropylene fibers due to temperature exposure.

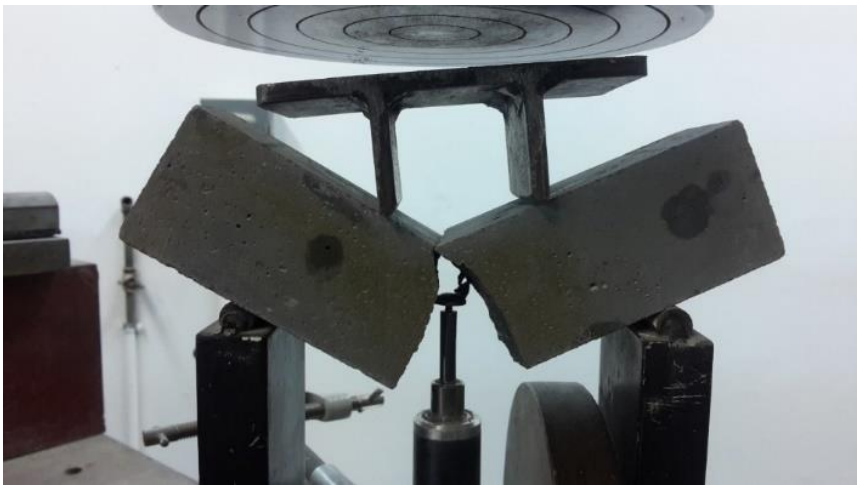

Figure 4.73: Typical flexural failure of specimen exposed to elevated temperatures

The ductile failure of control specimens and brittle failure of specimens exposed to elevated temperature are evident also from the plots of load deflection curves, as shown in Figure 4.74.

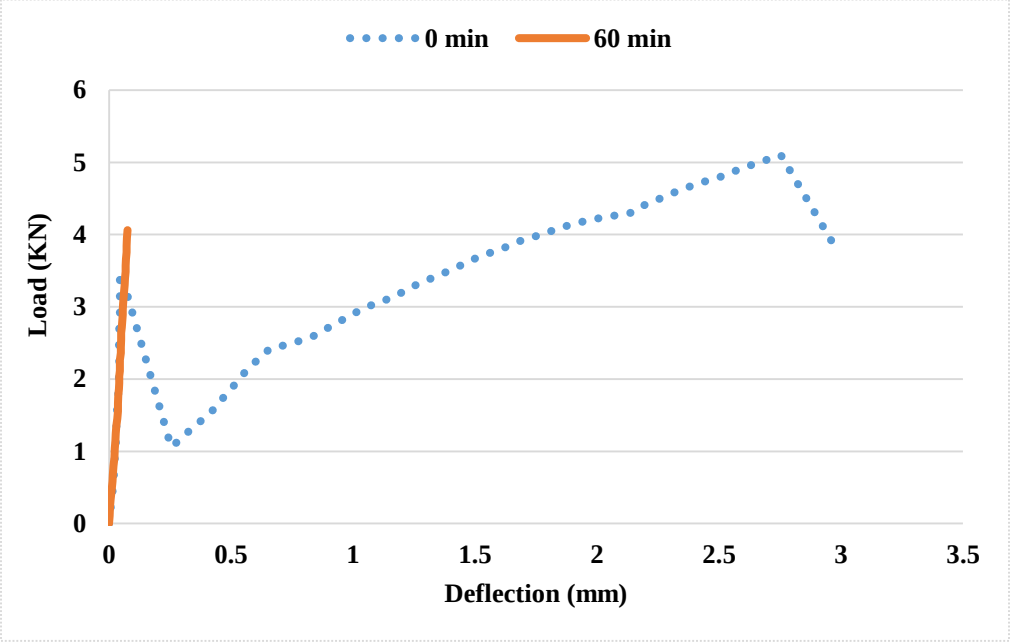

Figure 4.74: Typical load-deflection curves obtained through flexure tests of control and heated specimens

b) Flexural strength test results

Average modulus of rupture (MOR) of the control specimens and specimens subjected to elevated temperature of 300^{o}C for 60 min, 120 min, 180 min, 240 min and 300 min are summarized in Table 4.49. The ratios of the MOR after a particular exposure duration to the MOR of control specimens (MOR_T/MOR) are presented in Table 4.49. Based on the data presented in Tables 4.49 and 4.50, discussions were made regarding the effect of fiber content and duration of elevated temperature and the effect of type of UHPC on MOR.

Table 4.49: MOR of UHPC mixtures containing polypropylene fibers exposed to elevated temperatures

Mixture ID	MOR (MPa)					
	control	60 min	120 min	180 min	240 min	300 min
MP01	10.62	13.89	11.00	9.92	9.82	9.44
MP02	10.70	12.85	11.61	9.73	9.50	9.19
MP03	11.25	11.81	10.63	9.70	9.40	9.40
MP04	12.05	12.10	10.41	9.05	9.01	8.52
MPN1	9.20	11.80	10.30	9.72	9.70	9.04
MPN2	9.43	12.52	10.58	9.65	9.40	9.07
MPN3	10.89	11.39	9.82	9.02	9.15	9.10
MPN4	11.44	11.56	9.57	9.09	8.65	8.55
MPL1	9.77	12.41	10.91	9.77	9.72	9.14
MPL2	10.32	12.41	11.33	9.68	9.23	9.14
MPL3	10.94	11.45	9.78	9.57	9.39	9.04
MPL4	12.02	12.10	10.19	9.01	8.88	8.70

Table 4.50: MOR_T/MOR of UHPC mixtures containing polypropylene fibers exposed to elevated temperatures

Mixture ID	MOR_T/MOR				
	60 min	120 min	160 min	240 min	300 min
MP01	1.31	1.04	0.93	0.92	0.89
MP02	1.20	1.09	0.91	0.89	0.86
MP03	1.05	0.94	0.86	0.84	0.84
MP04	1.00	0.86	0.75	0.75	0.71
MPN1	1.28	1.12	1.06	1.05	0.98
MPN2	1.33	1.12	1.02	1.00	0.96
MPN3	1.05	0.90	0.83	0.84	0.84
MPN4	1.01	0.84	0.79	0.76	0.75
MPL1	1.27	1.12	1.00	0.99	0.94
MPL2	1.20	1.10	0.94	0.89	0.89
MPL3	1.05	0.89	0.87	0.86	0.83
MPL4	1.01	0.85	0.75	0.74	0.72

i. Effect of fiber content and duration of elevated temperature on MOR

The plots of MOR versus exposure duration data corresponding to different fiber contents are shown in Figures 4.75 through 4.77 for UHPC mixture with silica fume alone, blend of silica fume and natural pozzolana, and blend of silica fume and limestone powder, respectively.

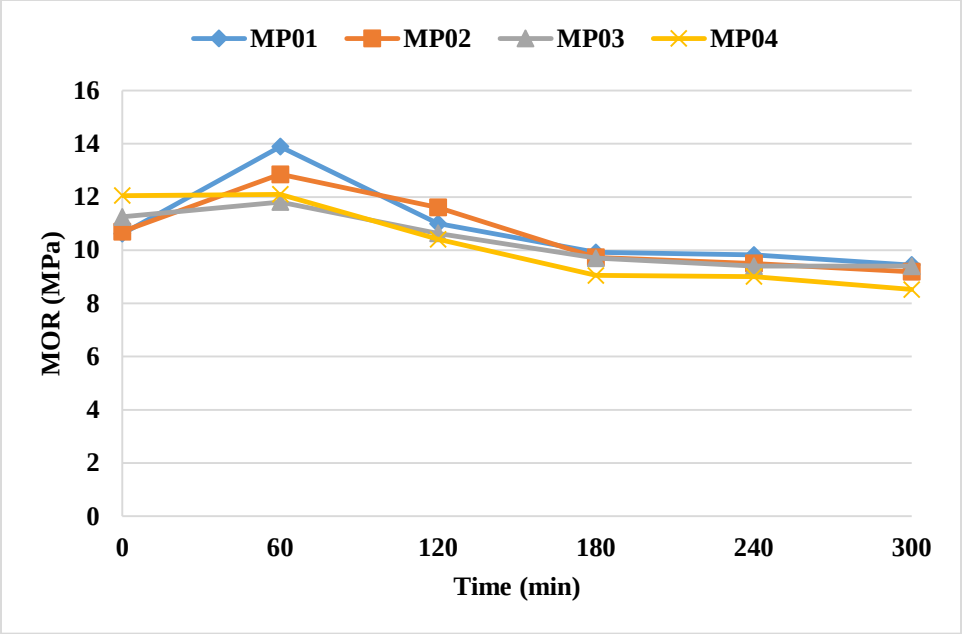

Figure 4.75: Variation of MOR with exposure duration for UHPC with silica fume and different polypropylene fiber contents

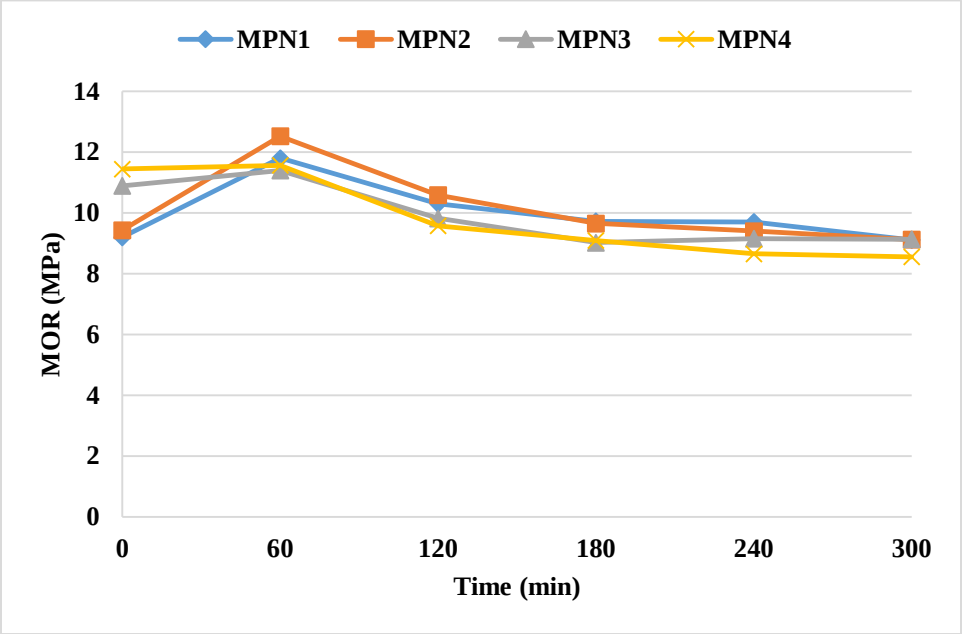

Figure 4.76: Variation of MOR with exposure duration for UHPC with blend of silica fume and natural pozzolana and different polypropylene fiber contents

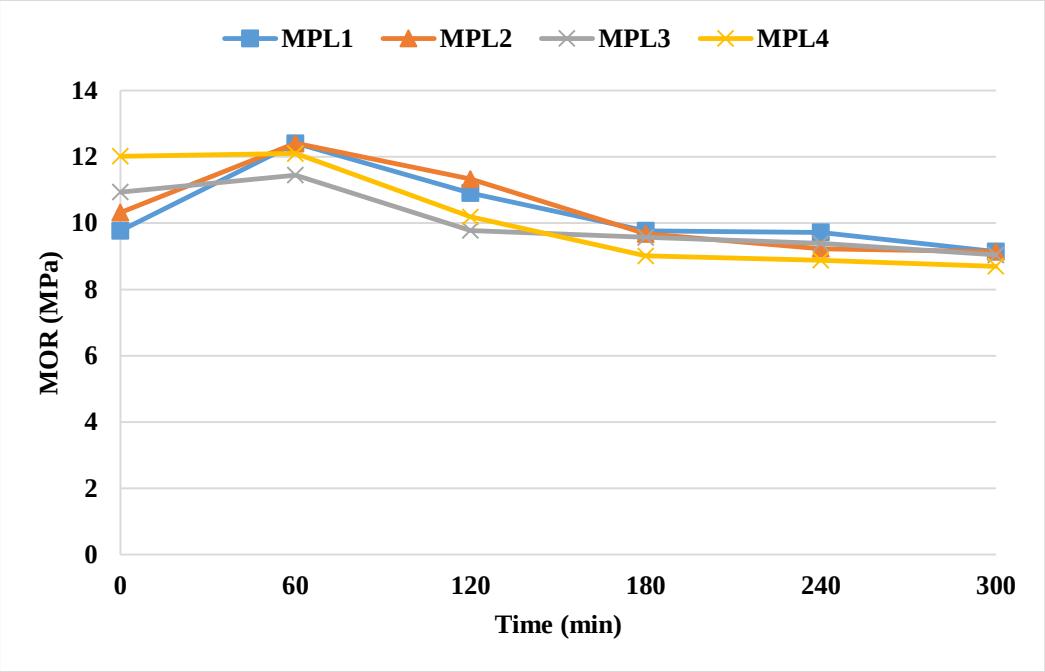

Figure 4.77: Variation of MOR with exposure duration for UHPC with blend of silica fume and limestone powder and different polypropylene fiber contents

It can be seen from the data in Figures 4.75 through 4.77 that for control specimens, the MOR of the specimens with higher fiber content was slightly higher showing the effect of fiber content on MOR without exposure to the elevated temperature. After 60 minutes of exposure to elevated temperature, the specimens of each type of UHPC mixture showed an increased MOR. It is noted from Table 4.50 that an increase of 0 to 31% of strength took place in first 60 minutes of exposure. However, beyond 60 minutes of exposure, the MOR decreased with the increase of exposure duration. After 300 minutes of exposure, the strength decreased to 2 to 29%. The fiber content has a negligible effect on MOR. The increase in MOR up to 60 minutes of exposure is due positive heat-curing effect on densification of concrete matrix. However, the formation of micro cracks and melting of polypropylene fibers at longer exposure duration caused the reduction in MOR.

The analysis of variance (ANOVA) of the MOR data presented in Table 4.49 for all three UHPC mixtures are presented in Tables 4.51 through 4.53.

Table 4.51: ANOVA table for MOR of polypropylene fibers reinforced UHPC mixture with silica fume only

Source of variation	SS	DOF	MS	F	P	F_{cr}	Significance criteria P< 0.05 and F > F_{cr}
Exposure duration	36.3	5	7.26	22.6	1.70×10^{-06}	2.9	**Significant**
Fiber content	1.21	3	0.40	1.26	3.24×10^{-01}	3.2	**Insignificant**
Error	4.81	15	0.32				
Total	42.3	23					

Table 4.52: ANOVA table for MOR of polypropylene fibers reinforced UHPC mixture with silica fume and natural pozzolana

Source of variation	SS	DOF	MS	F	P	F_{cr}	Significance criteria P< 0.05 and F > F_{cr}
Exposure duration	21.6	5	4.3	10.9	1.39×10^{-04}	2.90	**Significant**
Fiber content	0.3	3	0.1	0.26	8.56×10^{-01}	3.29	**Insignificant**
Error	5.9	15	0.4				
Total	27.8	23					

Table 4.53: ANOVA table for MOR of polypropylene fibers reinforced UHPC mixture with silica fume and limestone powder

Source of variation	SS	DOF	MS	F	P	F_{cr}	Significance criteria P< 0.05 and F > F_{cr}
Exposure duration	26.9	5	5.4	15.1	2.13×10^{-05}	2.9	**Significant**
Fiber content	0.37	3	0.12	0.4	7.89×10^{-01}	3.2	**Insignificant**
Error	5.34	15	0.36				
Total	32.6	23					

From the ANOVA results, as presented in Tables 4.51 through 4.53, it can be observed that for all three UHPC mixtures, exposure duration has a significant effect on MOR due to a very high F-value and very low P-value. However, the effect of fiber content is insignificant on MOR.

Empirical model for MOR in terms of exposure duration and fiber content, as obtained through regression analysis, is given as:

$$MOR = a + b(T) + c(T^2) + d(F) + e(F^2)$$

Where:

MOR is modulus of rupture (MPa)

a, *b*, *c*, *d* and *e* are regression coefficients, as given in Table 4.54 for all three UHPC mixtures

T is exposure duration (0, 60, 120, 180, 240, and 360 minutes)

F is fiber content (0.1, 0.2, 0.3, and 0.4% by mass of mixture)

Table 4.54: Values of regression coefficients for MOR of UHPC mixtures with polypropylene fibers

UHPC mixture	*a*	*b*	*c*	*d*	*e*	R^2
Mixture with silica fume only	12.3	-0.00605	-0.00001	-2.1317	0.250	0.64
Mixture with silica fume and natural pozzolana	10.7	-0.00302	-0.00001	2.2358	-5.875	0.47
Mixture with silica fume and limestone powder	11.6	-0.00450	-0.00001	-1.44167	1.41667	0.60

A low value of regression coefficient, R^2, for each of the UHPC mixtures, as shown in Table 4.54, indicate lack of fit of the data.

ii. Effect of type of UHPC mixture on MOR

The plots of MOR of three UHPC mixtures at different exposure durations are shown in Figures 4.78 through 4.80, for 0.1, 0.2, 0.3, and 0.4%, respectively. It can be observed from the data in Figure 4.78 through 4.80 that at any exposure duration and fiber content, there is not much difference between the MOR of the three mixtures. Therefore, it can be concluded that the performance of all three UHPC is comparable.

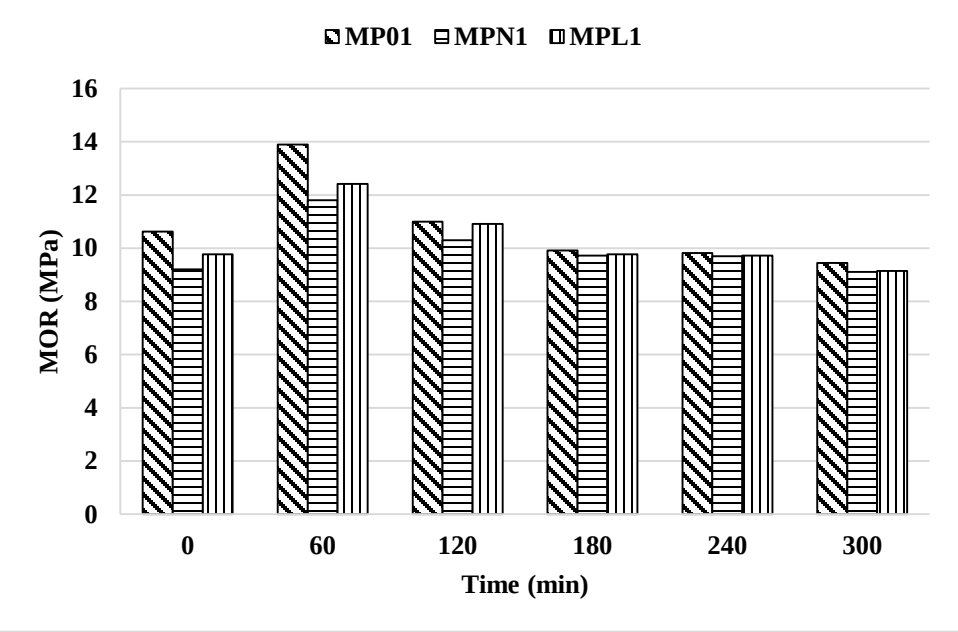

Figure 4.78: MOR vs exposure duration for UHPC mixtures with 0.1% polypropylene fibers

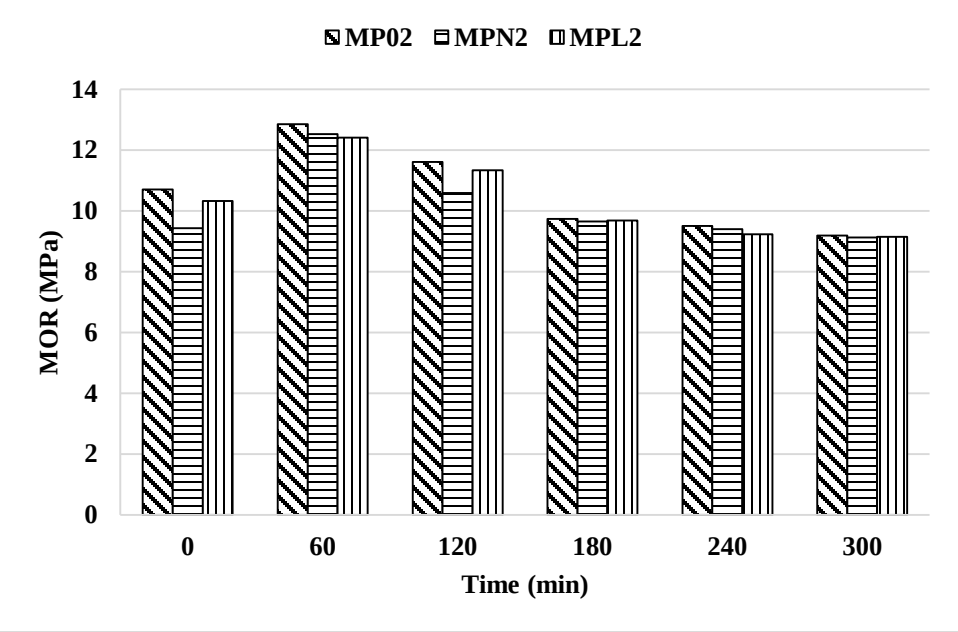

Figure 4.79: MOR vs exposure duration for UHPC mixtures with 0.2% polypropylene fibers

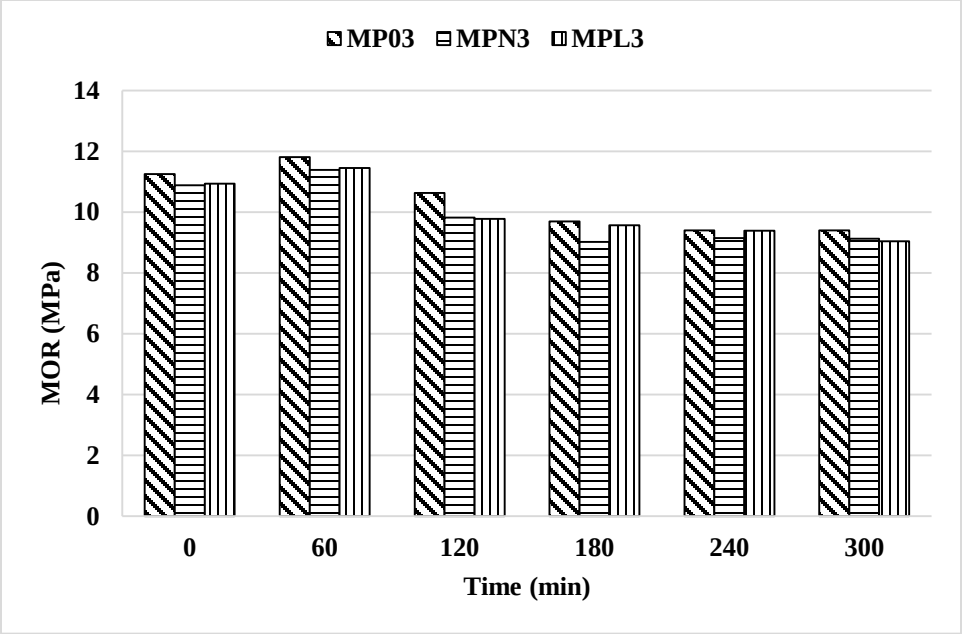

Figure 4.80: MOR vs exposure duration for UHPC mixtures with 0.3% polypropylene fibers

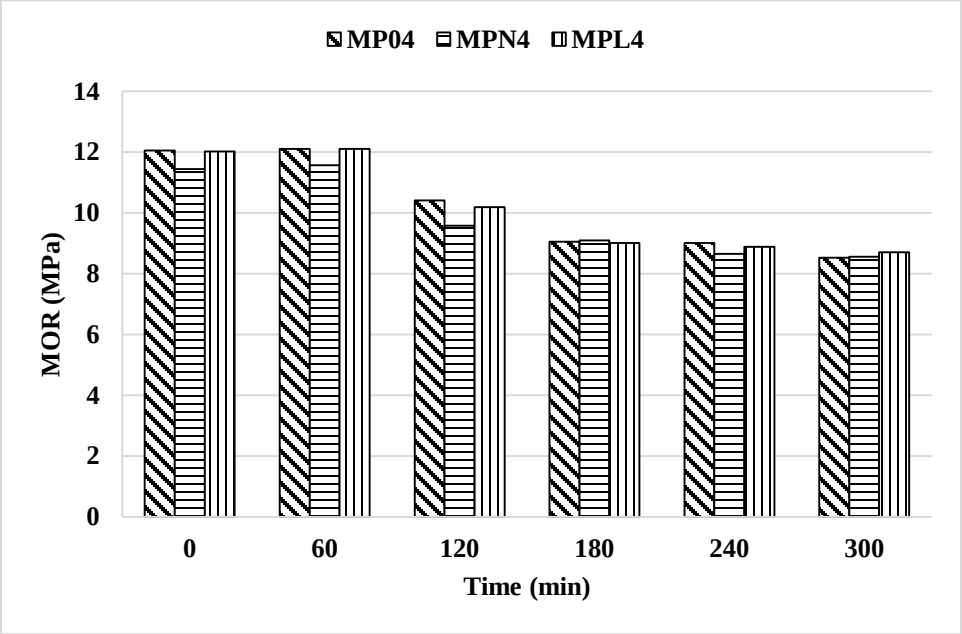

Figure 4.81: MOR vs exposure duration for UHPC mixtures with 0.4% polypropylene fibers

4.2.5 Splitting Tensile Strength

a) Failure modes in slitting tensile strength test

Figure 4.82 is showing failure modes of control specimens subjected to splitting tensile strength test. At peak load, only fine cracks were developed without any splitting of the specimens confirming that the failure was ductile for the specimens of all UHPC mixtures with different fiber contents.

Figure 4.82: Typical splitting failure of control specimens

Figure 4.83 is showing failure modes of specimens subjected to 60 minutes of exposure and tested for splitting tensile strength. It can be observed that at the peak load, the specimens after 60 minutes of exposure had more damage than that of control specimens, however, remained intact without a clear splitting indicating that still some polypropylene fibers were present inside the core of the concrete.

Figure 4.83: Typical splitting failure of specimens subjected to 60 minutes of exposure

Figure 4.84 is showing failure modes of specimens subjected to more than 60 minutes of exposure and tested for splitting tensile strength. It can be observed that at the peak load, the specimens after more than 60 minutes of exposure had clear splitting indicating that all polypropylene fibers were lost due to melting and mixtures turned to be brittle.

Figure 4.84: Typical splitting failure of specimens subjected to more than 60 minutes of exposures

b) Splitting tensile strength test results

Average splitting tensile strength of the control specimens and specimens subjected to elevated temperature of 300^{o}C for 60 min, 120 min, 180 min, 240 min and 300 min are presented in the Table 4.55. The ratios of the splitting tensile strength after a particular exposure duration to the splitting tensile strength of control specimens $(f_{st})_T/f_{st}$ are presented in Table 4.56. Based on the data presented in Tables 4.55 and 4.56, discussions were made regarding the effect of fiber content and duration of elevated temperature and the effect of type of UHPC on splitting tensile strength.

Table 4.55: Splitting tensile strength of UHPC mixtures containing polypropylene fibers exposed to elevated temperatures

Mixture ID	Splitting tensile strength, f_{st}, (MPa)					
	control	60 min	120 min	180 min	240 min	300 min
MP01	10.33	12.98	11.59	10.3	9.6	8.86
MP02	10.34	12.63	11.3	10.12	9.9	9.26
MP03	10.99	12.81	10.63	10.1	9.56	9.12
MP04	12.02	12.43	10.67	9.38	9.32	9.13
MPN1	10.08	11.99	10.71	9.26	8.88	8.20
MPN2	10.23	12.56	10.37	9.88	9.4	9.17
MPN3	10.94	12.44	10.07	9.96	9.56	8.66
MPN4	11.57	12.02	10.4	9.23	8.76	8.52
MPL1	10.10	12.41	10.18	9.33	9.02	8.65
MPL2	10.12	12.41	11.17	9.86	9.25	9.23
MPL3	10.89	12.64	10.59	9.35	8.95	8.20
MPL4	11.87	12.11	10.19	9.50	9.12	8.99

Table 4.56: $(f_{st})_T/f_{st}$ of UHPC mixtures containing polypropylene fibers exposed to elevated temperatures

Mixture ID	$(f_{st})_T/f_{st}$				
	60 min	**120 min**	**160 min**	**240 min**	**300 min**
MP01	1.26	1.12	1.00	0.93	0.86
MP02	1.22	1.09	0.98	0.96	0.90
MP03	1.17	0.97	0.92	0.87	0.83
MP04	1.03	0.89	0.78	0.78	0.76
MPN1	1.19	1.06	0.92	0.88	0.81
MPN2	1.23	1.01	0.97	0.92	0.90
MPN3	1.14	0.92	0.91	0.87	0.79
MPN4	1.04	0.90	0.80	0.76	0.74
MPL1	1.23	1.01	0.92	0.89	0.86
MPL2	1.23	1.10	0.97	0.91	0.91
MPL3	1.16	0.97	0.86	0.82	0.75
MPL4	1.02	0.86	0.80	0.77	0.76

i. Effect of fiber content and duration of elevated temperature on splitting tensile strength

The plots of splitting tensile strength versus exposure duration data corresponding to different fiber contents are shown in Figures 4.85 through 4.87 for UHPC mixture with silica fume alone, blend of silica fume and natural pozzolana, and blend of silica fume and limestone powder, respectively.

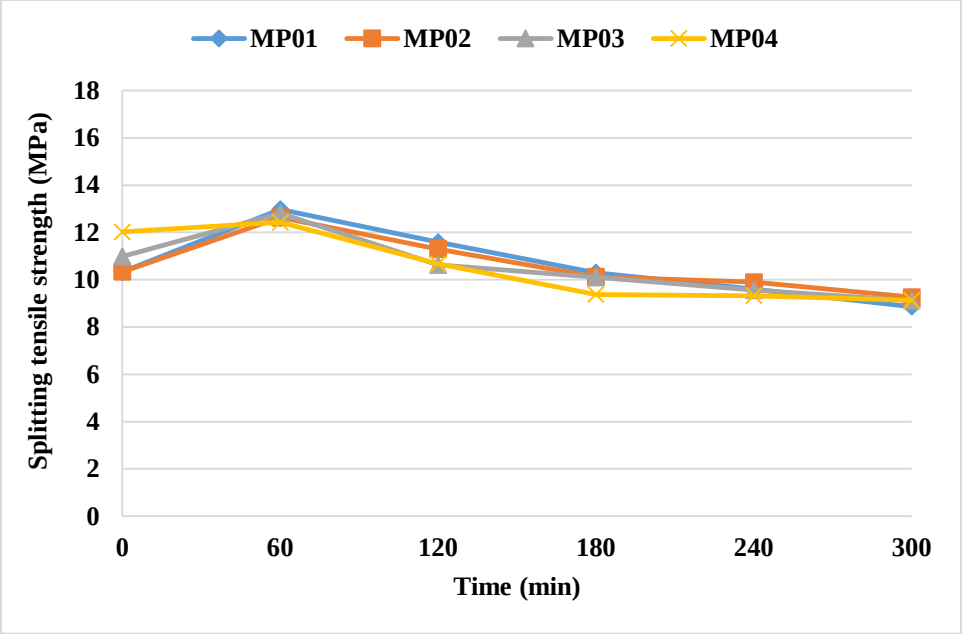

Figure 4.85: Variation of splitting tensile strength with exposure duration for UHPC with silica fume and different polypropylene fiber contents

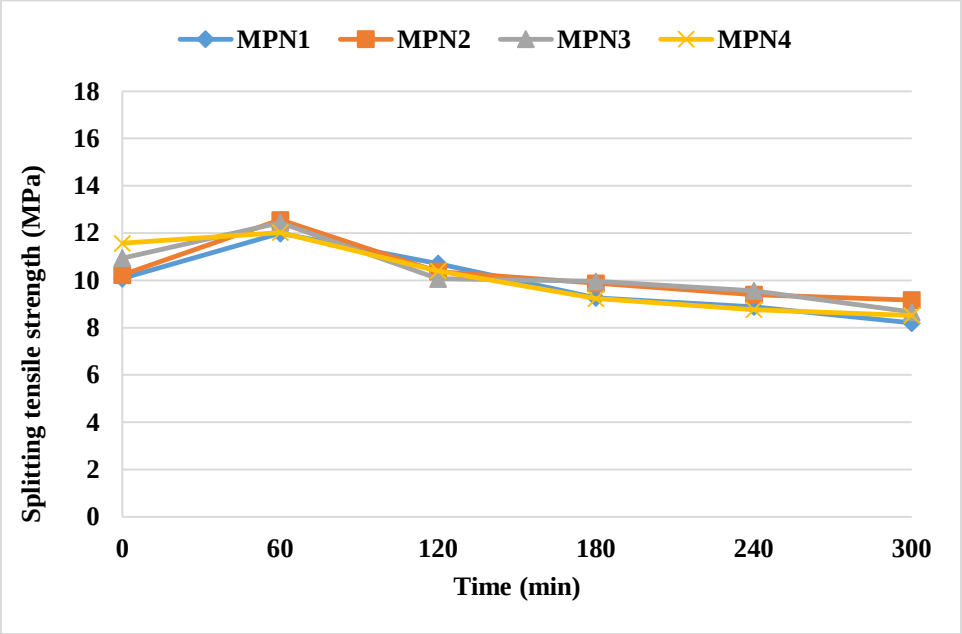

Figure 4.86: Variation of splitting tensile strength with exposure duration for UHPC with blend of silica fume and natural pozzolana and different polypropylene fiber contents

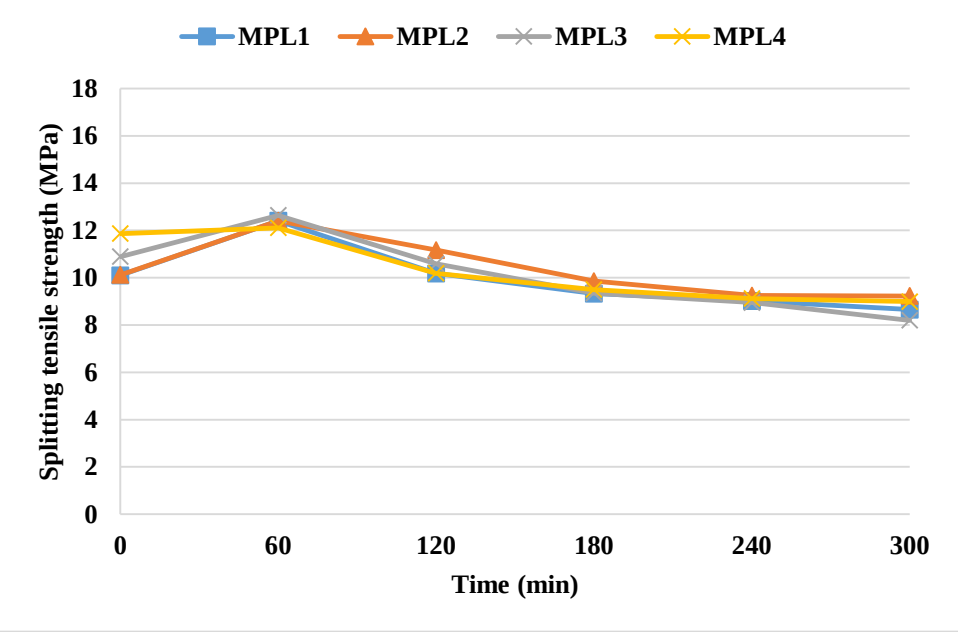

Figure 4.87: Variation of splitting tensile strength with exposure duration for UHPC with blend of silica fume and limestone powder and different polypropylene fiber contents

It can be seen from Figures 4.85 through 4.87 that in case of each type of UHPC mixture, the splitting tensile strength increased after 60 minutes of exposure. However, beyond 60 minutes of exposure, the splitting tensile strength decreased with the increase of exposure duration. It is observed from Table 4.56 that an increase of 3 to 26% of strength took place in first 60 minutes of exposure. After 300 minutes of exposure, the strength decreased by 9 to 26%. The fiber content has a negligible effect on splitting tensile strength.

The analysis of variance (ANOVA) of the splitting tensile strength data presented in Table 4.55 for all three UHPC mixtures are presented in Tables 4.57 through 4.59.

Table 4.57: ANOVA table for splitting tensile strength of polypropylene fibers reinforced UHPC mixture with silica fume only

Source of variation	SS	DOF	MS	F	P	F_{cr}	Significance criteria P< 0.05 and F > F_{cr}
Exposure duration	33.7	5	6.74	29.4	3.04×10^{-07}	2.9	**Significant**
Fiber content	0.05	3	0.02	0.08	9.72×10^{-01}	3.3	**Insignificant**
Error	3.44	15	0.23				
Total	37.2	23					

Table 4.58: ANOVA table for splitting tensile strength of polypropylene fibers reinforced UHPC mixture with silica fume and natural pozzolana

Source of variation	SS	DOF	MS	F	P	F_{cr}	Significance criteria P< 0.05 and F > F_{cr}
Exposure duration	33.6	5	6.71	39.06	4.42×10^{-08}	2.9	**Significant**
Fiber content	0.7	3	0.23	1.37	2.91×10^{-01}	3.3	**Insignificant**
Error	2.58	15	0.17				
Total	36.8	23					

Table 4.59: ANOVA table for splitting tensile strength of polypropylene fibers reinforced UHPC mixture with silica fume and limestone powder

Source of variation	SS	DOF	MS	F	P	F_{cr}	Significance criteria P< 0.05 and F > F_{cr}
Exposure duration	35.93	5	7.19	34.48	1.04×10^{-07}	2.90	**Significant**
Fiber content	0.59	3	0.20	0.95	4.44×10^{-01}	3.29	**Insignificant**
Error	3.13	15	0.21				
Total	39.64	23					

From the ANOVA results, as presented in Tables 4.57 through 4.59, it can be observed that for all three UHPC mixtures, exposure duration has significant effect on splitting tensile strength due to a very high F-value and very low P-value. However, the effect of fiber content is insignificant.

Empirical model for splitting tensile strength in terms of exposure duration and fiber content, as obtained through regression analysis, is given as:

$$f_{st} = a + b(T) + c(T^2) + d(F) + e(F^2)$$

Where:

f_{st} is splitting tensile strength (MPa)

a, *b*, *c*, *d* and *e* are regression coefficients, as given in Table 4.60 for all three UHPC mixtures

T is exposure duration (0, 60, 120, 180, 240, and 360 minutes)

F is fiber content (0.1, 0.2, 0.3, and 0.4% by mass of mixture)

Table 4.60: Values of regression coefficients for splitting tensile strength of UHPC mixtures with polypropylene fibers

UHPC mixture	***a***	***b***	***c***	***d***	***e***	R^2
Mixture with silica fume only	11.6	0.00011	-0.00003	-0.099	-0.63	0.64
Mixture with silica fume and natural pozzolana	10.4	-0.0029	-0.00002	8.235	-15.08	0.69
Mixture with silica fume and limestone powder	10.9	-0.0038	-0.00002	3.288	-4.96	0.65

A low value of regression coefficient, R^2, for each of the UHPC mixtures, as shown in Table 4.60, indicate lack of fit of the data.

ii. Effect of type of UHPC mixture on splitting tensile strength

The plots of splitting tensile strength of three UHPC mixtures at different exposure durations are shown in Figures 4.88 through 4.90, for 0.1, 0.2, 0.3, and 0.4%, respectively. It can be observed from Figures 4.88 through 4.90 that at any exposure duration and fiber content, there is not much difference between the splitting tensile strengths of the three mixtures. Therefore, it can be concluded that the performance of all three UHPC is comparable.

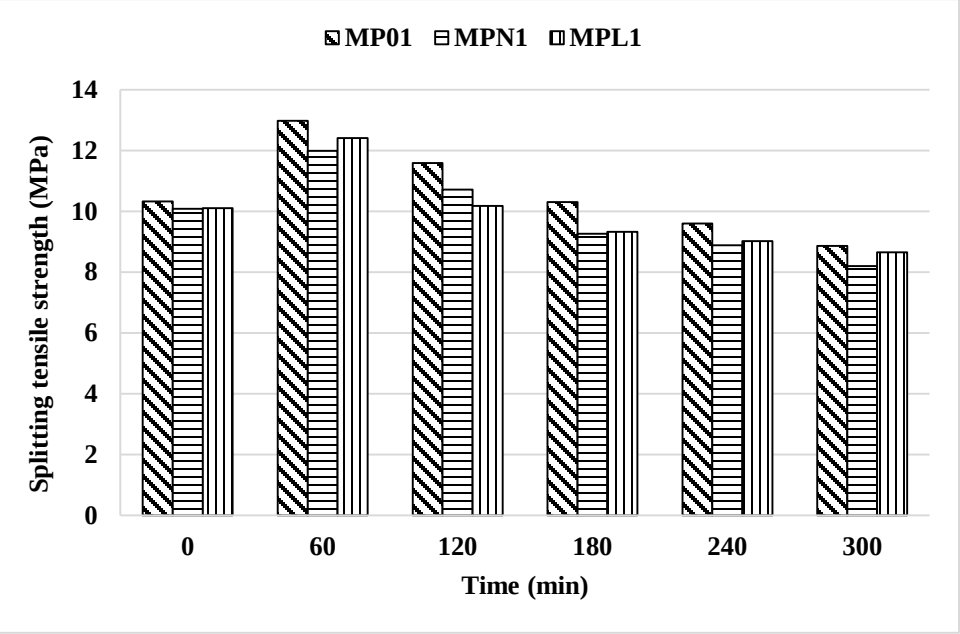

Figure 4.88: Splitting tensile strength vs exposure duration for UHPC mixtures with 0.1% polypropylene fibers

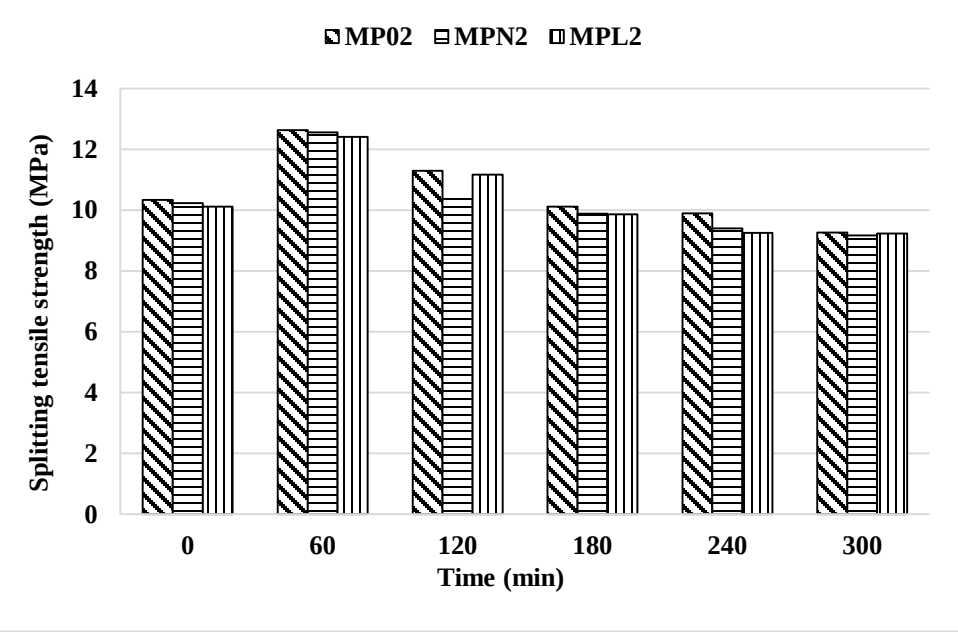

Figure 4.89: Splitting tensile strength vs exposure duration for UHPC mixtures with 0.2% polypropylene fibers

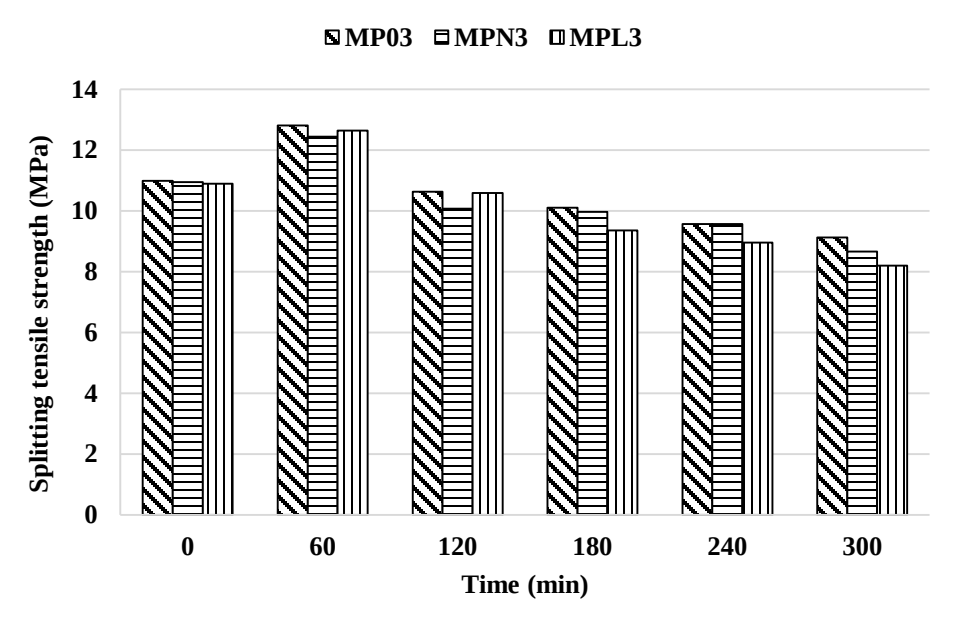

Figure 4.90: Splitting tensile strength vs exposure duration for UHPC mixtures with 0.3% polypropylene fibers

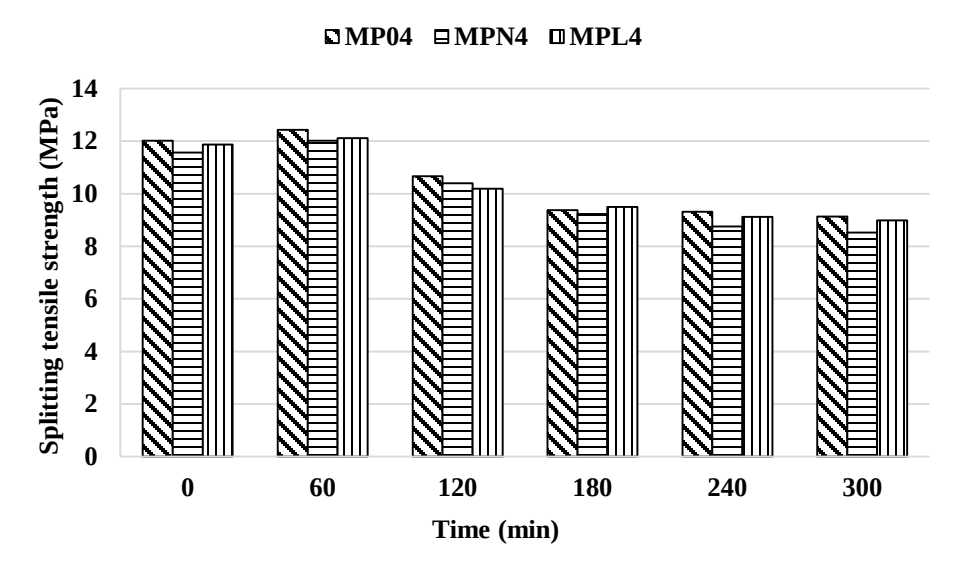

Figure 4.91: Splitting tensile strength vs exposure duration for UHPC mixtures with 0.4% polypropylene fibers

4.3 UHPC Mixtures Subjected to Heat-Cool Cycles

4.3.1 Compressive Strength

Average compressive strength of the control specimens and specimens exposed to heat-cool cycles are shown in Table 4.61. The ratios of the compressive strength after a particular cyclic period to the compressive strength of control specimens, $(f'_c)_C/f'_c$ are summarized in Table 4.62. Based on the data presented in Tables 4.61 and 4.61, discussions were made regarding the effect of type of mixture and number of cycles on the compressive strength.

Table 4.61: Compressive strength of UHPC mixtures exposed to heat-cool cycles

Mixture ID	Compressive Strength (MPa)		
	Control	90 Cycles	180 Cycles
MS06	147.7	170.5	190.3
MSN6	145.4	165.8	179.9
MSL6	146.8	163.8	178.7

Table 4.62: $(f'_c)_C/f'_c$ of UHPC mixtures exposed to heat-cool cycles

Mixture ID	$(f'_c)_C/f'_c$	
	90 Cycles	180 Cycles
MS06	1.15	1.29
MSN6	1.14	1.24
MSL6	1.12	1.22

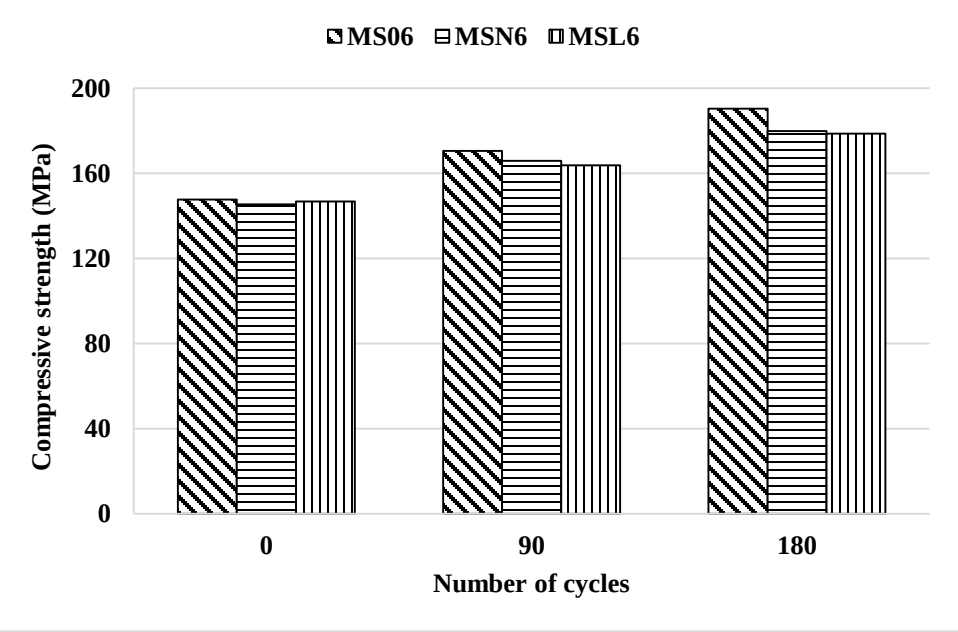

Figure 4.92: Compressive strength vs heat-cool cycles

It can be seen from the data in Figure 4.92, in case of each type of UHPC mixture, the compressive strength increases with an increase in number of heat cool cycles. It is

observed from the data in Table 4.62 that an increase of 22 to 29% of strength took place after 180 heat-cool cycles. The increase in strength may be attributed to the heat curing of the specimens.

4.3.2 Modulus of Elasticity

Average modulus of elasticity (MOE) of the control specimens and specimens exposed to heat-cool cycles are summarized in Table 4.63. The ratios of the MOE after a particular cyclic period to the MOE of control specimens (MOE_C/MOE) are summarized in Table 4.64. Based on the data presented in Tables 4.63 and 4.64, discussions were made regarding the effect of type of mixture and number of cycles on MOE.

Table 4.63: MOE of UHPC mixtures exposed to heat-cool cycles

Mixture ID	MOE (GPa)		
	Control	90 Cycles	180 Cycles
MS06	48.8	51.2	51.3
MSN6	49.4	51.3	51.4
MSL6	49.8	51.8	51.9

Table 4.64: MOE_C/MOE of UHPC mixtures exposed to heat-cool cycles

Mixture ID	MOE_C/MOE	
	90 Cycles	180 Cycles
MS06	1.05	1.05
MSN6	1.04	1.04
MSL6	1.04	1.04

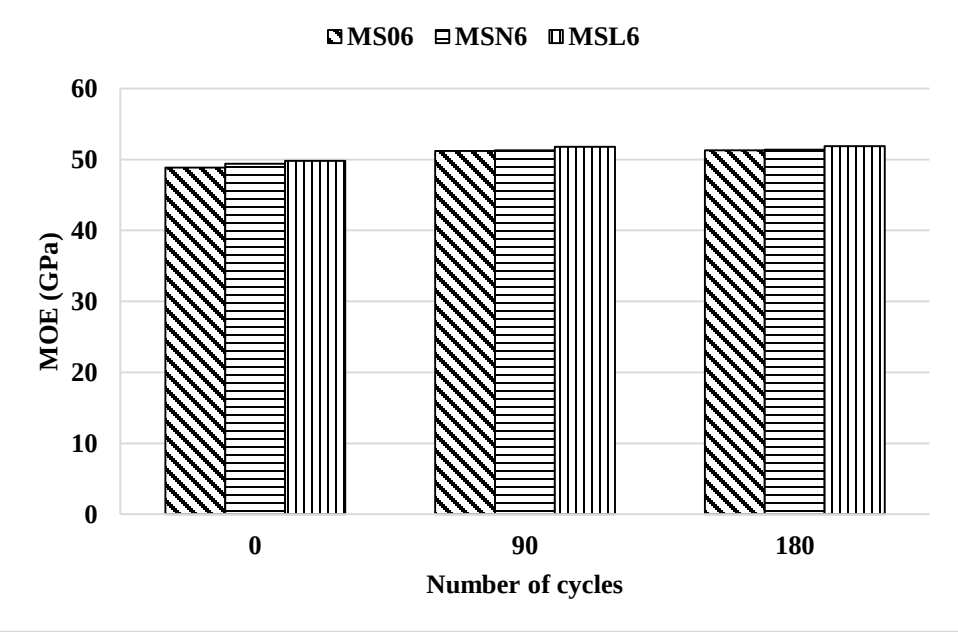

Figure 4.93: MOE vs heat-cool cycles

It can be seen from the data in Figure 4.93, in case of each type of UHPC mixture, the MOE increased a little with the increase in number of heat-cool cycles. It is observed from the data in Table 4.64 that an increase of only 4 to 5% of MOE took place after 180 heat-cool cycles.

4.3.3 Flexural Strength

Average modulus of rupture (MOR) of the control specimens and specimens exposed to heat-cool cycles are summarized in the Table 4.65. The ratios of the MOR after a particular cyclic period to the MOR of control specimens (MOR_C/MOR) are shown in Table 4.66. Based on the data presented in Tables 4.65 and 4.66, discussions were made regarding the effect of type of mixture and number of cycles on MOR.

Table 4.65: MOR of UHPC mixtures exposed to heat-cool cycles

Mixture ID	MOR(MPa)		
	Control	90 Cycles	180 Cycles
MS06	34.16	36.49	33.57
MSN6	33.41	34.65	33.02
MSL6	33.45	34.88	32.57

Table 4.66: MOR_C/MOR of UHPC mixtures exposed to heat-cool cycles

Mixture ID	MOR_C/MOR	
	90 Cycles	180 Cycles
MS06	1.07	0.98
MSN6	1.04	0.99
MSL6	1.04	0.97

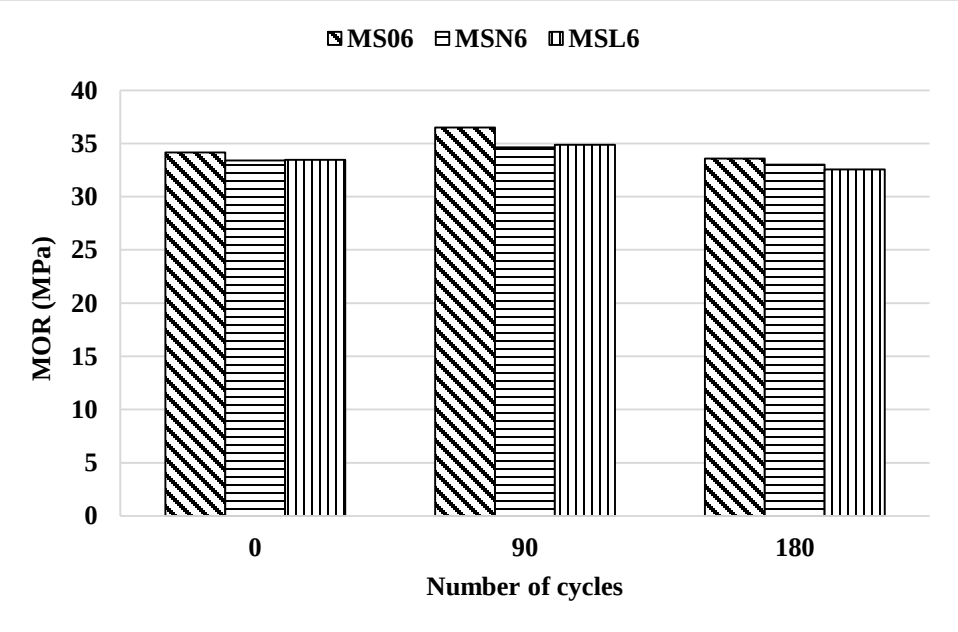

Figure 4.94: MOR vs heat-cool cycles

It can be seen from the data in Figure 4.94, in case of each type of UHPC mixture, the MOR increased until 90 heat-cool cycles then a reduction was observed after 180 cycles. It is observed from the data in Table 4.66 that an increase of 4 to 7% of strength took place after 90 heat-cool cycles. After 180 cycles, a reduction of 1 to 3 % was observed.

4.3.4 Splitting Tensile Strength

Average splitting tensile strength of the control specimens and specimens exposed to heat-cool cycles are summarized in the Table 4.67. The ratios of the splitting tensile strength after a particular cyclic period to the splitting tensile strength of control specimens $(f_{st})_C/f_{st}$ are summarized in Table 4.68. Based on the data presented in Tables 4.67 and 4.68, discussions were made regarding the effect of type of mixture and number of cycles on splitting tensile strength.

Table 4.67: Splitting tensile strength of UHPC mixtures exposed to heat-cool cycles

Mixture ID	Splitting tensile strength (MPa)		
	Control	90 Cycles	180 Cycles
MS06	20.09	21.3	21.35
MSN6	19.5	20.17	20.82
MSL6	18.44	18.65	18.78

Table 4.68: $(f_{st})_C/f_{st}$ of UHPC mixtures exposed to heat-cool cycles

Mixture ID	$(f_{st})_C/f_{st}$	
	90 Cycles	180 Cycles
MS06	1.06	1.06
MSN6	1.03	1.07
MSL6	1.01	1.02

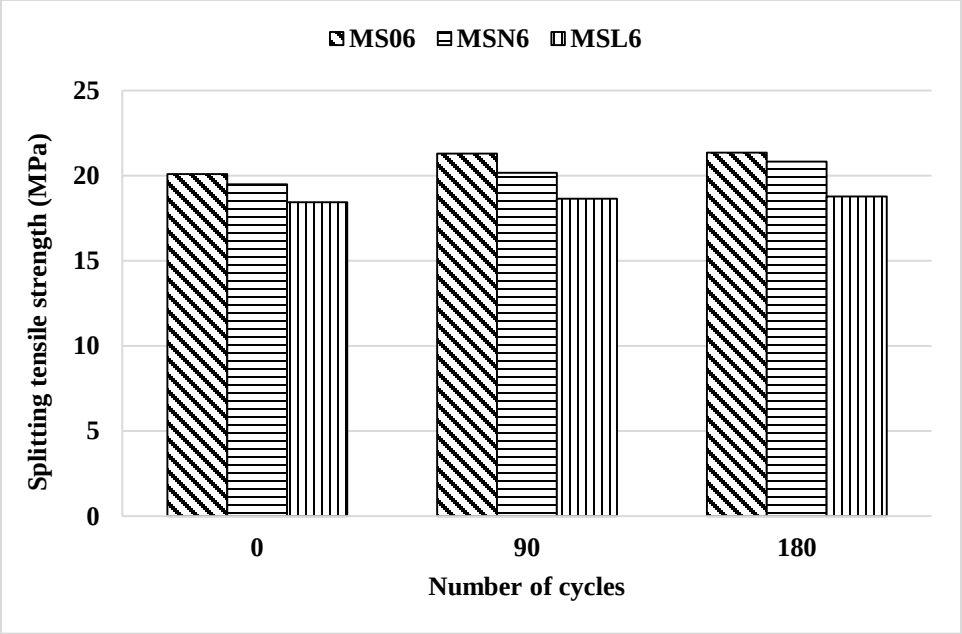

Figure 4.95: Splitting tensile strength vs heat-cool cycles

It can be seen from the data in Figure 4.95, in case of each type of UHPC mixture, the splitting tensile increased slightly with the heat-cool cyclic exposure. It is observed from the data in Table 4.68 that an increase of 2 to 7% of strength took place after 180 heat-cool cycles. The increase in strength may be attributed to the heat curing of the specimens.

4.3.5 Fracture Toughness

Average critical stress intensity factor (K_{ic}) of the control specimens and specimens exposed to heat-cool cycles are summarized in the Table 4.69. The ratios of the K_{ic} after a particular cyclic period to the K_{ic} of control specimens $(K_{ic})_C/K_{ic}$ are summarized in Table 4.70. Based on the data presented in Tables 4.69 and 4.70, discussions were made regarding the effect of type of mixture and number of cycles on K_{ic}.

Table 4.69: Critical stress intensity factor (K_{ic}) of UHPC mixtures exposed to heat-cool cycles

Mixture ID	K_{ic} (MPa.m$^{1/2}$)		
	Control	90 Cycles	180 Cycles
MS06	5.7	6.4	6.9
MSN6	5.4	5.8	6.2
MSL6	5.7	6.2	6.7

Table 4.70: $(K_{ic})_C/K_{ic}$ of UHPC mixtures exposed to heat-cool cycles

Mixture ID	$(K_{ic})_C/K_{ic}$	
	90 Cycles	180 Cycles
MS06	1.12	1.21
MSN6	1.07	1.15
MSL6	1.09	1.18

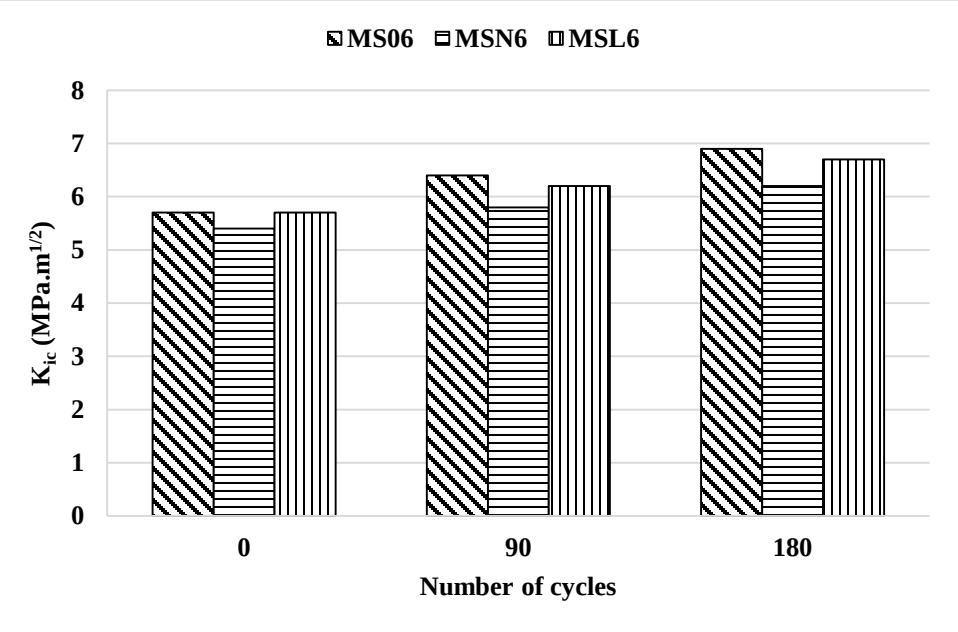

Figure 4.96: K_{ic} vs heat-cool cycles

It can be seen from the data in Figure 4.96, in case of each type of UHPC mixture, that the K_{ic} increased after the heat-cool cyclic exposure. An increase of 15 to 21% of K_{ic} was found

after 180 heat-cool cycles. The increase in K_{ic} may be attributed to the heat curing of the specimens.

4.3.6 Water Permeability

Average water penetration depth of the control specimens and specimens exposed to heat-cool cycles are summarized in the Table 4.71. Based on the data presented in Table 4.71, discussions were made regarding the effect of type of mixture and number of cycles on water Penetration Depth.

Table 4.71: Water penetration depth of UHPC mixtures exposed to heat-cool cycles

Mixture ID	Water Penetration Depth (mm)		
	Control	90 Cycles	180 Cycles
MS06	0	0	0
MSN6	0	0	0
MSL6	0	0	0

It is observed from the data in Table 4.71 that water penetration depth is zero for control and the specimens subjected to heat-cool cycles as well, which shows that the UHPC is highly impermeable even after the adverse exposures.

4.3.7 Rapid Chloride Ion Permeability

Average rapid chloride ion permeability of the control specimens and specimens exposed to heat-cool cycles are summarized in the Table 4.72. Based on the data presented in Table 4.72, discussions were made regarding the effect of type of mixture and number of cycles on rapid chloride ion permeability.

Table 4.72: Rapid chloride ion permeability of UHPC mixtures exposed to heat-cool cycles

Mixture ID	Rapid chloride ion permeability (Coulombs)		
	Control	90 Cycles	180 Cycles
MS06	53	32	39
MSN6	85	49	48
MSL6	70	53	57

It is observed from the data in Table 4.72 that all the UHPC mixtures had rapid chloride ion permeability less than 100 Coulombs, which indicate that all the mixtures performed well against rapid chloride ion permeability even after 180 hat-cool cycles.

4.3.8 Corrosion Current Density

Average corrosion current density of the control specimens and specimens exposed to heat-cool cycles are summarized in Table 4.73. Based on the data presented in Table 4.73, discussions were made regarding the effect of type of mixture and number of cycles on corrosion current density.

Table 4.73: Corrosion current density of UHPC mixtures exposed to heat-cool cycles

Mixture ID	Corrosion current density ($\mu A/cm^2$)		
	Control (After 9 months exposure to chloride)	90 Cycles (After 6 months exposure to chloride)	180 Cycles (After 3 months exposure to chloride)
MS06	0.044	0.036	0.010
MSN6	0.060	0.049	0.029
MSL6	0.059	0.042	0.024

It is observed from the data in Table 4.73 that even after 180 heat-cool cycles, the corrosion current density is still in the passive range.

4.4 UHPC Mixtures Subjected to Wet-Dry Cycles

4.4.1 Compressive Strength

Average compressive strength of the control specimens and specimens exposed to wet-dry cycles are summarized in the Table 4.74. The ratios of the compressive strength after a particular cyclic period to the compressive strength of control specimens $(f'_c)_C/f'_c$ are summarized in Table 4.75. Based on the data presented in Tables 4.74 and 4.75, discussions were made regarding the effect of type of mixture and number of cycles on the compressive strength.

Table 4.74: Compressive strength of UHPC mixtures exposed to wet-dry cycles

Mixture ID	Compressive Strength (MPa)		
	Control	90 Cycles	180 Cycles
MS06	147.7	161.2	159.5
MSN6	145.4	155.9	155.3
MSL6	146.8	159.3	158.2

Table 4.75: $(f'_c)_T/f'_c$ of UHPC mixtures exposed to wet-dry cycles

Mixture ID	$(f'_c)_C/f'_c$	
	90 Cycles	180 Cycles
MS06	1.09	1.08
MSN6	1.07	1.07
MSL6	1.09	1.08

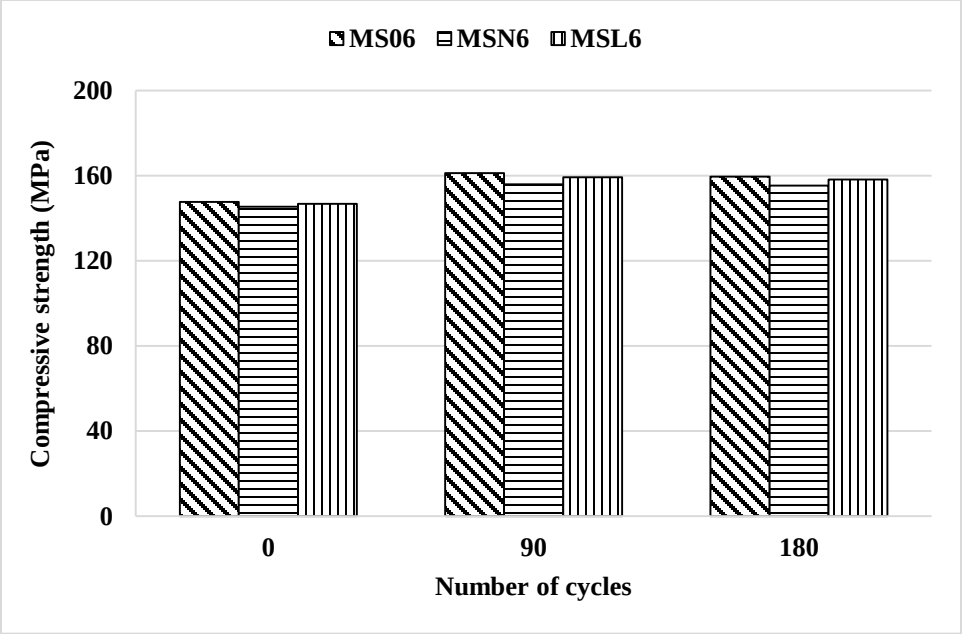

Figure 4.97: Compressive strength vs wet-dry cycles

It can be seen from the data in Figure 4.97 that in case of each type of UHPC mixture, the compressive strength increased after 90 cycles of wet-dry cycles. However, strength remained almost same after 180 cycles. It is observed from the data in Table 4.75 that an increase of 7 to 9% of strength took place after 90 wet-dry cycles. After 180 cycles, the total increase was 7 to 8%. The increase may be attributed to the moist-curing of the specimens.

4.4.2 Modulus of Elasticity

Average modulus of elasticity (MOE) of the control specimens and specimens exposed to wet-dry cycles are summarized in the Table 4.76. The ratios of the MOE after a particular cyclic period to the MOE of control specimens (MOE_C/MOE) are summarized in Table 4.77. Based on the data presented in Tables 4.76 and 4.77, discussions were made regarding the effect of type of mixture and number of cycles on MOE.

Table 4.76: MOE of UHPC mixtures exposed to wet-dry cycles

Mixture ID	MOE (GPa)		
	Control	90 Cycles	180 Cycles
MS06	48.86	51.2	49.5
MSN6	49.4	51.9	50.2
MSL6	51.9	52	51.2

Table 4.77: MOEc/MOE of UHPC mixtures exposed to wet-dry cycles

Mixture ID	MOEc/MOE	
	90 Cycles	180 Cycles
MS06	1.05	1.01
MSN6	1.05	1.02
MSL6	1.00	0.99

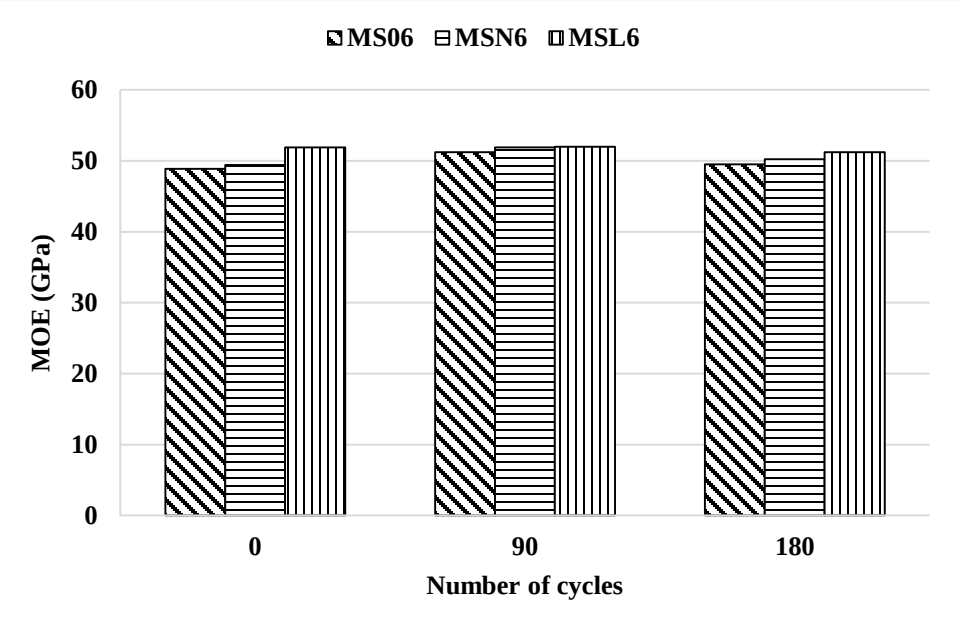

Figure 4.98: MOE vs wet-dry cycles

It can be seen from the data Figure 4.98, in case of each type of UHPC mixture, the MOE is increasing a little after 90 wet-dry cycles. It is observed from the data in Table 4.77 that

an increase of 0 to 5% of strength took place after 90 wet-dry cycles. After 180 cycles the change is not appreciable as compared to control specimens.

4.4.3 Flexural Strength

Average modulus of rupture (MOR) of the control specimens and specimens exposed to wet-dry cycles are summarized in the Table 4.78. The ratios of the MOR after a particular cyclic period to the MOR of control specimens (MOR_C/MOR) are summarized in Table 4.79. Based on the data presented in Tables 4.78 and 4.79, discussions were made regarding the effect of type of mixture and number of cycles on MOR.

Table 4.78: MOR of UHPC mixtures exposed to wet-dry cycles

Mixture ID	MOR(MPa)		
	Control	90 Cycles	180 Cycles
MS06	34.16	35.23	37.16
MSN6	33.41	33.99	34.03
MSL6	33.45	34.23	36.4

Table 4.79: MOR_C/MOR of UHPC mixtures exposed to wet-dry cycles

Mixture ID	MOR_C/MOR	
	90 Cycles	180 Cycles
MS06	1.03	1.09
MSN6	1.02	1.02
MSL6	1.02	1.09

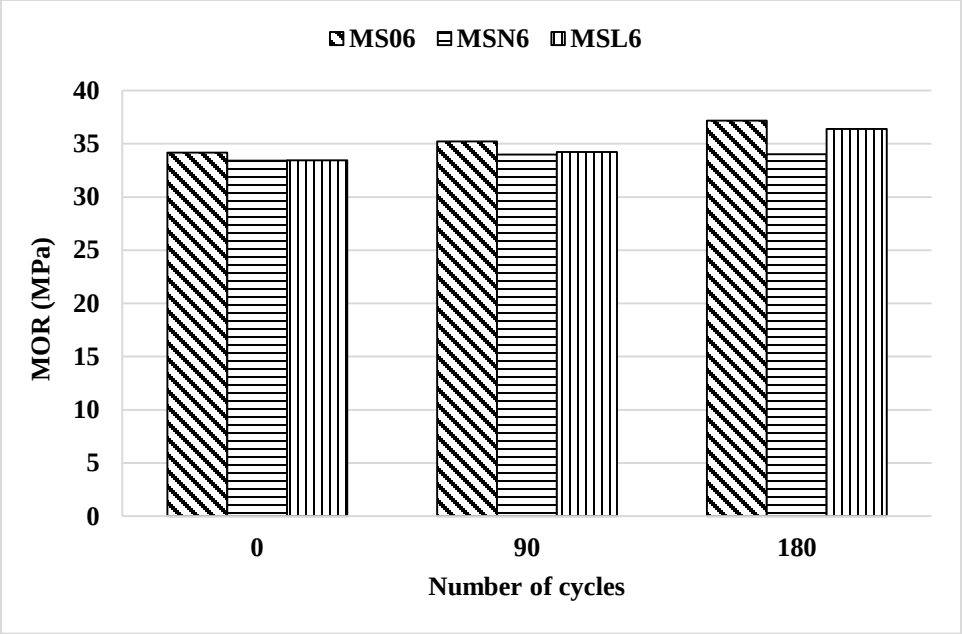

Figure 4.99: MOR vs wet-dry cycles

It can be seen from the data in Figure 4.99, in case of each type of UHPC mixture, the MOR is increasing after 180 cycles. It is observed from the data in Table 4.79 that an increase of 2 to 9% of strength took place after 180 wet-dry cycles.

4.4.4 Splitting Tensile Strength

Average splitting tensile strength of the control specimens and specimens exposed to wet-dry cycles are summarized in the Table 4.80. The ratios of the splitting tensile strength after a particular cyclic period to the splitting tensile strength of control specimens $(f_{st})_C/f_{st}$ are summarized in Table 4.81. Based on the data presented in Tables 4.80 and 4.81, discussions were made regarding the effect of type of mixture and number of cycles on splitting tensile strength.

Table 4.80: Splitting tensile strength of UHPC mixtures exposed to wet-dry cycles

Mixture ID	Splitting tensile strength (MPa)		
	Control	90 Cycles	180 Cycles
MS06	20.09	20.56	17.06
MSN6	19.5	18.18	16.54
MSL6	18.44	16.87	15.18

Table 4.81: $(f_{st})_C/f_{st}$ of UHPC mixtures exposed to wet-dry cycles

Mixture ID	$(f_{st})_C/f_{st}$	
	90 Cycles	180 Cycles
MS06	1.02	0.85
MSN6	0.93	0.85
MSL6	0.91	0.82

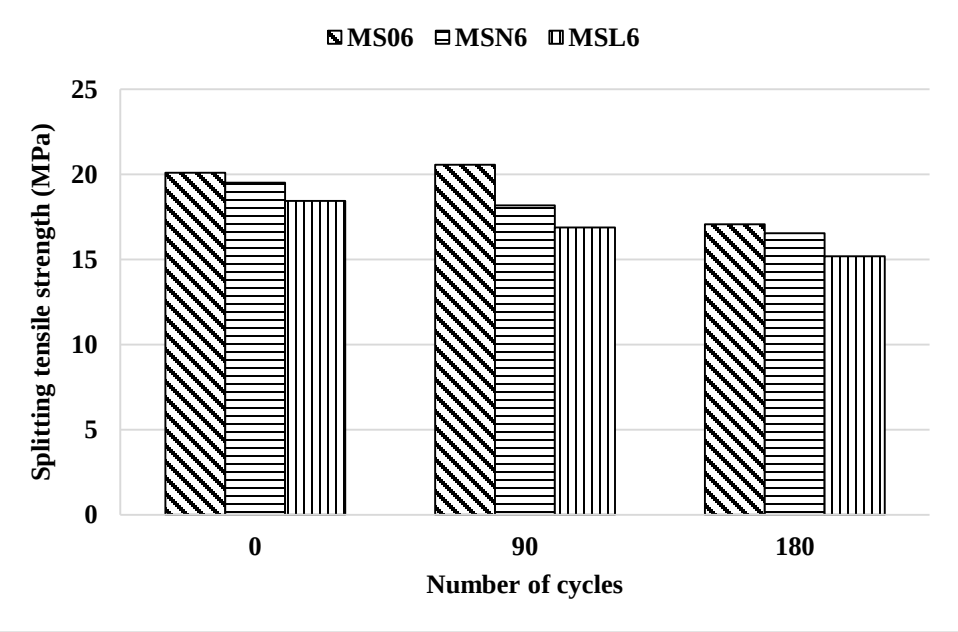

Figure 4.100: Splitting tensile strength vs wet-dry cycles

It can be observed from the data in Figure 4.100, in case of each type of UHPC mixture, the splitting tensile strength decreased after 180 cycles. A decrease of 15 to 17% in splitting tensile strength was observed after 180 cycles.

4.4.5 Fracture Toughness

Average critical stress intensity factor (K_{ic}) of the control specimens and specimens exposed to wet-dry cycles are summarized in the Table 4.82. The ratios of the K_{ic} after a particular cyclic period to the K_{ic} of control specimens $(K_{ic})_C/K_{ic}$ are summarized in Table 4.83. Based on the data presented in Tables 4.82 and 4.83, discussions were made regarding the effect of type of mixture and number of cycles on K_{ic}.

Table 4.82: Critical stress intensity factor (K_{ic}) for UHPC mixtures exposed to wet-dry cycles

Mixture ID	K_{ic} (MPa.m$^{1/2}$)		
	Control	90 Cycles	180 Cycles
MS06	5.7	6.4	6.7
MSN6	5.4	5.7	6.2
MSL6	5.7	6	6.6

Table 4.83: $(K_{ic})_C/K_{ic}$ for UHPC mixtures exposed to wet-dry cycles

Mixture ID	$(K_{ic})_C/K_{ic}$	
	90 Cycles	180 Cycles
MS06	1.12	1.18
MSN6	1.06	1.15
MSL6	1.05	1.16

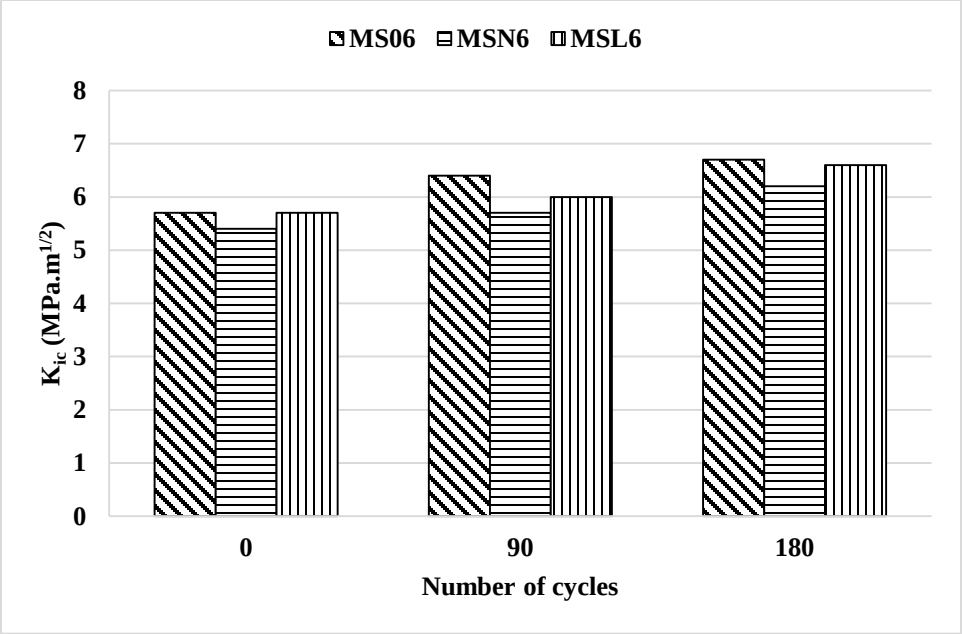

Figure 4.101: K_{ic} vs wet-dry cycles

It can be seen from the data in Figure 4.101, in case of each type of UHPC mixture, that the K_{ic} increased after the wet-dry cyclic exposure. An increase of 15 to 18% of K_{ic} was found after 180 wet-dry cycles. The increase in K_{ic} may be attributed to the moist curing of the specimens.

4.4.6 Water Permeability

Average water penetration depth of the control specimens and specimens exposed to wet-dry cycles are summarized in the Table 4.84. Water penetration depth is zero for control and the specimens undergone the cyclic exposures as well, which shows that the UHPC is highly impermeable and it remains highly impermeable even after the adverse exposures.

Table 4.84: Water penetration depth for UHPC mixtures exposed to wet-dry cycles

Mixture ID	Water penetration depth (mm)		
	Control	90 Cycles	180 Cycles
MS06	0	0	0
MSN6	0	0	0
MSL6	0	0	0

It is observed from the data in Table 4.84 that water penetration depth is zero for control and the specimens subjected to wet-dry cycles as well, which shows that the UHPC is highly impermeable even after the adverse exposures.

4.4.7 Rapid Chloride Ion Permeability

Average rapid chloride ion permeability of the control specimens and specimens exposed to wet-dry cycles are summarized in the Table 4.85. Based on the data presented in Table 4.85, discussions were made regarding the effect of type of mixture and number of cycles on rapid chloride ion permeability.

Table 4.85: Rapid chloride ion permeability for UHPC mixtures exposed to wet-dry cycles

Mixture ID	Rapid chloride ion permeability (Coulombs)		
	Control	90 Cycles	180 Cycles
MS06	53	21	17
MSN6	85	26	29
MSL6	70	38	32

It is observed from the data in Table 4.85 that all the UHPC mixtures had rapid chloride ion permeability less than 100 Coulombs, which indicate that all the mixtures performed well against rapid chloride ion permeability even after 180 wet-dry cycles.

4.4.8 Corrosion Current Density

Average corrosion current density of the control specimens and specimens exposed to wet-dry cycles are summarized in the Table 4.86. Based on the data presented in Table 4.86, discussions were made regarding the effect of type of mixture and number of cycles on corrosion current density.

Table 4.86: Corrosion current density for UHPC mixtures exposed to wet-dry cycles

Mixture ID	Corrosion current density ($\mu A/cm^2$)		
	Control (After 9 months exposure to chloride)	**90 Cycles (After 6 months exposure to chloride)**	**180 Cycles (After 3 months exposure to chloride)**
MS06	0.044	0.111	0.078
MSN6	0.060	0.104	0.086
MSL6	0.059	0.149	0.074

It is observed from the data in Table 4.86 that even after 180 heat-cool cycles, the corrosion current density is still in the passive range.

CHAPTER 5

CONCLUSIONS AND RECOMMENDATIONS

Based on the findings of the present work following conclusions are drawn:

5.1 UHPC Mixtures with Steel Fibers Subjected to Elevated Temperature (300ºC)

(i) UHPC mixtures with steel fibers can withstand elevated temperature of up to 300ºC safely. Explosive spalling was observed when temperature was increased beyond 350ºC.

(ii) UHPC mixtures with steel fibers showed ductile failure when tested in compression, flexure, and splitting. The exposure to elevated temperature did not change the ductile failure mode.

(iii) The compressive strength increased with an increase in the duration of exposure to elevated temperature and steel fiber content. The effect of duration of exposure to elevated temperature was more significant than that of fiber content. The increase in compressive strength after 300 minutes of exposure to elevated temperature was in the range of 31 to 53%.

(iv) The modulus of elasticity decreased with increase in the duration of exposure to elevated temperature. After 300 minutes of exposure, the reduction in modulus of elasticity was found to be in the range of 24 to 37%. The fiber content had insignificant effect.

(v) The modulus of toughness, an indicator of resistance against failure under compression, increased with an increase in the duration of exposure to the elevated temperature. Both factors, exposure duration and fiber content, affected the modulus of toughness. The modulus of toughness increased in the range of about 50 to 150% after 300 minutes of exposure to the elevated temperature.

(vi) The flexural strength decreased with an increase in the duration of exposure to elevated temperature. The decrease was lesser at higher content. Although, both exposure duration and fiber content affected the flexural strength, fiber content was found to be a major factor. A decrease of flexural strength in the range of 12 to 27% was noted after an exposure for 300 minutes.

(vii) There was a very little impact of the elevated temperature on the splitting tensile strength. However, splitting tensile strength was higher at higher fiber content.

5.2 UHPC Mixtures with Polypropylene Fibers Subjected to Elevated Temperature (300^{o}C)

(i) UHPC mixtures with polypropylene fibers can withstand elevated temperature until 300^{o}C safely.

(ii) UHPC mixtures with polypropylene fibers, not exposed to elevated temperature, exhibited ductile failure when tested in compression, flexure, and splitting. However, when subjected to elevated temperature beyond 60 minutes, failure mode was brittle under all tests.

(iii) The compressive strength increased with the duration of exposure to the elevated temperature. Both exposure duration and fiber content were found to have a significant effect on the compressive strength. The increase in compressive strength

with an increase in the exposure duration is lesser at higher fiber content. A 14 to 33% increase in the compressive strength was noted after 300 minutes of exposure.

(iv) The modulus of elasticity decreased with an increase in the duration of exposure to elevated temperature. Exposure duration as well as fiber content were found to have a significant effect on the modulus of elasticity. The decrease in modulus of elasticity was found to be in the range of 23 to 40% after an exposure duration of 300 minutes.

(v) The modulus of toughness increased with an increase in the exposure duration. The increase was in the range of 31 to 143% after 300 minutes of exposure. The effect of both exposure duration and fiber content were significant.

(vi) The flexural strength increased in the range of 0 to 33% when the specimens of UHPC mixtures were exposed to elevated temperature for first 60 minutes. However, beyond 60 minutes of exposure, the flexural strength decreased with an increase in the exposure duration. The decrease was in the range of 2 to 29% after 300 minutes of exposure. The fiber content had no significant effect on the flexural strength of the UHPC mixtures exposed to elevated temperature.

(vii) Like flexural strength, splitting tensile strength also increased in the range of 2 to 26% as the UHPC specimens were exposed to elevated temperature for the first 60 minutes. However, beyond 60 minutes of exposure, the splitting tensile strength decreased with an extension of the exposure duration. A loss of splitting tensile strength took place in the range of 9 to 26% as specimens were exposed to elevated temperature for a period of 300 minutes.

5.3 UHPC Mixtures Subjected to Cyclic Exposures

(i) There was no significant adverse effect of the cyclic exposures on mechanical properties and durability characteristics up to 180 cycles of thermal and moisture variations (Rather almost all mechanical properties were slightly improved due the curing effect of cyclic exposures).

5.4 Recommendations

(i) All three UHPC mixtures containing steel fibers can be used safely and advantageously to withstand an exposure to elevated temperature up to 300°C and cyclic thermal and moisture variations.

(ii) The use of UHPC mixtures containing plastic fibers alone is not advantageous for exposure to the elevated temperature.

5.5 Recommendations for further studies

Since the UHPC mixtures were damaged due to explosive spalling when temperature exceeded 350°C, it is important to explore the possibility of enhancing the resistance of UHPC mixtures against explosive spalling. Therefore, based on the information from the recent literature, it is recommended to conduct a study on the evaluation of fire resistance of UHPC mixtures containing hybrid fibers (mixture of steel and polypropylene fibers). This would enable in revealing the maximum level of elevated temperature at which explosive spalling will take place.

REFERENCES

[1] P. Richard and M. Cheyrezy, “Composition of reactive powder concretes,” Cem. Concr. Res., vol. 25, no. 7, pp. 1501–1511, 1995.

[2] C. DAURIAC, “Special concrete may give steel stiff competition,” Seattle Dly. J. Commer., 1997.

[3] I. Y. A. HAKEEM, “Characterization of an ultra-high performance concrete,” 2011.

[4] G. Benjamin A., “Material Property Characterization of Ultra-High Performance Concrete,” 2006.

[5] S. Ahmad, I. Hakeem, and M. Maslehuddin, “Development of UHPC mixtures utilizing natural and industrial waste materials as partial replacements of silica fume and sand,” Sci. World J., vol. 2014, 2014.

[6] J. Ma and H. Schneider, “Properties of ultra-highperformance concrete,” Leipzig Annu. Civ. Eng. Rep., vol. 7, pp. 25–32, 2002.

[7] A. Zubair, “A study of mix design and mechanical properties of reactive powder concrete (RPC) utilizing fine quartz sand,” King Fahd University of Petroleum and Minerals, 2012.

[8] P. Y. Blais and M. Couture, “Precast, Prestressed Pedestrian Bridge - World’s first reactive powder concrete structure,” PCI J., vol. 44, pp. 60–71, 1999.

[9] A. Y. Shareef, “A Study on Durability Properties of Ultra-High Performance Concrete (UHPC) utilizing Local Fine Quartz Sand,” King Fahd University of Petroleum and Minerals, 2013.

[10] H. Yazici, H. Yiğiter, A. Ş. Karabulut, and B. Baradan, “Utilization of fly ash and ground granulated blast furnace slag as an alternative silica source in reactive powder concrete,” Fuel, vol. 87, no. 12, pp. 2401–2407, 2008.

[11] G. Long, X. Wang, and Y. Xie, “Very-high-performance concrete with ultrafine powders,” Cem. Concr. Res., vol. 32, no. 4, pp. 601–605, 2002.

[12] F. de Larrard and T. Sedran, “Optimization of ultra-high-performance concrete by the use of a packing model,” Cem. Concr. Res., vol. 24, no. 6, pp. 997–1009, 1994.

[13] K. Sobolev, “The development of a new method for the proportioning of high-performance concrete mixtures,” Cem. Concr. Compos., vol. 26, no. 7, pp. 901–907,

2004.

[14] C. P. Vernet, “Ultra-Durable Concretes: Structure at the Micro- and Nanoscale,” MRS Bull., vol. 29, no. 05, pp. 324–327, 2004.

[15] K. Wille, A. E. Naman, and G. J. Parra-Montesinos, “Ultra - High Performance Concrete with Compressive Strength Exceeding 150 MPa (22ksi) : A Simpler Way,” ACI Mater. J., vol. 108, no. 1, pp. 46–53, 2011.

[16] B. A. Graybeal, “Compressive Behavior of Ultra-High-Performance Fiber-Reinforced Concrete,” ACI Mater. J., vol. 146, no. 104, pp. 146–152, 2007.

[17] J. Dugat, N. Roux, and G. Bernier, “Mechanical properties of reactive powder concretes,” Mater. Struct., vol. 29, no. May, pp. 233–240, 1996.

[18] N. Roux, C. Andrade, and M. A. Sanjuan, “EXPERIMENTAL STUDY OF DURABILITY OF REACTIVE POWDER CONCRETES,” J. Mater. Civ. Eng., vol. 8, no. February, pp. 1–6, 1996.

[19] M. Cheyrezy, V. Maret, L. Frouin, D. S. Bouygues, and S. Quentin, “Microstructure analysis of RPC (Reactive powder concrete),” Cem. Concr. Res., vol. 25, no. 7, pp. 1491–1500, 1995.

[20] H. Zanni, M. Cheyrezy, V. Maret, S. Philippot, and P. Nieto, “Investigation of hydration and pozzolanic reaction in reactive powder concrete (RPC) using 29Si NMR,” Cem. Concr. Res., vol. 26, no. 1, pp. 93–100, 1996.

[21] W. Zheng, H. Li, and Y. Wang, “Compressive behaviour of hybrid fiber-reinforced reactive powder concrete after high temperature,” Mater. Des., vol. 41, pp. 403–409, 2012.

[22] Y. Tai, H. Pan, and Y. Kung, “Mechanical properties of steel fiber reinforced reactive powder concrete following exposure to high temperature reaching 800 ◦ C,” Nucl. Eng. Des., vol. 241, no. 7, pp. 2416–2424, 2011.

[23] C. Liu and J. Huang, “Fire performance of highly flowable reactive powder concrete,” Constr. Build. Mater., vol. 23, no. 5, pp. 2072–2079, 2009.

[24] V. R. Kodur, “Fiber reinforcement for minimizing spalling in HSC structural members exposed to fire,” Innov. fibre-reinforced Concr. value, ACI Spec. Publ. SP, vol. 216, pp. 221–36, 2003.

[25] Z. P. Bazant and W. Thonguthai, “Pore Pressure and Drying of Concrete at High Temperature,” J. Eng. Mech. Div., vol. 104, pp. 1059–1079, 1978.

[26] Z. P. Bazant and W. Thonguthai, “Pore Pressure in Heated Concrete Walls: Theoretical Prediction,” Mag. Concr. Res., vol. 31, pp. 67–76, 1979.

[27] H. So, J. Yi, J. Khulgadai, and S. So, “Properties of Strength and Pore Structure of Reactive Powder Concrete Exposed to High Temperature,” ACI Mater. J., no. 111, pp. 335–346, 2014.

[28] W. Zheng, H. Li, and Y. Wang, “Compressive stress – strain relationship of steel fiber-reinforced reactive powder concrete after exposure to elevated temperatures,” Constr. Build. Mater., vol. 35, pp. 931–940, 2012.

[29] W. Zheng, B. Luo, and Y. Wang, “Compressive and tensile properties of reactive powder concrete with steel fibres at elevated temperatures,” Constr. Build. Mater., vol. 41, pp. 844–851, 2013.

[30] W. Z. Zheng, H. Y. Li, Y. Wang, and H. Y. Xie, “Tensile Properties of Steel Fiber-Reinforced Reactive Powder Concrete after High Temperature,” Adv. Mater. Res., vol. 413, pp. 270–276, 2011.

[31] G.-F. Peng, Y.-R. Kang, Y.-Z. Huang, X.-P. Liu, and Q. Chen, “Experimental Research on Fire Resistance of Reactive Powder Concrete,” Adv. Mater. Sci. Eng., vol. 2012, pp. 1–6, 2012.

[32] M. Canbaz, “The effect of high temperature on reactive powder concrete,” Constr. Build. Mater., vol. 70, pp. 508–513, 2014.

[33] S. Ahmad and I. Hakeem, “Effect of curing , fibre content and exposures on compressive strength and elasticity of UHPC,” Adv. Cem. Res., vol. 27, no. 4, pp. 233–239, 2015.

[34] I. Hakeem, A. K. Azad, and S. Ahmad, “Effect of Steel Fibers and Thermal Cycles on Fracture Properties of Ultra-High-Performance Concrete,” J. Test. Eval., vol. 41, no. 3, p. 20120182, 2013.

[35] A. K. Azad, I. Hakeem, and S. Ahmad, “Effect of cyclic exposure and fibre content on tensile properties of ultra-high- performance concrete,” vol. 25, no. 5, pp. 273–280, 2013.

[36] Z. Wang, Q. Zeng, L. Wang, Y. Yao, and K. Li, “Corrosion of rebar in concrete under cyclic freeze-thaw and Chloride salt action,” Constr. Build. Mater., vol. 53, pp. 40–47, 2014.

[37] C. S. Poon, Z. H. Shui, and L. Lam, “Compressive behavior of fiber reinforced high-performance concrete subjected to elevated temperatures,” Cem. Concr. Res., vol. 34, no. 12, pp. 2215–2222, 2004.

[38] L. Taerwe and a. V. Gysel, “Influence of Steel Fibers on Design Stress-Strain Curve for High-Strength Concrete,” J. Eng. Mech., vol. 122, no. 8, pp. 695–704, 1996.

[39] M. C. Nataraja, N. Dhang, and A. P. Gupta, “Stress-strain curves for steel-fiber reinforced concrete under compression,” Cem. Concr. Compos., vol. 21, no. 5–6, pp. 383–390, 1999.

[40] A. C. Bordelon, “Fracture Behavior of Concrete Materials for Rigid Pavement Systems,” vol. M.S. Thesi, 2007.

[41] O. Shah, Surendra P. , Stuart E., Swartz, Chengsheng, Fracture Mechanics of Concrete: Applications of Fracture Mechanics to Concrete, Rock and Other Quasi-Brittle Materials. .

[42] S. Aydin, H. Yazici, and B. Baradan, “High temperature resistance of normal strength and autoclaved high strength mortars incorporated polypropylene and steel fibers,” Constr. Build. Mater., vol. 22, no. 4, pp. 504–512, 2008.

[43] Y. F. Chang, Y. H. Chen, M. S. Sheu, and G. C. Yao, “Residual stress-strain relationship for concrete after exposure to high temperatures,” Cem. Concr. Res., vol. 36, no. 10, pp. 1999–2005, 2006.

VITAE

Personal Information

Name **: MEHBOOB RASUL**

Father's Name **:** NADEEM RASUL ASIF

Date of Birth **:** October 13, 1991

Nationality **:** Pakistani

Residential Address **:** St#2, Nawab Colony, AliPur Road, Hafizabad, Punjab, Pakistan

Email **:** mehboob174@gmail.com

Educational Qualification

S.No.	Name of Institution	Degree	Passing Year	CGPA
1.	King Fahd University of Petroleum and Minerals, Dhahran, Saudi Arabia	M.S. Civil Engineering (Structures)	May 2016	**3.500/ 4.0**
2.	University of Engineering and Technology, Lahore, Pakistan	B.Sc. Civil Engineering	August 2012	**3.558 / 4.0**

Professional Experience

1. **Employer : National University of Computer and Emerging Sciences, Lahore**

   Period **:** August 2012 - August 2013

   Position **:** Lab Engineer

2. **Employer : Communication and Works Department, Govt. of Punjab, Pakistan**

   Period **:** August 2013 - January 2014

   Position **:** Deputy District Officer (Roads)

Membership

Registered Engineer with Pakistan Engineering Council